UNIVERSITY OF CALIFORNIA, SAN DIEGO

Mechanisms of effector secretion in the *Yersinia* type III secretion system

A dissertation submitted in partial satisfaction of the requirements for the degree of Doctor of Philosophy

in

Chemistry

by

Romila Mukerjea

Committee in charge:

Professor Partho Ghosh, Chair
Professor Thomas Hermann
Professor Simpson Joseph
Professor Kit Pogliano
Professor Navtej Toor

2014

The dissertation of Romila Mukerjea is approved, and it is acceptable in quality and form for publication on microfilm and electronically:

Chair

University of California, San Diego

2014

DEDICATION

I would like to dedicate this dissertation to my parents,

thank you Babi and Ma for everything but most of all for your love.

TABLE OF CONTENTS

LIST OF ABBREVIATIONS

T3S – type III secretion

T3S4 –type III substrate specificity switch

S1- streptavidin binding aptamer

MS2CP – MS2 coat protein

GFP – green fluorescent protein

SBP – streptavidin binding peptide

Yop- *Yersinia* outer protein

Ysc – *Yersinia* secretion component

3-Ala -alanine substitution mutant

5-Ala- alanine substitution mutant

HCR – highly conserved region

Syc –specific Yop chaperone

WT - wild type

LIST OF FIGURES

LIST OF TABLES

ACKNOWLEDGEMENTS

I first and foremost would like to acknowledge Professor Partho Ghosh in his guidance and support throughout my graduate career. His mentorship, honesty, and patience (especially during the writing process of manuscripts and this thesis) have been amazing throughout my graduate career.

I would like to thank my parents, Rupendra and Ilora Mukerjea, for their constant support. My father, Rupendra, instilled in me a love of science at a very young age and for that I thank him. I also thank him for his incessant "Dad jokes". I thank my mother, Ilora, for being my best friend and cheerleader throughout my life but especially in the last few year of graduate school. I also thank her for being my personal stylist. I know I would not have been able to accomplish anything without both of my parents support and love (although I may have referred to this love as borderline obsession). I would like to thank my brother, Rudi, for his support and always supplying me with comedy bits and witty one-liners when I was stressed out. I also thank him for being my go to person for anything sports related.

I would like to thank the current and former members of the Partho Ghosh lab for their help and support both inside and outside of lab. I would like to thank my awesome office mates, Kharissa Shaw and Sumit Handa for keeping the office jovial and fun. I would like to thank Chelsea Stewart for the delicious baked goods she would bring to lab. I would like to thank Cosmo Buffalo, Adrian Bahn, and Henry Quach for keeping the lab lively and fun. I would like to thank Brent Hamaoka for his jubilant and lively personality.

I would like to thank my fellow graduate school friends; Dr. Diana Rios Ourthiague, Dr. Karen Fortmann, and Dr. Rachel Tsui for helping me survive graduate school. I know I couldn't have gotten through this without your help and support. I am #blessed to be able to call you my friends and I appreciate you all so much.

I would like to thank my committee members for their suggestions throughout my graduate career.

Chapter 2, in full, is a reprint of material as it appears in Rodgers L, Mukerjea R, Birtalan S, Freiberg D, Ghosh, P. "A solvent-exposed patch in chaperone-bound YopE is required for translocation by the type III secretion system" *Journal of Bacteriology* 2010 192(12):3114-22. The dissertation author was a contributing author of this material.

Chapter 3, in full, is a reprint of material as it appears in Gamez A, Mukerjea R, Alayyoubi M, Ghassemian M, Ghosh P. "The structure and interactions of the cytoplasmic domain of the *Yersinia* type III secretion protein YscD." *Journal of Bacteriology* 2012; 194(21):5949-58. The dissertation author was a primary investigator and author of this material along with Alicia Gamez.

Chapter 4, in full, is a reprint of material as it appears in Mukerjea R, Ghosh P. "Functionally essential interaction between *Yersinia* YscO and the T3S4 domain of YscP." *Journal of Bacteriology* 2013 195(20):4631-8. The dissertation author was the primary investigator and author of this material.

VITA

Education

2008-2014	University of California San Diego, La Jolla, CA Doctor of Philosophy in Chemistry
2004-2008	Iowa State University, Ames, IA Bachelor of Science in Biochemistry

Publications (* marks primary authorship)

Mukerjea R. and Ghosh, P. 2013. Functionally essential interaction between *Yersinia* YscO and the T3S4 domain of YscP.Type III Secretion System. *J. Bacteriol*. 195:4631-8.

Gamez, A*. and **Mukerjea, R***., Alayyoubi, M., Ghassemian, M., and Ghosh. P. 2012. Structure and interactions of the cytoplasmic domain of the Yersinia type III secretion protein YscD. *J. Bacteriol.* 194:5949-58.

Rodgers L, **Mukerjea R**, Birtalan S, Friedberg D, Ghosh P. 2010. A solvent-exposed patch in chaperone-bound YopE is required for translocation by the type III secretion system. *J Bacteriol*. 192:3114-22.

Mukerjea, Ro., Mukerjea, R. and Robyt, J.F. 2009. Starch biosynthesis: experiments on how starch granules grow *in vivo*. *Carbohydr. Res*. 344:67-73
Mukerjea, Ru., Slocum, G., **Mukerjea, Ro**., and Robyt, J. F. 2006. Significant differences in the activities of α-amylases in the absence and presence of polyethylene glycol assayed on eight starches solubilized by two methods. *Carbohydr. Res*. 341: 2049-2054.

Mukerjea, Ro., Mukerjea, R. and Robyt, J.F. 2006.Controlled peeling of the surfaces of starch granules by gelatinization in aqueous dimethyl sulfoxide at selected temperatures. *Carbohydr. Res*. 341:757-765.

Abstracts at Scientific Meetings

Mukerjea R and Ghosh P. (2013) "Functionally essential interaction between *Yersinia* YscO and the T3S4 domain of YscP" Microbial Adhesion and Signal Transduction Gordon Research Conference (Poster)

ABSTRACT OF THE DISSERTATION

Mechanisms of effector secretion in the *Yersinia* type III secretion system

by

Romila Mukerjea

Doctor of Philosophy in Chemistry

University of California, San Diego, 2014

Professor Partho Ghosh, Chair

Pathogens utilize a variety of mechanisms to survive and reproduce within their host. The type III secretion (T3S) system is a pathogenic mechanism employed by many gram negative bacteria, including *Salmonella*, *Pseudomonas*, *Escherichia coli*, and *Yersinia*, the last of which is responsible for the bubonic plague (*Y. pestis*) as well as gastrointestinal infections (*Y. enterocolitca* and *Y. pseudotuberculosis*). The T3S system is made up of approximately 20-25 proteins which form a needle-like

complex with similarity to the bacterial flagellum. *Yersinia* spp. utilize this system to translocate effectors into the host cell. These effectors enable *Yersinia* to evade host immune responses and ensure bacterial survival. This dissertation aims to answer questions regarding the mechanisms of effector secretion by the *Yersinia* T3S. In this dissertation, I present contributions I have made to published papers on the translocation of the effector YopE as well as structural and functional characteristics of an inner membrane protein of the T3S injectisome, YscD. I present my findings on the functional characteristics of an essential T3S component, YscO. I further show how protein-protein interactions between YscO and the T3S molecular ruler, YscP, dictate T3S function.

In this dissertation, I also present methods for identifying potential binding partners to the secretion and translocation signals of the effector YopE. I present the construction of two vectors to use the RaPID and reverse-CLIP techniques for the identification of binding partners to the 5'mRNA signal of YopE. Both of these techniques utilize *in vivo* crosslinking and streptavidin affinity purification coupled with tandem mass spectrometry. Finally, I present potential binding partners to the first 80 amino acids of YopE which encompass the 5'/N-terminal signal as well as the chaperone binding (Cb) region. Using streptavidin affinity purification coupled with tandem mass spectrometry, I found that the inner rod protein YscI and the ATPase regulator YscL selectively bind wild-type $YopE_{1-80}$ and a non-translocating mutant of YopE called 3-Ala_{1-80}. I also found that the T3S gate-keeper YopN selectively binds 3-Ala_{1-80} and not wild-type $YopE_{1-80}$.

Chapter 1:

General Introduction

INTRODUCTION

Pathogens and host immune systems are constantly trying to "outsmart" one another. As hosts develop ways to combat infection, pathogens in turn develop methods to invade hosts and evade host immune responses. One method of pathogenesis employed by many gram-negative bacteria is the type III secretion, or T3S, system (Figure 1.1a). This system involves the injection of virulence factors into the host cell to combat the host immune response and further propagate infection.

The T3S system is present in animal and plant pathogens, including *Salmonella, Pseudomonas, Escherichia Coli,* and *Yersinia,* the last of which is responsible for the bubonic plague (*Y. pestis*) as well as gastrointestinal infections (*Y. enterocolitca and Y. pseudotuberculosis*). *Y. enterocolitca and Y. pseudotuberculosis* gain entry into the host using the oral route through contaminated food or water (Ramamurthi and Schneewind, 2002). Eventually the bacteria reach the terminal ilium and breach the intestinal epithelium upon encountering M cells, which are specialized immune cells that sample the contents of the intestinal lumen and transfer these contents to the host lymph system (Ramamurthi and Schneewind, 2002). At this point, pathogenic *Yersinia* come in contact with macrophages and initiates the type III secretion system.

The T3S system of *Yersinia spp*. is one of the more widely studied T3S systems to date as the T3S was first discovered in *Y. enterocolitica* and *Y.*

pseduotuberculosis (Salmond and Reeves, 1993). Researchers were first examining an arrest in growth of the bacteria in a low calcium environment (Portnoy et al., 1984). It was later discovered that this low calcium response, or LCR, was due to the shifting of bacterial resources to the production of virulence factors, known as effectors (Ramamurthi and Schneewind, 2002). In the case of *Yersinia* spp. these effectors are referred to as *Yersinia* outer proteins, or Yops. These Yops are then secreted and/or translocated into the host cell using the *Yersinia* T3S apparatus.

The T3S apparatus involves the assembly of a needle-like complex comprised of approximately 20-25 proteins. Approximately 8-10 proteins are conserved amongst many T3S systems as well as parts of the basal body of the bacterial flagellum (Ghosh, 2004). The bacterial flagellar and T3S systems appear to have evolved independently from a common ancestor as both systems have protein secretion in common (Ghosh, 2004). Bacterial flagellar assembly requires secretion of flagellar subunits in a process powered by a flagellar ATPase (Ghosh, 2004). Similarly, the T3S system of protein transport also uses ATP as its energizer and depends on an ATPase as well as a transmembrane ionic potential (Ghosh, 2004; Woestyn et al., 1994). The T3S multimeric protein complex is made up a basal body consisting of multiple rings which span the inner and outer bacterial membranes. A protruding needle completes the formation of the T3S apparatus and this needle-complex is referred to as an injectisome (Cornelis, 2006). Protein components that comprise the inner membrane ring have been

identified for a number of different T3S systems (Ghosh, 2004). The assembly of the T3S apparatus occurs in a highly ordered fashion with the formation of the basal body occurring first, followed by secretion of needle components.

The T3S needle is formed by helical polymerization of the protein YscF into a cylindrical hollow tube of ~ 60 nm in length and ~ 25 Å in diameter for *Yersinia* (Cornelis, 2006). Once the T3S molecular ruler, YscP, determines the appropriate length of the needle, a switch occurs (Agrain et al., 2005; Edqvist et al., 2003; Journet et al., 2003), changing the substrates from needle components to Yops. Although the mechanism of how this switch occurs has not been determined, the importance of the cytoplasmic domain of the inner membrane protein YscU has been implicated (Riordan and Schneewind, 2008; Wood et al., 2008). Additionally the inner rod protein, YscI, has been predicted to be involved in this substrate switching as well (Wood et al., 2008).

The switch from needle components to Yops induces the secretion of the translocator Yops, YopB and YopD. These Yops appear to form the pore in the host cell membrane and are required for translocation of the effector Yops are virulence factors and contain two or three specific regions of interest. The first is the secretion signal, which has been mapped to the first 15 codons or amino acids for all Yops. This signal, referred to as the 5'/N-terminal signal here, has been shown to be sufficient for secretion into the media, and in some effectors, translocation into host cells (Figure 1.1.b). The naming of the 5'/N-terminal signal originates from the fact that evidence has shown the signal for secretion resides in

the first ~15 codons of the mRNA encoding the effector (Anderson and Schneewind, 1997), and evidence also exists that the secretion signal resides in the N-terminal ~15 amino acid residues of the effector (Lloyd et al., 2001). These two different sorts of signals may both be utilized, but at different times of infection. Some Yops have a second region of interest, which is located downstream of the N-terminal signal and is responsible for binding a T3S chaperone.

Chaperones of the T3S system are compact (~14 kD), acidic (pI 4-5) proteins which form globular dimers and bind one or only a few effectors. This binding interaction is localized to a specific region of the cognate effector, generally spanning amino acids ~25-100. Some effectors do not have cognate chaperones and are translocated independently of chaperone action (Ghosh, 2004). However, an effector that has a chaperone binding region, requires the binding of the cognate T3S chaperone for translocation into the host cell (Sorg et al., 2005).

The third region of interest in the effector is the region that directly interacts with targets within host cells. This region specifies the effector activities, either catalytic or host cell target binding, in the host cell, and are encoded by domains that usually follow the chaperone-binding region (Ghosh, 2004).

The effector YopE is a well-studied effector and is a Rho GTPase-activating (RhoGAP) protein that disrupts the actin cytoskeleton and disables phagocytosis in the host cell (Black and Bliska, 2000; Von Pawel-Rammingen et

al., 2000). YopE contains both a 5'/N-terminal signal and a chaperone-binding (Cb) region (Anderson and Schneewind, 1997; Lloyd et al., 2001) as well as a Rho-GAP domain (Von Pawel-Rammingen et al., 2000).

The aim of this dissertation is to examine mechanisms of effector secretion by characterizing different injectisome or injectisome-associated components as well as the secretion and translocation signals of the effector YopE. Chapter 2 is a reprint of a manuscript that I contributed to and presents experiments examining the putative translocation signal of the YopE. In this chapter, we identified a set of residues in the YopE Cb region that are required for translocation but not for other aspects of YopE function such as SycE binding, secretion into the extrabacterial milieu, and stability in mammalian cells. These residues referred to as 3-Ala and 5-Ala form a solvent-exposed patch on the surface of the chaperone-bound Cb region of YopE, and suggest the chaperone bound Cb region of an effector serves as a signal for translocation. Chapter 3 is a reprint of a manuscript that I contributed to and presents information on the structural and functional characteristics of a domain of the injectisome component, YscD. In this chapter we reported the 2.52-Å resolution structure of the cytoplasmic domain of YscD, YscDc, and found two loop regions necessary for T3S function. These two loops, L3 and L4 indicated a role in effector secretion through dissociation of the chaperone SycH from its effector YopH. These findings lead to the hypothesis that the loop regions L3 and L4 induced a protein complex formation that stalled the T3S apparatus. Chapter 4 is a reprint of

a manuscript on which I was the primary author. This chapter examines YscO, which is an essential component of the T3S in *Yersinia*. I found regions of YscO which were highly conserved amongst YscO orothologs and using model-guided mutagenesis targeted these surface exposed regions of YscO with multiple alanine substitutions. Most of the mutations abrogated T3S with a loss of function. While all YscO mutant proteins interacted with the chaperone SycD, only functional versions of YscO interacted with the T3S molecular ruler YscP. I presented evidence that the YscO-YscP interaction was direct and that the type III secretion substrate specificity switch (T3S4) domain of YscP was sufficient for this interaction.

In Chapters 5 and 6, I present an examination of the secretion and translocation signals of the effector YopE. In Chapter 5, I present the construction of two vectors to identify potential binding partners of the 5' secretion signal of *yopE* mRNA using reverse-CLIP and RaPID techniques. These two techniques used RNA aptamers fused to the 5' mRNA signal sequence of *yopE* and utilized the high affinity of streptavidin as a means of affinity purifying components associated with 5' signal. I found the RaPID technique to be a more promising option than the reverse-CLIP technique. I also discuss future steps and directions with these techniques. In Chapter 6, I present potential binding partners to the first 80 amino acids of the *Yersinia* effector YopE ($YopE_{1-80}$) using a similar technique of streptavidin affinity purification coupled to tandem mass spectrometry. I found that the inner rod protein YscI and the ATPase regulator YscL were selectively

bound by wild-type $YopE_{1-80}$ and a non-translocating mutant $3\text{-}Ala_{1-80}$ whereas the T3S gate-keeper YopN was selectively bound by $3\text{-}Ala_{1-80}$.

FIGURES AND TABLES

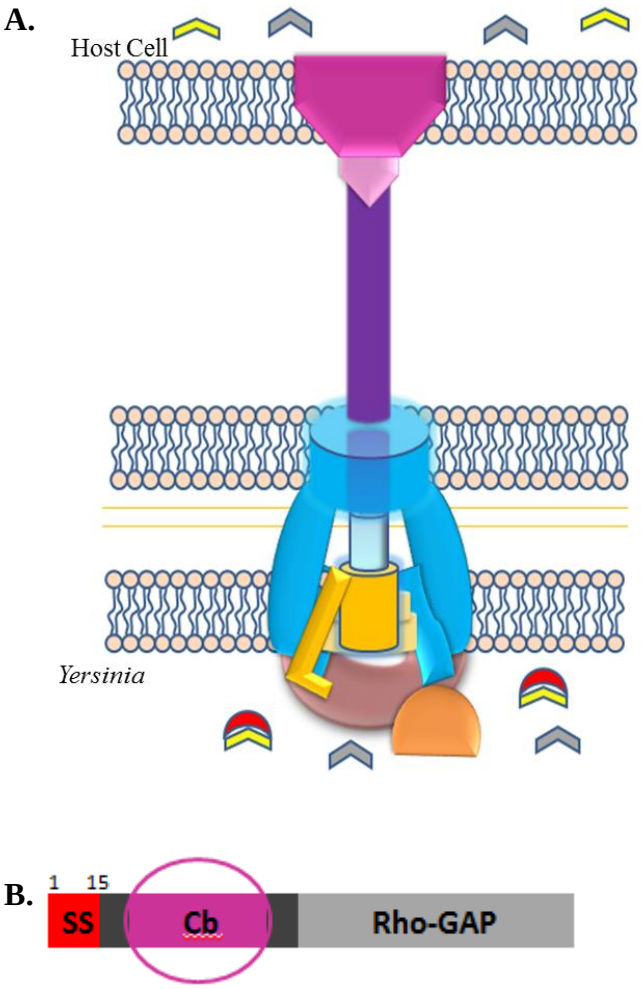

Figure 1.1 Schematic of the type III secretion system and the effector YopE.
A. Schematic of T3S of *Yersinia* in the presence of a host cell. The T3S needle apparatus is comprised of 20-25 proteins which span both inner and outer membranes of the bacterium (blue, yellow, cyan, brown and orange) and include a protruding needle structure (purple). This apparatus is used to secrete and/or translocate Yops (pink, magenta, gray, and yellow). Yops (chevron) with or without a chaperone (red crescent) are indicated.
B. Schematic of the effector YopE indicating three distinct regions including the secretion signal (SS), chaperone binding region (Cb) and the catalytic domain (Rho-GAP)

REFERENCES

Agrain, C., Callebaut, I., Journet, L., Sorg, I., Paroz, C., Mota, L.J., and Cornelis, G.R. (2005). Characterization of a Type III secretion substrate specificity switch (T3S4) domain in YscP from Yersinia enterocolitica. Mol. Microbiol. *56*, 54–67.

Anderson, D.M., and Schneewind, O. (1997). A mRNA signal for the type III secretion of Yop proteins by Yersinia enterocolitica. Science *278*, 1140–1143.

Cornelis, G.R. (2006). The type III secretion injectisome. Nat. Rev. Microbiol. *4*, 811–825.

Diepold, A., Amstutz, M., Abel, S., Sorg, I., Jenal, U., and Cornelis, G.R. (2010). Deciphering the assembly of the Yersinia type III secretion injectisome. EMBO J. *29*, 1928–1940.

Edqvist, P.J., Olsson, J., Lavander, M., Sundberg, L., Forsberg, A., Wolf-Watz, H., and Lloyd, S.A. (2003). YscP and YscU regulate substrate specificity of the Yersinia type III secretion system. J. Bacteriol. *185*, 2259–2266.

Ghosh, P. (2004). Process of Protein Transport by the Type III Secretion System. Microbiol. Mol. Biol. Rev. *68*, 771–795.

Journet, L., Agrain, C., Broz, P., and Cornelis, G.R. (2003). The needle length of bacterial injectisomes is determined by a molecular ruler. Science *302*, 1757–1760.

Lloyd, S.A., Norman, M., Rosqvist, R., and Wolf-Watz, H. (2001). Yersinia YopE is targeted for type III secretion by N-terminal, not mRNA, signals. Mol. Microbiol. *39*, 520–531.

Von Pawel-Rammingen, U., Telepnev, M.V., Schmidt, G., Aktories, K., Wolf-Watz, H., and Rosqvist, R. (2000). GAP activity of the Yersinia YopE cytotoxin specifically targets the Rho pathway: a mechanism for disruption of actin microfilament structure. Mol. Microbiol. *36*, 737–748.

Ramamurthi, K.S., and Schneewind, O. (2002). Type iii protein secretion in yersinia species. Annu. Rev. Cell Dev. Biol. *18*, 107–133.

Riordan, K.E., and Schneewind, O. (2008). YscU cleavage and the assembly of Yersinia type III secretion machine complexes. Mol. Microbiol. *68*, 1485–1501.

Sorg, J.A., Miller, N.C., and Schneewind, O. (2005). Substrate recognition of type III secretion machines –testing the RNA signal hypothesis. Cell. Microbiol. *7*, 1217–1225.

Woestyn, S., Allaoui, A., Wattiau, P., and Cornelis, G.R. (1994). YscN, the putative energizer of the Yersinia Yop secretion machinery. J. Bacteriol. *176*, 1561–1569.

Wood, S.E., Jin, J., and Lloyd, S.A. (2008). YscP and YscU Switch the Substrate Specificity of the Yersinia Type III Secretion System by Regulating Export of the Inner Rod Protein YscI. J. Bacteriol. *190*, 4252–4262.

Chapter 2:

A solvent-exposed patch in chaperone-bound YopE is required for translocation by the type III secretion system

In this chapter, I performed secretion assays to test for the secretion of YopE by *Y. pseudotuberculosis*126 (YP126); *Y. pseudotuberculosis* 126 (*ΔyopE*) expressing wild-type YopE (WT), YopE-3Ala (3Ala), and YopE-5Ala (5Ala); and wild-type YopE secreted by *Y. pseudotuberculosis* 126 (*ΔyopB*. I used western blots (probing with anti-YopE and anti-DnaK) of supernatants and cell pellets from *Y. pseudotuberculosis* strains induced to secrete due to a shift to low Ca^{2+} concentration and growth at 37 °C. My contribution was represented in Figure 4 of the manuscript.

ABSTRACT

Most effector proteins of bacterial type III secretion (T3S) systems require chaperone proteins for translocation into host cells. Such effectors are bound by chaperones in a conserved and characteristic manner, with the chaperone-binding (Cb) region of the effector wound around the chaperone in a highly extended conformation. This conformation has been suggested to serve as a translocation signal in promoting the association between the chaperone-effector complex and a bacterial component required for translocation. We sought to test a prediction of this model by identifying a potential association site for the *Yersinia pseudotuberculosis* chaperone-effector pair SycE-YopE. We identified a set of residues in the YopE Cb region that are required for translocation, but are dispensable for expression, SycE binding, secretion into the extrabacterial milieu, or stability in mammalian cells. These residues form a solvent-exposed patch on the surface of the chaperone-bound Cb region, and thus their effect on translocation is consistent with the structure of the chaperone-bound Cb region serving as a signal for translocation.

INTRODUCTION

The type III secretion (T3S) system is crucial to the virulence of a large number of Gram-negative bacterial pathogens (Cornelis, 2006; Feldman et al., 2002). These pathogens use the T3S system to translocate effector proteins from the bacterial cytosol directly into the interior of host cells. Typically, effectors contribute to the virulence of the pathogen by modifying or interacting with specific host cell targets. Effector proteins are arranged in modular fashion, with sequence elements required for translocation located within their N-terminal ~100-150 residues and domains that interact with host components following (Ghosh, 2004; Schesser et al., 1996). For most effectors, including the extensively characterized *Yersinia* effector YopE (23 kDa), two different N-terminal sequence elements are required for translocation into host cells. The first, termed here signal 1 (S1), occurs at the very N-terminus and spans ~10-15 residues (Figure 2.1A). The S1 element is highly degenerate in sequence (Quenee and Schneewind, 2007), and in YopE the S1 region has been shown to be structurally disordered (Rodgers et al., 2008). While the S1 element is sufficient for the non-physiological process of secretion of effectors into the extrabacterial milieu, it is not sufficient for translocation into host cells (Schesser et al., 1996; Sory et al., 1995).

For translocation a second sequence element, termed the chaperone-binding (Cb)region, is required (Figure 2.1A) (Sory et al., 1995). The

Cb region, which consists of ~50-100 residues downstream of S1, promotes translocation only when bound by a member of the effector-dedicated chaperone protein family (Woestyn et al., 1996).

The chaperone protein is dissociated from the effector by a T3S ATPase (Akeda and Galán, 2005), as shown in *Salmonella*, and remains in the bacterial cytosol upon transport of the effector (Frithz-Lindsten et al., 1995). There are a large number of such effector-dedicated chaperones, as each individual chaperone protein binds just a single or in some cases a few effectors. These chaperones are divergent in sequence (≤20% identity), but have similar protein folds, dimeric oligomerization states, and effector-binding modes (Birtalan and Ghosh, 2001; Birtalan et al., 2002; Büttner et al., 2005; van Eerde et al., 2004; Lilic et al., 2006; Locher et al., 2005; Luo et al., 2001; Phan et al.; Schubot et al., 2005; Singer et al., 2004; Stebbins and Galán, 2001). In this binding mode, the Cb region of the effector winds around the surface of the dimeric chaperone in highly extended fashion (Figure 1B and 1C). The chaperone-bound Cb region lacks independent tertiary structure but has short α-helical, β-strand, and random coil stretches that contact the chaperone. This mode has been observed for the Cb region of YopE (residues 23-78) bound to its homodimeric chaperone SycE (29 kDa per dimer) (Birtalan et al., 2002), as well as in a number of other chaperone-effector complexes (Lilic et al., 2006; Phan et al.; Schubot et al., 2005; Stebbins and Galán, 2001). The structural conservation among these chaperone-effector pairs is especially striking because the various effectors have no obvious sequence

relationship to one another in their Cb regions. However, recent work shows that the chaperone-Cb region binding mode can be predicted from *de novo* models (Hu et al., 2009).

The functional significance of the conserved chaperone-Cb region structure is not yet clear, but this structure has been suggested to constitute a translocation signal (Birtalan et al., 2002). It has been proposed that the conformation of the chaperone-bound Cb region promotes association between the chaperone-effector complex and a bacterial component required for translocation, *i.e.,* a receptor that recognizes this three-dimensional translocation signal. Consistent with this hypothesis, recent evidence indicated that the chaperone SycE brings about the structuring of an otherwise unstructured Cb region in YopE (Rodgers et al., 2008). Nuclear magnetic resonance studies demonstrated that the Cb region of YopE in its free state was unstructured and flexible, and that it underwent a pronounced disorder-to-order transition upon SycE binding. The effect of SycE was strictly localized to the Cb region, while other portions of YopE, including the S1 region and the C-terminal RhoGAP domain, were impervious to SycE binding. Additional lines of evidence also support the translocation signal model of chaperone action (Boyd et al., 2000; Cheng and Schneewind, 1999; Wulff-Strobel et al., 2002).

We sought here to test a prediction of the translocation signal model. This is the prediction that the surface of the chaperone-Cb region complex ought to provide a receptor-binding site. We surmised that mutation of such a solvent-

exposed site in the Cb region of YopE would affect translocation but not chaperone binding. Mutations of residues in the Cb region that contact the chaperone have already been shown to reduce translocation (Birtalan et al., 2002; Lilic et al., 2006; Schesser et al., 1996).

These are simple to explain. They diminish the affinity of the effector for the chaperone. In contrast, residues in the Cb region that are exposed in the chaperone-Cb complex, and hence available to form a receptor-binding site, have not yet been shown to be important for translocation. We now report the identification of such residues in the YopE Cb region. These residues are crucial for translocation but not for other aspects of YopE, including steady-state expression, binding to SycE, secretion, or stability in mammalian cells. These results are consistent with a translocation signal model of action for the chaperone-bound Cb region, and identify a potential receptor-binding site.

MATERIALS AND METHODS

Expression and Purification of SycEΔ122-YopE(Cb) constructs

SycEΔ122 (residues 1-121) and wild-type, 3Ala (V23A/E25A/S32A), or 5Ala (V23A/E25A/S27A/R29A/S32A) YopE(Cb) (residues 1-80) were expressed in inducible fashion in *Escherichia coli* BL21 (DE3) using a bicistronic vector derived from pET28b (Novagen). Bacteria were induced for protein expression at mid-log growth phase with 1 mM isopropyl β-D-1-thiogalactopyranoside (IPTG) and grown further at room temperature for 3 h. Bacteria were harvested by centrifugation, resuspended in 150 mM NaCl, 50 mM phosphate buffer (pH 8.0), and 10 mM β-mercaptoethanol (βME), and lysed by sonication. Polyethyleneimine was added to the lysate to a final concentration of 0.5% and the solution was centrifuged. The supernatant, which contained SycEΔ122-YopE(Cb), was then further precipitated with 50% saturated $(NH_4)_2SO_4$. The resulting pellet, which contained SycEΔ122-YopE(Cb), was resuspended and dialyzed in 20 mM NaCl, 30 mM Tris, pH 8.0, 10 mM βME. SycEΔ122-YopE(Cb) was purified by anion-exchange (Poros HQ/M), cation-exchange (Poros HS/M), and size-exclusion (Superdex 75) chromatography.

SycE-his (residues 1-130), which contains a C-terminal his-tag, was expressed in *E. coli* BL21 (DE3) using a pET28b (Novagen) as described above, and purified as described for his-tagged SycE-YopE complexes (Rodgers et al., 2008).

Guanidine Denaturation

Wild-type, 3Ala, and 5Ala SycEΔ122-YopE(Cb) were concentrated to 1.55 μM in 100 mM NaCl and 10 mM phosphate buffer, pH 8.0. Likewise, SycE-his was concentrated to 0.775 μM (dimer) in the same buffer. Proteins were denatured through stepwise, automated titration (Hamilton Microlab 500 titrator) with a solution consisting of 5.7 M guanidine, 100 mM NaCl, 10 mM phosphate buffer, pH 8.0, and either 1.55 μM SycEΔ122-YopE(Cb) (in the case of denaturation of this complex) or 0.775 μM SycE-his (in the case of its denaturation) in order to maintain a constant protein concentration. The concentration of guanidine was checked by refractometry. Protein samples were stirred for 10 min between titration steps (to reach equilibrium, as determined empirically), and the circular dichroism signal at 222 nm was monitored for 15 seconds on an Aviv 202 circular dichroism spectrometer. Denaturation data were fit with a two-state folding model, with the pre- and post-transition baselines treated to have a linear dependence on the concentration of denaturant, as described previously (Ferreiro et al., 2007).

Strain and plasmid construction

The serogroup III *Y. pseudotuberculosis* strain 126 (a gift from James Bliska) has previously been described (Bölin et al., 1982), as have *Y. pseudotuberculosis* 126 (Δ*yopB*) (Palmer et al., 1998) and *Y. pseudotuberculosis* 71 (Bölin and Wolf-Watz, 1984). A strain derived from *Y. pseudotuberculosis* 126

in which the coding sequence for *yopE* was precisely replaced by the coding sequence for aminoglycoside 3'-phosphotransferase (*kan*^{R}) was constructed by standard allelic exchange methods using the suicide vector pSB890 (Palmer et al., 1998) and bacterial mating with *E. coli* S17-1Δpir. The site of integration was verified by DNA sequencing.

Expression of wild-type YopE, YopE-3Ala, and YopE-5Ala in *Y. pseudotuberculosis* 126 (Δ*yopE*) was achieved with a 2.9-kb low-copy plasmid derived from pKK223-3 which carries the ampicillin resistance gene and the *tacl* promoter (Brosius and Holy, 1984).

For expression of wild-type YopE, YopE-3Ala, and YopE-5Ala in HeLa cells, pcDNA3.1+ (Invitrogen) was used.

***Y. pseudotuberculosis* expression of YopE**

Strains of *Y. pseudotuberculosis* were grown overnight at 26 ºC in Luria broth (LB) or brain-heart infusion (BHI) medium with appropriate antibiotics (30 µg/ml kanamycin, or also including 30 µg/ml carbenicillin). To examine expression of YopE under non-secreting conditions, cultures were diluted into LB or BHI containing 2.5 mM $CaCl_2$ and appropriate antibiotics to a final A_{600} of 0.1, grown for 1 h at 26 ºC, at which time IPTG was added to a final concentration of 1 mM; cultures were then grown for a further 2 h at 37 ºC. After this time, the quantity of cells in each sample was set to equivalent levels by diluting cultures to a final A_{600} of 0.3, and bacterial cells were harvested by centrifugation (10 min, 4

ºC, 4,000 x g). Cell pellets were lysed by the addition of 5 mg/ml lysozyme and 5 mg/ml DNase, and by resuspending and boiling in SDS-PAGE sample buffer. Samples were analyzed by western blot, as below.

Y. pseudotuberculosis secretion of YopE

Strains of *Y. pseudotuberculosis* were cultured by shaking overnight at 26 ºC in 3 ml LB or BHI with appropriate antibiotics. Bacterial cultures were diluted into LB or BHI containing 10 mM ethylene glycol tetraacetic acid (EGTA), 10 mM $MgCl_2$ and appropriate antibiotics as to a final A_{600} of 0.1. Cultures were grown with shaking for 1 h at 26 °C. IPTG was added to a final concentration of 1 mM, and cultures were grown with shaking for 2 hours at 37 °C or instead for a further hr at 26 °C followed by 3 hr at 37 °C. Both protocols produced similar results. Following this period, cells were separated from the culture medium by centrifugation (10 min, 4 ºC, 4,000 x g), and the culture medium was boiled with SDS-PAGE sample buffer for western blot analysis. The cell pellets were lysed as above, and resuspended and boiled in SDS-PAGE sample buffer for western blot analysis as well. As a negative control, bacterial strains were diluted into BHI containing 2.5 mM $CaCl_2$ after the overnight growth.

Western blotting

Samples were resolved by 12% SDS-PAGE and transferred to a PVDF

membrane (Amersham). Membranes were blocked with 5% milk in TBS (50 mM Tris, pH 8.0, 150 mM NaCl) or TBS including 0.1% Tween (TBST) for 1 hr at 26 ºC or 12 hr at 4 °C. Primary antibody (anti-YopE polyclonal antibodies were a gift from J. Bliska; anti-SycE polyclonal antibodies were described previously (Rodgers et al., 2008); anti-DnaK monoclonal antibody were from Abcam; and anti-□-tubulin monoclonal antibodies were from Santa Cruz Biotechnology) diluted in 5% bovine serum albumin (in TBS) or 5% milk (in TBST) was added and incubated for 50 min at 26 °C or 12 h at 4 ºC. Membranes were washed 4-8 times with 20-30 ml TBS or TBST (3-5 minutes per wash), and 20-25 ml of secondary antibody (HRP-conjugated rabbit anti-mouse, Santa Cruz) was added and incubated for 30-45 min at 26 ºC. Membranes were washed 4-8 times with 20-30 ml TBS or TBST (3-5 minutes per wash), and immunodetection was carried out on X-ray film with ECL plus (Amersham) according to the manufacturer's instructions. Densitometry of X-ray film was performed using ImageJ. Quantifications were ascertained to be within the linear range of measurement.

In cases in which membranes were stripped and reprobed, a stripping solution consisting of 67% guanidine hydrochloride, 50 µM ethylene diamine tetraacetic acid, 50 mM glycine, pH 10.8, 2.5 mM KCl, and 1.4 mM βME was incubated with the membrane for 10 min. The membrane was then washed once with H_2O and then with TBS for 5 min. Primary and secondary antibodies were added as above.

Translocation Assay

HeLa cells were routinely cultured in Dulbecco's modified Eagle's medium (DMEM, Cellgro) supplemented with 10% fetal bovine serum (FBS), glutamine, streptomycin, and penicillin in a 5% CO_2 humidified incubator at 37 ºC. HeLa cells were split 18 hours prior to infection, and plated at a density of 2 x 106 cells per 10 cm dish. Two hours prior to infection, adherent cells were washed twice with phosphate buffered saline (PBS) at 37 ºC and incubated in unsupplemented DMEM (i.e., without FBS, penicillin, streptomycin, or glutamine). The proteasome inhibitor MG 132 (Calbiochem) and the actin polymerization inhibitor cytochalasin D (Biomol) were added to final concentrations of 5 µM and 1 µg/ml, respectively. HeLa cells were then incubated for 2 h at 37 ºC, 5% CO_2.

The infection was allowed to proceed for 150 min at 37 ºC, 5%CO_2. Non-adherent cells were removed with three 15 ml washes of cold PBS, and following the aspiration of the last wash, papain was added to digest extracellular proteins (150 µl from a 0.25 mg/ml papain stock in PBS with 2 mM dithiothreitol). After 30 seconds, 140 µl of the papain solution was removed, leaving a thin layer of papain coating the HeLa monolayer. This digestion proceeded for 20 min at 26 °C, and was stopped by the addition of E-64 (90 µl of a 10 µg/ml solution). The cells were incubated in E-64 for 5 min before the addition of 400 µl lysis buffer (1% Triton X-100, 10% glycerol, 150 mM NaCl, 10 mM Tris, pH 8.0), which remained on the cells for 5 min. Cell lysates were collected by scraping, and then

clarified by centrifugation (10 min, 16,000 x g, 4 ºC). The clarified lysate was passed through a 0.22 µm cutoff filter to remove intact cells and debris. The total protein concentration of the lysate was quantified by a Lowry assay (Bio-Rad DC-protein detection kit). Lysate volumes were adjusted with lysis buffer to make protein concentrations equivalent among samples. Typical concentrations were 1-2 mg/ml as determined by comparison to a BSA standard. SDS-PAGE sample buffer (4X) was added, and samples were boiled for 10 minutes and centrifuged (1 min, 16,000 x g, 26 °C). Samples were analyzed by western blot.

Transfection

HeLa cells were cultured as above, and plated at a density of 1.5 x 105 cells per 9.6 cm2 well 18 hr prior to transfection. Thirty minutes prior to transfection, adherent cells were washed twice with PBS (37 ºC) and incubated in 1.9 ml unsupplemented DMEM. Two micrograms of the expression vector pcDNA3.1+ containing *yopE*, *yopE 3Ala* or *yopE 5Ala* was diluted to 95 µl with unsupplemented DMEM, and 5 µl FuGENE HD (Roche) was added. The resulting 100 µl solution was added to each well, and cells were incubated for 5 h at 37 ºC, 5% CO_2. The medium was then removed by aspiration and replaced with DMEM supplemented with 10% FBS, glutamine, streptomycin, and penicillin. Cells were incubated an additional 22 h (37 ºC, 5% CO_2), and the culture medium was removed by aspiration. Cells were lysed by the addition of 200 µl lysis buffer, which remained on the cells for five minutes. Cell lysates were collected

by scraping, and SDS-page sample buffer (4X) was added to the samples prior to analysis by SDS-PAGE and western blotting.

RESULTS

We targeted residues in the YopE Cb region for alanine-substitution that are solvent-exposed when the Cb region is bound to SycE (Birtalan et al., 2002). Based on previously noted similarities between the Cb regions of YopE and the *Salmonella* effector SptP (Birtalan et al., 2002), we focused on YopE Val23, Glu25 and Ser32. These residues were substituted with alanine, and this triple alanine substitution mutant (V23A/E25A/S32A) was designated YopE-3Ala. The side chains of these residues do not contact SycE (Birtalan et al., 2002), and thus their substitution was not expected to affect binding to SycE. The surface patch defined by these three residues is neighbored by Ser27 and Arg29 (Figure 2.1D), which make polar contacts with SycE but also have solvent-exposed portions. Because polar interactions usually contribute more to specificity than affinity, we substituted Ser27 and Arg29 with alanine along with Val23, Glu25, and Ser32 to increase the chances of disrupting a potential receptor-binding site. The quintuple alanine substitution mutant (V23A/E25A/S27A/R29A/S32A) was designated YopE-5A.

Affinity for SycE

The affinities of the YopE-3Ala and YopE-5Ala alanine-substitution mutants for SycE were determined and compared to that of wild-type YopE. To carry this out, complexes containing SycE dimers and either wild-type or mutant

versions of a YopE Cb fragment (*i.e.*, Cb-3Ala or Cb-5Ala) were coexpressed in *E. coli* and purified. The Cb fragment (residues 1-80) was used in lieu of intact YopE to simplify the analysis. The Cb region is the only portion of YopE that interacts with SycE, and this interaction is independent of other portions of YopE (Birtalan et al., 2002; Rodgers et al., 2008). The version of SycE used in this experiment, called SycE□122, was originally designed for structure determination and lacks its last eight residues. These last eight residues are flexible and do not contact YopE (Birtalan et al., 2002).

The purified complexes were subjected to reversible unfolding with guanidine, and the progress of unfolding was monitored by circular dichroism at 222 nm. As shown previously (Birtalan et al., 2002), the midpoint of unfolding for free SycE was lower than that for SycE-YopE(Cb) (Figure 2.2). This difference reflects the binding energy derived from the association between SycE and YopE, and is thus a measure of the binding affinity between SycE and YopE. A mutation that results in a decrease in the SycE-YopE affinity would be manifested as a decrease in the guanidine concentration required for unfolding (as compared to the guanidine concentration required for unfolding of wild-type SycE-YopE). As predicted from structural grounds, the triple alanine substitution in YopE had no effect on SycE-YopE affinity. SycEΔ122-YopE(Cb-3Ala) had a midpoint of unfolding of 2.30 ± 0.01 M guanidine (standard error of the mean), which is identical to the 2.30 M ± 0.02 M guanidine midpoint of wild-type

SycEΔ122-YopE(Cb) (Figure 2.2). In comparison, SycEΔ122-YopE(Cb-5A) had a slightly lower midpoint of unfolding at 2.23 ± 0.01 M guanidine, indicative of a small loss in affinity for SycE (Figure 2.2). These results indicate that the combined alanine substitutions of YopE Val23, Glu25, and Ser32 have no influence on the affinity of the Cb region for SycE, and that the additional alanine substitutions of Ser27 and Arg29 have a only a slight effect.

Expression and Secretion by *Y. pseudotuberculosis*

We next asked whether the alanine-substitution affected expression and secretion of YopE by *Y. pseudotuberculosis*. Wild-type YopE, YopE-3Ala, and YopE-5Ala were expressed under the inducible control of the *tac* promoter from a low-copy plasmid (Brosius and Holy, 1984) in *Y. pseudotuberculosis* 126 (*ΔyopE*). In this *ΔyopE* strain, the entire coding sequence for *yopE* was substituted by that of aminoglycoside 3'-phosphotransferase **(***kan*^{R}), and the loss of YopE expression was verified by western blot. YP126, YP126 (*ΔyopE*), and the YP126 (*ΔyopE*) strains expressing plasmid-encoded wild-type YopE, YopE-3Ala, and YopE-5Ala all had equivalent growth rates (data not shown).

The steady-state expression level of plasmid-encoded YopE was compared to that of YopE expressed from its native promoter on the pIB plasmid of *Y. pseudotuberculosis* 126 (Palmer et al., 1998). These experiments were carried out under non-secreting conditions through the inclusion of Ca^{2+} in the growth medium at 37 °C. A western blot showed that plasmid-encoded, wild-type YopE

was produced at a level equivalent to that of natively encoded YopE (Figure 2.3A). This steady-state expression level was also equivalent to that of YopE-3Ala and YopE-5Ala. The number of cells analyzed for these experiments was normalized, as was verified by detecting DnaK on the same blot. Quantification of western blots from multiple independent experiments showed that the steady-state level of YopE expression was statistically indistinguishable among these strains (Figure 2.3B, ANOVA *P*-value = 0.85). These results are consistent with the observation that the YopE-3Ala and YopE-5Ala substitution mutants have the same or nearly the same affinity for SycE as wild-type YopE. Loss of binding to SycE has previously been demonstrated to lower the level of YopE due to degradation (Cheng and Schneewind, 1999; Cheng et al., 1997; Frithz-Lindsten et al., 1995; Wattiau and Cornelis, 1993).

Type III secretion of alanine-substitution mutants

We next asked whether the alanine substitutions had an effect on the secretion of YopE. The process of type III secretion into the extrabacterial milieu in the absence of host cells has similarities to translocation, but the requirements for the two processes differ. For example, while SycE is required for translocation of YopE, it is not required for secretion (Cheng and Schneewind, 1999; Cheng et al., 1997). A SycE-deficient strain contains ~2-fold lower steady-state levels of YopE than a wild-type strain, but the SycE-deficient strain secretes YopE at the same steady-state efficiency as the wild-type strain (Cheng et al., 1997). In

contrast, the SycE-deficient strain is entirely incapable of translocating YopE into HeLa cells (Cheng and Schneewind, 1999).

Type III secretion was induced by growing *Y. pseudotuberculosis* in low calcium medium at 37 °C, and secretion of YopE was monitored by western blotting of culture supernatants. YopE secretion occurred only when calcium was absent from the medium, consistent with the secretion being type III (Figure 2.4A). The level of secreted wild-type YopE was similar regardless of whether YopE was expressed from its native locus on the pIB plasmid or from the low-copy plasmid, as determined from quantification of western blots (Figure 2.4B). Most importantly, this experiment showed that the levels of secreted YopE-3Ala and YopE-5Ala were indistinguishable from that of wild-type YopE (Figure 2.4A and 2.4B).

We verified that equivalent numbers of bacterial cells were examined in these experiments, as shown by immunodetection of DnaK from the intrabacterial pool (Figure 4.4C). As expected from the equivalent steady-state expression levels of YopE, the levels of intrabacterial YopE were similar among these strains under secreting conditions (Figure 4.4C). Furthermore, DnaK was present only in the intrabacterial fraction and was not detected in the secreted fraction, verifying proper separation of secreted from intrabacterial pools.

In summary, these experiments demonstrated that the five residues in the Cb region targeted for mutagenesis are not consequential for secretion.

Translocation of alanine-substitution mutants

Having established that the alanine substitutions in YopE had no or little effect on the affinity for SycE and that the expression and secretion of YopE were not altered, we turned to examining translocation. Y. pseudotuberculosis strains expressing either wild type or alanine-substituted YopE were incubated with HeLa cells at a 50:1 multiplicity of infection. Prior to and during infection, HeLa cells were treated with the proteasome inhibitor MG-132 to prevent ubiquitin-mediated YopE degradation (Ruckdeschel et al., 2006). HeLa cells were also treated with the actin polymerization inhibitor cytochalasin D to prevent invasion of HeLa cells and to ensure that actin disruption, a downstream effect of YopE action, was equivalent in all infections (Mejía et al., 2008; Ruckdeschel et al., 2006).

After infection for 150 minutes, HeLa cells were selectively lysed with Triton X-100, leaving bacterial cells intact. We verified previously published evidence that Triton X-100 does not lyse *Y. pseudotuberculosis* (Mejía et al., 2008). We incubated *Y. pseudotuberculosis* in Triton X-100 and examined the soluble (i.e., supernatant) fraction resulting from this incubation by western blot (Figure 2.5A). We also included HeLa cell lysates in some of these incubations, in case components in the HeLa cell lysate promoted lysis of *Y. pseudotuberculosis*. In neither case did we detect lysis of *Y. pseudotuberculosis*, as assayed by the release of YopE (Figure 2.5A). We further verified that Triton X-100 did not lyse *Y. pseudotuberculosis* by examining for the presence of SycE, which is not

translocated (Frithz-Lindsten et al., 1995), in the supernatant and pellet fractions by western blot. SycE was detected only in the pellet (i.e., intrabacterial) fraction and not in the supernatant (i.e., translocated) fraction of a Triton X-100 lysate of infected HeLa cells (data not shown). As expected, YopE was detected in both fractions, confirming the existence of both intrabacterial and translocated pools of YopE (data not shown).

Having verified the experimental format, we then quantified the amount of translocated YopE. To establish the level of background contamination in HeLa cell lysate supernatants of untranslocated YopE, the same experiment was carried out with *Y. pseudotuberculosis* 126 (*ΔyopB*) (Palmer et al., 1998). YopB is required for translocation (Håkansson et al., 1996; Nordfelth and Wolf-Watz, 2001), and most likely contributes to forming a pore in the host cell membrane through which effectors are transported. YopB also promotes translocation via a signaling mechanism in mammalian cells (Mejía et al., 2008). Consistent with prior results, deletion of *yopB* had no effect on the steady-state expression level of YopE or the type III secretion of YopE (Figure 2.3) (Håkansson et al., 1996; Nordfelth and Wolf-Watz, 2001).

Strikingly, a major difference in translocation level between wild-type and alanine-substituted YopE mutants was seen. As compared to wild-type YopE, either encoded natively or on a low copy plasmid, YopE-3Ala and YopE-5Ala were translocated at levels that matched the background contamination level set by the *ΔyopB* strain (Figure 2.5B). The differences between the alanine-

substitution mutants and wild-type YopE were statistically significant (Figure 2.5C, ANOVA *P*-value< 0.01). These differences do not reflect loading errors, as equivalent amounts of total protein were loaded in each lane and equal loading was further verified by quantification of HeLa cell □-tubulin in these western blots (Figure 5B and 5D).

Although the alanine substitutions did not affect stability in *Y. pseudotuberculosis*, it remained possible that the differences observed between levels of translocated wild-type and alanine-substituted YopE were not due to translocation but instead differential stability in HeLa cells. To evaluate this possibility, we transfected HeLa cells with a mammalian expression vector encoding YopE, YopE-3Ala, or YopE-5Ala. We found that the steady-state levels of wild-type and alanine-substituted YopE were similar in HeLa cells (Figures 2.6A and B), indicating that the alanine substitutions did not alter the stability of YopE in HeLa cells.

We conclude from these results that the surface patch defined by Val23, Glu25, and Ser32 has a significant role in translocation. Mutation of these residues to alanine reduced the translocation level of YopE to background values, but did not alter other features of YopE.

DISCUSSION

Despite a wealth of structural and biochemical data on T3S chaperones and their interactions with effectors, the mechanism by which T3S chaperones promote translocation of effectors remains elusive. A growing body of evidence supports the notion that the specific structure of the effector Cb region when bound to the chaperone acts as a three-dimensional translocation signal. The surface of the highly extended Cb region in combination with the adjoining chaperone surface is envisaged to constitute a binding site for a T3S component required for translocation, i.e., a receptor. The identity of this putative receptor is currently unknown. Although *E. coli* and *Salmonella* T3S ATPases have been shown to bind chaperone-effector complexes, these events have not been shown to be dependent on the chaperone (Akeda and Galán, 2005; Gauthier and Finlay, 2003). Indeed, the *E. coli* effector Tir binds the T3S ATPase EscN in the absence of a chaperone (Gauthier and Finlay, 2003). In addition, SycE-YopE has not been detected to bind the *Yersinia* T3S ATPase YscN (Rodgers et al., 2008). Thus, the T3S ATPase is unlikely to be the chaperone-dependent receptor that explains the necessity for the chaperone in translocation.

Here, we tested a prediction of the translocation signal model. We reasoned that if binding of SycE-YopE to a receptor were required for translocation, then disruption of the potential receptor-binding site should disrupt translocation of YopE but should leave other properties of YopE unaltered. We

targeted residues that are solvent-exposed in the chaperone-bound conformation of the YopE Cb region, and constructed two alanine-substitution mutants:YopE-3Ala(V23A/E25A/S32A) and YopE-5Ala(V23A/E25A/S27A/-R29A/S32A). We found that the triple alanine substitution of YopE had no effect on the affinity for SycE, and that the quintuple alanine substitution had only a small effect. Further, these substitutions did not alter the steady-state expression level in *Y. pseudotuberculosis*, the efficiency of secretion by *Y. pseudotuberculosis*, or stability in HeLa cells. They did however have a large effect on translocation. The level of translocation for these substitution mutants was equivalent to that found for *Y. pseudotuberculosis* YP126 (*ΔyopB*), a strain that secretes but does not translocate effectors.

We chose a biochemical assay for translocation in lieu of mammalian cell reporter fusion assays (Anderson and Schneewind, 1997; Charpentier and Oswald, 2004; Jacobi et al., 1998; Jaumouillé et al., 2008; Rüssmann et al., 2002; Sory et al., 1995). This was due to concerns regarding potential artifacts of fusion partners. An example of such an artifact comes from studies of the fusion of dihydrofolate reductase (DHFR) to YopE. While biophysical evidence indicates that SycE does not promote unfolding of YopE but rather the opposite in bringing about structuring of YopE (Rodgers et al., 2008), the opposite seems to be true for YopE-DHFR fusions (Feldman et al., 2002). In addition, the biochemical assay provides a direct means for evaluating levels of translocated YopE.

One potential issue with the biochemical assay is possible contamination of fractions of translocated YopE with extrabacterial but non-translocated YopE (e.g., from lysis of bacterial cells). The biochemical assay depends on the selective lysis of mammalian cells using Triton X-100 (32). The selectivity of this detergent was confirmed in our experiments. Following published precedents, we used a *ΔyopB* strain to control for other sources of YopE contamination in the translocated fraction. While the level of translocated YopE (i.e., found in the supernatant of the Triton X-100 lysate) was always much higher for the wild-type strain as compared to the □*yopB* strain, a small amount of YopE was consistently found in the translocated fraction of infections carried out with the *ΔyopB* strain, as has been seen previously (Aili et al., 2006). Further experiments showed that the small amount of YopE observed for the *ΔyopB* strain was T3S-dependent. This was surmised from the fact that no YopE was detected in the translocated fraction from an infection with *Y. pseudotuberculosis* 71 (Bölin and Wolf-Watz, 1984), a strain containing a random transposon insertion that renders the T3S system inactive (Figure 2.7). It is possible that in the absence of YopB a small amount of YopE may leak into the extracellular media due to the lack of a tight junction between the T3S needle and the host cell membrane. Of note, this small amount of YopE was resistant to papain, which was added to remove extracellular YopE prior to lysis of HeLa cells. The papain resistance of this fraction of YopE contrasts with the papain sensitivity of soluble YopE, and may be due to insertion

of some small amount of YopE into the host cell membrane. Membrane insertion of YopE has been observed (Krall et al., 2004).

Most striking in our findings was the low translocation levels for YopE-3Ala and YopE-5Ala as compared to wild-type YopE. Having found no differences between these alanine-substitutions and wild-type YopE in processes that precede translocation (i.e., expression and SycE binding), we asked whether there was a difference in the behavior of the proteins following translocation, namely, in the stability of these proteins in HeLa cells. *Y. enterocolitica* YopE is degraded by the ubiquitin-proteasome pathway, with Lys75 being the site of ubiquitination (Ruckdeschel et al., 2006). While *Y. pseudotuberculosis* YopE has Gln instead of Lys at position 75, we nevertheless utilized the proteasome inhibitor MG-132 during the infection process. Furthermore, we transfected and expressed wild-type YopE and the alanine-substitutions in HeLa cells, and saw no differences in the levels of these proteins.

These results altogether indicate that the site defined by Val23, Glu25, and Ser32 is crucial for translocation. The location of this site at the N-terminus of the Cb region is consistent with recent results showing that the C-terminal portion of the YopE Cb region, residues 54-75, is not required for translocation (Isaksson et al., 2009). Instead, this C-terminal portion of the Cb region has been identified to promote localization of YopE to host cell membranes (Krall et al., 2004). Thus the chaperone may serve two purposes: It may template the formation of a specific structure in the N-terminal portion of the Cb region that is required for

translocation and it may also maintain the solubility in the bacterial cytosol of a C-terminal portion of the Cb region that is lipophilic (Krall et al., 2004; Letzelter et al., 2006).

We chose residues 23, 25, 27, 29, and 32 due to the structural and chemical similarities between chaperone-bound YopE and *Salmonella* SptP Cb regions. These were the first two effector Cb regions to be visualized in their chaperone-bound conformations (Birtalan et al., 2002; Stebbins and Galán, 2001). Succeeding work on other chaperone-bound Cb regions has shown a less tight correspondence of residues at these positions, suggesting the existence of interactions that differ in detail among effectors. While we favor the possibility that these residues constitute part of a receptor-binding site in the chaperone-effector complex, other possibilities cannot be excluded. Among these is the possibility that these residues are important in steps following dissociation of the chaperone, for example, in transiting from the T3S needle to the host cell membrane-inserted translocon. In either case, our work identifies a crucial set of functional residues in the Cb region and provides guidance for the direction of future mechanistic investigation.

FIGURES AND TABLES

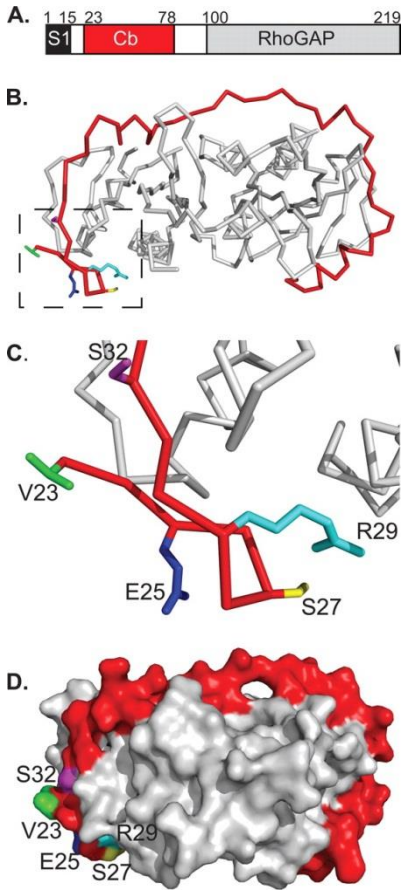

Figure 2.1 The SycE-YopE chaperone-effector complex.
A. Schematic of YopE domains. S1, signal 1; Cb, chaperone-binding region; RhoGAP, Rho GTPase activating protein domain. Residue numbers for domain boundaries are indicated.
B. Structure of the SycE-YopE(Cb) complex. The Cb region of YopE (red) and the SycE dimer (gray) are shown in Cα stick representation. Side chains that were mutated in the YopE Cb region are depicted: V23 (green), E25 (blue), S27 (yellow), R29 (cyan) and S32 (magenta). Molecular figures were made with PyMol (http://pymol.sourceforge.net).
C. Enlarged view of boxed region in panel B.
D. Molecular surface representation of the SycE-YopE(Cb) complex. The YopE(Cb) surface is in red, except for surfaces formed by V23 (green), E25 (blue), S27 (yellow), R29 (cyan) and S32 (magenta). The SycE homodimer is in gray.

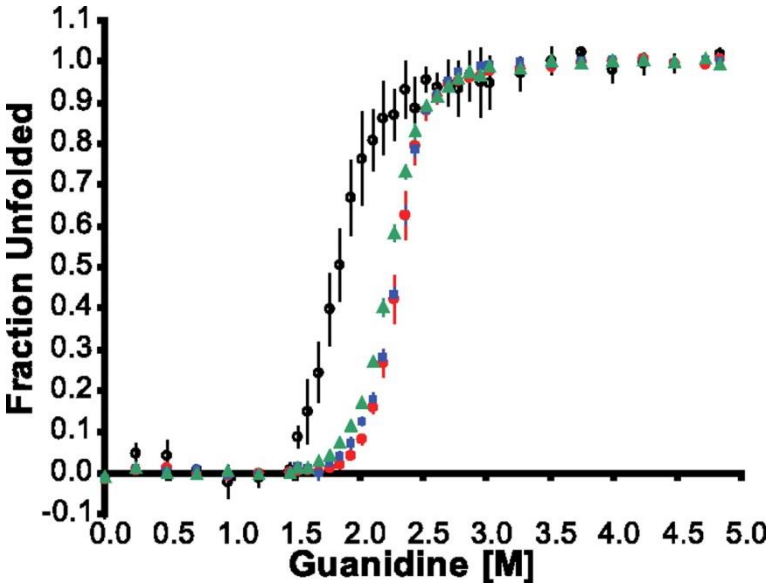

Figure 2.2 Affinity of the YopE Cb region for SycE.
Dependence of the fraction of unfolded protein on guanidine concentration, as determined by the circular dichroism signal at 222 nm. Wild-type SycEΔ122-YopE(Cb), red circles; SycE Δ122-YopE(Cb-3Ala), blue squares; SycE Δ122-YopE(Cb-5Ala), green triangles; and SycE-his, empty circles. Data were averaged from at least three independent experiments, and bars represent standard errors of the mean.

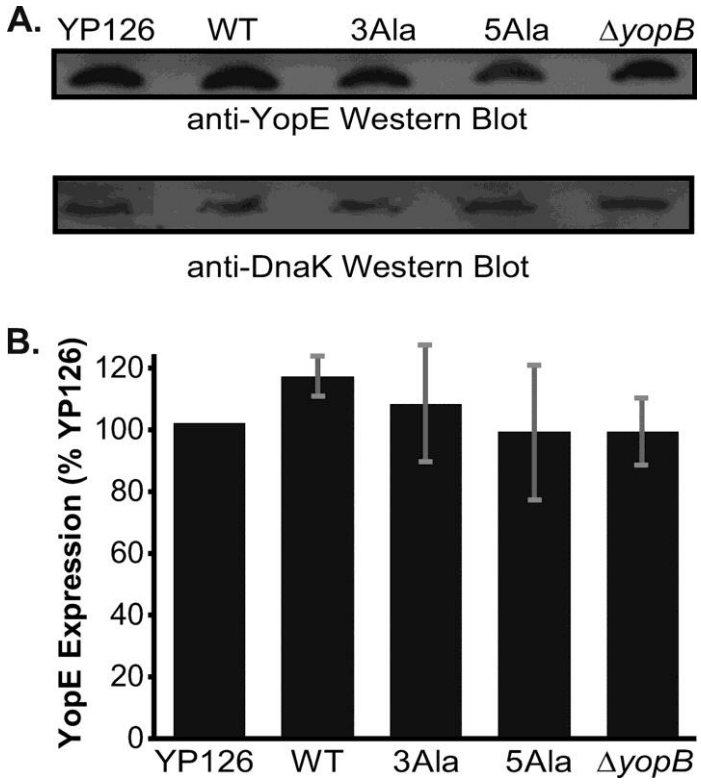

Figure 2.3 Expression of YopE in *Y. pseudotuberculosis*.
A. Western blot of steady-state expression level of YopE in *Y. pseudotuberculosis* grown at 37 °C under non-secreting conditions (top). YopE was detected with anti-YopE polyclonal antibodies. The number of cells analyzed was normalized, and as a loading control, DnaK was detected on the same blot with a monoclonal anti-DnaK antibody (bottom). YP126 is wild-type YopE expressed from its native locus on the pIB plasmid by *Y. pseudotuberculosis*126 (YP126). WT, 3Ala, and 5Ala are wild-type YopE, YopE-3Ala, and YopE-5Ala, respectively, expressed from a low-copy plasmid by *Y. pseudotuberculosis* 126 (*ΔyopE*). The last sample, *ΔyopB,* is wild-type YopE expressed from its native locus on the pIB plasmid by *Y. pseudotuberculosis* 126 (*ΔyopB*).
B. Quantification of YopE expression levels under nonsecreting conditions, assessed by Western blotting. Mean values from four independent experiments carried out in triplicate are depicted. These values were normalized to the expression level of YP126 and are expressed as percentages of the YP126 value. Gray bars represent standard errors of the means.

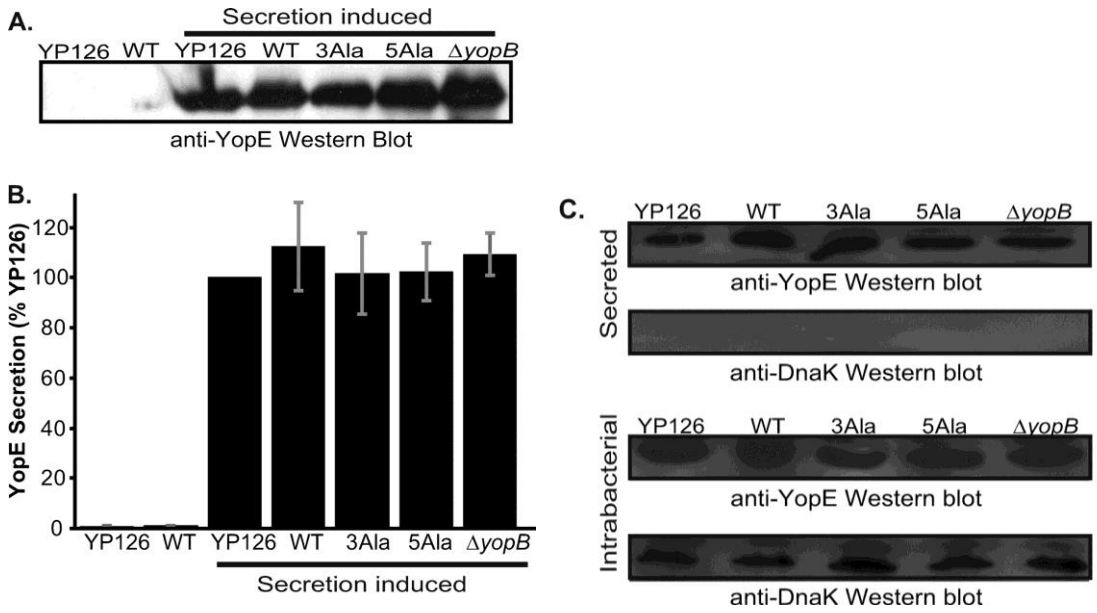

Figure 2.4 Secretion of YopE.

A. Western blot of wild-type YopE secreted by *Y. pseudotuberculosis*126 (YP126); wild-type YopE (WT), YopE-3Ala (3Ala), and YopE-5Ala (5Ala) secreted by *Y. pseudotuberculosis* 126 (*ΔyopE*); and wild-type YopE secreted by *Y. pseudotuberculosis* 126 (*ΔyopB*). Type III secretion was inhibited for the samples in the two left lanes by growth at 37 °C in 2.5 mM $CaCl_2$, while type III secretion was induced in the remaining samples by addition of 10 mM EGTA at 37 °C. Supernatants from *Y. pseudotuberculosis* cultures were separated by SDS-PAGE and probed with anti-YopE polyclonal antibodies.

B. Quantification of YopE secretion as assessed by western blot. Mean values from three independent experiments carried out in triplicate are depicted. These values are normalized to the secretion level of YP126 in T3S-inducing conditions and expressed as a percentage of YP126. Gray bars report standard errors of the mean.

C. Western blot of supernatants (top two blots) and cell pellets (bottom two blots) from *Y. pseudotuberculosis* strains induced to secrete due to a shift to low Ca^{2+} concentration and growth at 37 °C. Bacterial cultures were centrifuged to separate supernatant from pellet fractions. The first panel in each set shows YopE as detected by anti-YopE polyclonal antibodies, and the bottom panel in each set shows DnaK as detected on the same membrane by an anti-DnaK monoclonal antibody.

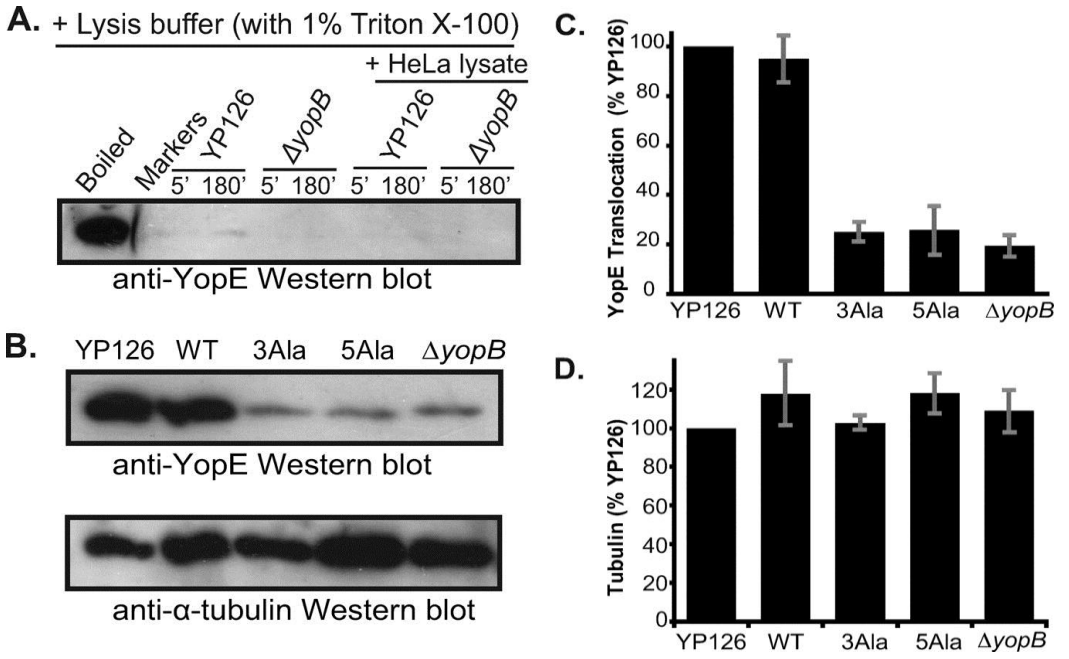

Figure 2.5 Translocation of YopE.
A. Western blot of YopE (top) in the supernatant fractions of *Y. pseudotuberculosis* YP126 or *Y. pseudotuberculosis* (*ΔyopB*) incubated for 5 or 180 minutes in HeLa cell lysis buffer (containing 1% Triton X-100), in the absence or presence of a HeLa cell lysate. As a positive control for YopE, YP126 was incubated in PBS and lysed by boiling in SDS-PAGE sample buffer ('Boiled').
B. Top, western blot of wild-type YopE translocated into HeLa cells by *Y. pseudotuberculosis*126 (YP126); wild-type YopE (WT), YopE-3Ala (3Ala), and YopE-5Ala (5Ala) translocated by *Y. pseudotuberculosis* 126 (*ΔyopE*); and wild-type YopE translocated by *Y. pseudotuberculosis* 126 (*ΔyopB*). Translocated fractions were separated by SDS-PAGE and probed with anti-YopE polyclonal antibodies. Bottom, the blot at the top was stripped and re-probed with anti-α-tubulin monoclonal antibodies.
C. Quantification of YopE translocation as assessed by western blot. Mean values from three independent experiments carried out in triplicate are depicted. These values are normalized to the translocation level of YP126 and expressed as a percentage of YP126. Gray bars report standard errors of the mean.
D. Quantification of α-tubulin in translocation samples as assessed by western blot. Mean values from three independent experiments carried out in triplicate are depicted. These values were normalized to the level of tubulin in the YP126 sample and expressed as a percentage of YP126. Gray bars report standard errors of the mean.

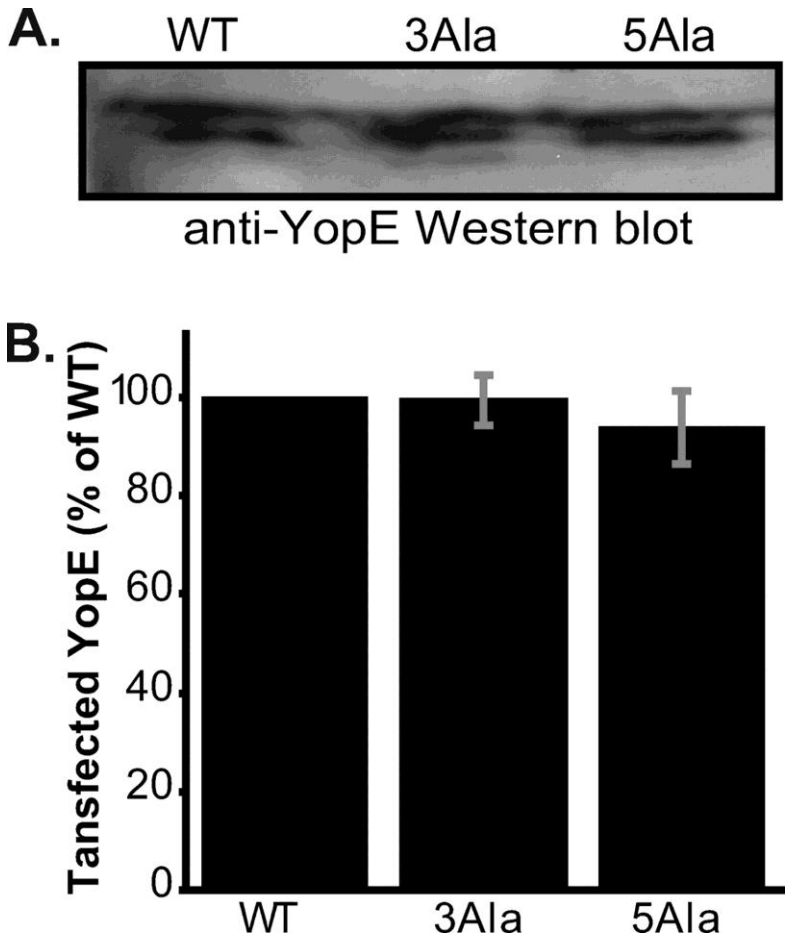

Figure 2.6 Transfection of YopE.
A. Western blot of HeLa cells expressing transfected wild-type YopE (WT), YopE-3Ala (3Ala), and YopE-5Ala (5Ala).
B. Quantification of YopE expressed in HeLa cells. Mean values from three independent experiments are reported. These values are normalized to the expression level of WT and expressed as a percentage of WT. Gray bars report standard error of the mean.

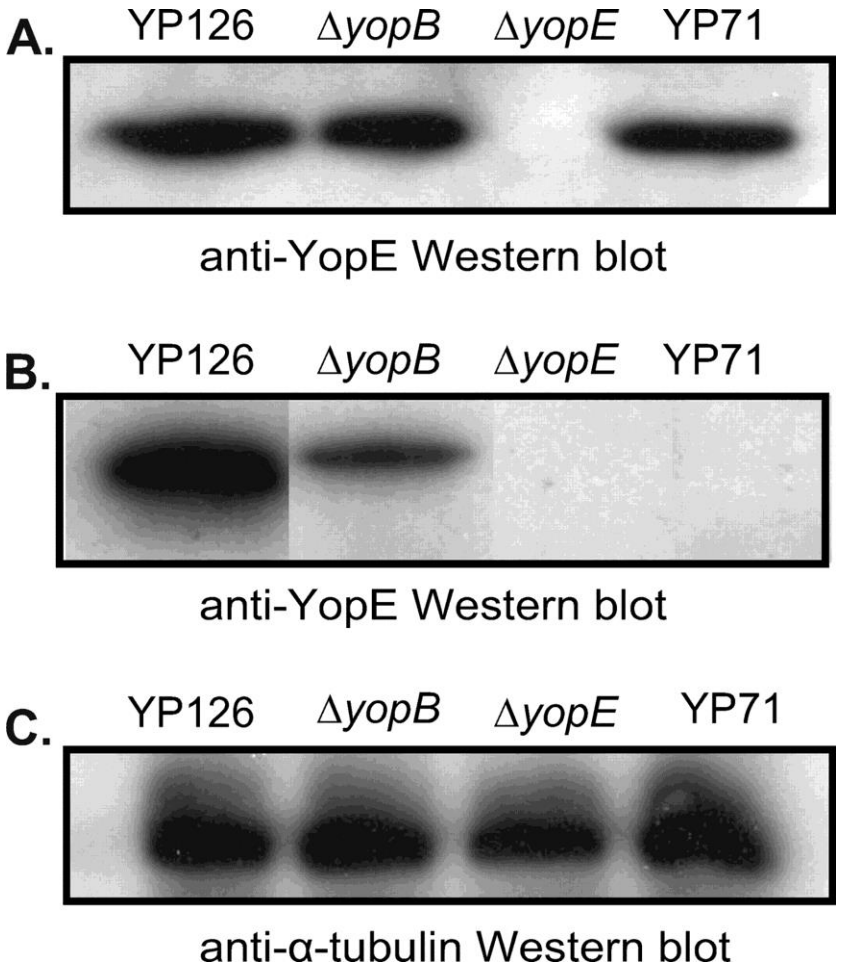

Figure 2.7 Expression and Translocation of YopE by YP71.
A. Western blot of YopE expressed by *Y. pseudotuberculosis* YP126, *Y. pseudotuberculosis* YP126 (*ΔyopB*), *Y. pseudotuberculosis* YP126 (*ΔyopE*), and *Y. pseudotuberculosis* YP71.
B. Western blot of YopE translocated by same strains as in panel A. Translocated fractions were separated by SDS-PAGE and probed with anti-YopE polyclonal antibodies. Samples are from the same blot, but lanes have been rearranged for the sake of consistency.
C. Western blot of samples from panel B probed with anti-α-tubulin monoclonal antibodies.

ACKNOWLEDGEMENTS

This works was supported by NIH grant T32 GM007240 (LR), the Universitywide AIDS Research Program (LR), and NIH grant R01 AI061452 (PG).

The abbreviations used are: T3S, type III secretion; Cb, chaperone-binding.

The text of this chapter, in full, is a reprint of the material as it appears in the *Journal of Baceteriology*. The dissertation author was the co-author and along with the primary author and other co-authors (L. Rodgers, S. Birtalan, D. Friedberg, and P.Ghosh) listed in this publication contributed to or supervised the research which forms the basis of this chapter.

REFERENCES

Aili, M., Isaksson, E.L., Hallberg, B., Wolf-Watz, H., and Rosqvist, R. (2006). Functional analysis of the YopE GTPase-activating protein (GAP) activity of Yersinia pseudotuberculosis. Cell. Microbiol. *8*, 1020–1033.

Akeda, Y., and Galán, J.E. (2005). Chaperone release and unfolding of substrates in type III secretion. Nature *437*, 911–915.

Anderson, D.M., and Schneewind, O. (1997). A mRNA signal for the type III secretion of Yop proteins by Yersinia enterocolitica. Science *278*, 1140–1143.

Birtalan, S., and Ghosh, P. (2001). Structure of the Yersinia type III secretory system chaperone SycE. Nat. Struct. Biol. *8*, 974–978.

Birtalan, S.C., Phillips, R.M., and Ghosh, P. (2002). Three-dimensional secretion signals in chaperone-effector complexes of bacterial pathogens. Mol. Cell *9*, 971–980.

Bölin, I., and Wolf-Watz, H. (1984). Molecular cloning of the temperature-inducible outer membrane protein 1 of Yersinia pseudotuberculosis. Infect. Immun. *43*, 72–78.

Boyd, A.P., Lambermont, I., and Cornelis, G.R. (2000). Competition between the Yops of Yersinia enterocolitica for delivery into eukaryotic cells: role of the SycE chaperone binding domain of YopE. J. Bacteriol. *182*, 4811–4821.

Brosius, J., and Holy, A. (1984). Regulation of ribosomal RNA promoters with a synthetic lac operator. Proc. Natl. Acad. Sci. U. S. A. *81*, 6929–6933.

Büttner, C.R., Cornelis, G.R., Heinz, D.W., and Niemann, H.H. (2005). Crystal structure of Yersinia enterocolitica type III secretion chaperone SycT. Protein Sci. Publ. Protein Soc. *14*, 1993–2002.

Charpentier, X., and Oswald, E. (2004). Identification of the secretion and translocation domain of the enteropathogenic and enterohemorrhagic Escherichia coli effector Cif, using TEM-1 beta-lactamase as a new fluorescence-based reporter. J. Bacteriol. *186*, 5486–5495.

Cheng, L.W., and Schneewind, O. (1999). Yersinia enterocolitica type III secretion. On the role of SycE in targeting YopE into HeLa cells. J. Biol. Chem. *274*, 22102–22108.

Cheng, L.W., Anderson, D.M., and Schneewind, O. (1997). Two independent type III secretion mechanisms for YopE in Yersinia enterocolitica. Mol. Microbiol. *24*, 757–765.

Cornelis, G.R. (2006). The type III secretion injectisome. Nat. Rev. Microbiol. *4*, 811–825.

Van Eerde, A., Hamiaux, C., Pérez, J., Parsot, C., and Dijkstra, B.W. (2004). Structure of Spa15, a type III secretion chaperone from Shigella flexneri with broad specificity. EMBO Rep. *5*, 477–483.

Feldman, M.F., Müller, S., Wüest, E., and Cornelis, G.R. (2002). SycE allows secretion of YopE-DHFR hybrids by the Yersinia enterocolitica type III Ysc system. Mol. Microbiol. *46*, 1183–1197.

Ferreiro, D.U., Cervantes, C.F., Truhlar, S.M.E., Cho, S.S., Wolynes, P.G., and Komives, E.A. (2007). Stabilizing IkappaBalpha by "consensus" design. J. Mol. Biol. *365*, 1201–1216.

Frithz-Lindsten, E., Rosqvist, R., Johansson, L., and Forsberg, A. (1995). The chaperone-like protein YerA of Yersinia pseudotuberculosis stabilizes YopE in the cytoplasm but is dispensible for targeting to the secretion loci. Mol. Microbiol. *16*, 635–647.

Gauthier, A., and Finlay, B.B. (2003). Translocated intimin receptor and its chaperone interact with ATPase of the type III secretion apparatus of enteropathogenic Escherichia coli. J. Bacteriol. *185*, 6747–6755.

Ghosh, P. (2004). Process of protein transport by the type III secretion system. Microbiol. Mol. Biol. Rev. MMBR *68*, 771–795.

Håkansson, S., Schesser, K., Persson, C., Galyov, E.E., Rosqvist, R., Homblé, F., and Wolf-Watz, H. (1996). The YopB protein of Yersinia pseudotuberculosis is essential for the translocation of Yop effector proteins across the target cell plasma membrane and displays a contact-dependent membrane disrupting activity. EMBO J. *15*, 5812–5823.

Hu, X., Lee, M.S., and Wallqvist, A. (2009). Interaction of the disordered Yersinia effector protein YopE with its cognate chaperone SycE. Biochemistry (Mosc.) *48*, 11158–11160.

Isaksson, E.L., Aili, M., Fahlgren, A., Carlsson, S.E., Rosqvist, R., and Wolf-Watz, H. (2009). The membrane localization domain is required for intracellular

localization and autoregulation of YopE in Yersinia pseudotuberculosis. Infect. Immun. *77*, 4740–4749.

Jacobi, C.A., Roggenkamp, A., Rakin, A., Zumbihl, R., Leitritz, L., and Heesemann, J. (1998). In vitro and in vivo expression studies of yopE from Yersinia enterocolitica using the gfp reporter gene. Mol. Microbiol. *30*, 865–882.

Jaumouillé, V., Francetic, O., Sansonetti, P.J., and Tran Van Nhieu, G. (2008). Cytoplasmic targeting of IpaC to the bacterial pole directs polar type III secretion in Shigella. EMBO J. *27*, 447–457.

Krall, R., Zhang, Y., and Barbieri, J.T. (2004). Intracellular membrane localization of pseudomonas ExoS and Yersinia YopE in mammalian cells. J. Biol. Chem. *279*, 2747–2753.

Lilic, M., Vujanac, M., and Stebbins, C.E. (2006). A common structural motif in the binding of virulence factors to bacterial secretion chaperones. Mol. Cell *21*, 653–664.

Locher, M., Lehnert, B., Krauss, K., Heesemann, J., Groll, M., and Wilharm, G. (2005). Crystal structure of the Yersinia enterocolitica type III secretion chaperone SycT. J. Biol. Chem. *280*, 31149–31155.

Luo, Y., Bertero, M.G., Frey, E.A., Pfuetzner, R.A., Wenk, M.R., Creagh, L., Marcus, S.L., Lim, D., Sicheri, F., Kay, C., Haynes ,C., Finlay, BB., Strynadka, NC. (2001). Structural and biochemical characterization of the type III secretion chaperones CesT and SigE. Nat. Struct. Biol. *8*, 1031–1036.

Mejía, E., Bliska, J.B., and Viboud, G.I. (2008). Yersinia controls type III effector delivery into host cells by modulating Rho activity. PLoS Pathog. *4*, e3.

Nordfelth, R., and Wolf-Watz, H. (2001). YopB of Yersinia enterocolitica is essential for YopE translocation. Infect. Immun. *69*, 3516–3518.

Palmer, L.E., Hobbie, S., Galán, J.E., and Bliska, J.B. (1998). YopJ of Yersinia pseudotuberculosis is required for the inhibition of macrophage TNF-α production and downregulation of the MAP kinases p38 and JNK. Mol. Microbiol. *27*, 953–965.

Phan, J., Tropea, J.E., and 2004, D.S.W. Structure of the Yersinia pestis type III secretion chaperone SycH in complex with a stable fragment of YscM2. Acta Crystallogr D *60*, 1591–1599.

Quenee, L.E., and Schneewind, O. (2007). Ubiquitin-Yop hybrids as probes for post-translational transport by the Yersinia type III secretion pathway. Mol. Microbiol. *65*, 386–400.

Rodgers, L., Gamez, A., Riek, R., and Ghosh, P. (2008). The type III secretion chaperone SycE promotes a localized disorder-to-order transition in the natively unfolded effector YopE. J. Biol. Chem. *283*, 20857–20863.

Ruckdeschel, K., Pfaffinger, G., Trulzsch, K., Zenner, G., Richter, K., mann, J.H.-, and Aepfelbacher, M. (2006). The proteasome pathway destabilizes Yersinia outer protein E and represses its antihost cell activities. J Immunol.

Rüssmann, H., Kubori, T., Sauer, J., and Galán, J.E. (2002). Molecular and functional analysis of the type III secretion signal of the Salmonella enterica InvJ protein. Mol. Microbiol. *46*, 769–779.

Schesser, K., Frithz-Lindsten, E., and Wolf-Watz, H. (1996). Delineation and mutational analysis of the Yersinia pseudotuberculosis YopE domains which mediate translocation across bacterial and eukaryotic cellular membranes. J. Bacteriol. *178*, 7227–7233.

Schubot, F.D., Jackson, M.W., Penrose, K.J., Cherry, S., Tropea, J.E., Plano, G.V., and Waugh, D.S. (2005). Three-dimensional structure of a macromolecular assembly that regulates type III secretion in Yersinia pestis. J. Mol. Biol. *346*, 1147–1161.

Singer, A.U., Desveaux, D., Betts, L., Chang, J.H., Nimchuk, Z., Grant, S.R., Dangl, J.L., and Sondek, J. (2004). Crystal structures of the type III effector protein AvrPphF and its chaperone reveal residues required for plant pathogenesis. Struct. Lond. Engl. 1993 *12*, 1669–1681.

Sory, M.P., Boland, A., Lambermont, I., and Cornelis, G.R. (1995). Identification of the YopE and YopH domains required for secretion and internalization into the cytosol of macrophages, using the cyaA gene fusion approach. Proc. Natl. Acad. Sci. U. S. A. *92*, 11998–12002.

Stebbins, C.E., and Galán, J.E. (2001). Maintenance of an unfolded polypeptide by a cognate chaperone in bacterial type III secretion. Nature *414*, 77–81.

Wattiau, P., and Cornelis, G.R. (1993). SycE, a chaperone-like protein of Yersinia enterocolitica involved in Ohe secretion of YopE. Mol. Microbiol. *8*, 123–131.

Woestyn, S., Sory, M.P., Boland, A., Lequenne, O., and Cornelis, G.R. (1996). The cytosolic SycE and SycH chaperones of Yersinia protect the region of YopE

and YopH involved in translocation across eukaryotic cell membranes. Mol. Microbiol. *20*, 1261–1271.

Wulff-Strobel, C.R., Williams, A.W., and Straley, S.C. (2002). LcrQ and SycH function together at the Ysc type III secretion system in Yersinia pestis to impose a hierarchy of secretion. Mol. Microbiol. *43*, 411–423.

Chapter 3:

The structure and interactions of the cytoplasmic domain of the *Yersinia* type III secretion protein YscD

In this chapter, I performed secretion assays to test for the effect on secretion by YscD and the L3/L4 mutants of YscD as detected by SDS-PAGE of culture supernatants. I further used western blots to test for intrabacterial expression of YscD. I also performed circular dichroism on purified YscD, L3, and L4 mutants. My contributions are represented by Figures. 3.3 and 3.5.

ABSTRACT

The virulence of a large number of Gram-negative bacterial pathogens depends on the type III secretion (T3S) system, which transports select bacterial proteins into host cells. An essential component of the *Yersinia* T3S system is YscD, a single-pass inner membrane protein. We report here the 2.52 Å resolution structure of the cytoplasmic domain of YscD, called YscDc. The structure confirms that YscDc consists of a forkhead-associated (FHA) fold, which in many but not all cases specifies binding to phosphothreonine. YscDc, however, lacks the structural properties associated with phosphothreonine-binding, and thus most likely interacts with partners in a phosphorylation-independent manner. Structural comparison highlighted two loop regions, L3 and L4, as potential sites of interactions. Alanine substitutions of L3 and L4 had no deleterious effects on protein structure or stability, but abrogated T3S in a dominant-negative manner. To gain insight into the function of L3 and L4, we identified proteins associated with YscD by affinity purification coupled to mass spectrometry. The lipoprotein YscJ was found associated with wild-type YscD, as was the effector YopH. Notably, the L3 and L4 substitution mutants interacted with more YopH than did wild-type YscD. These substitution mutants also interacted with SycH (the specific chaperone for YopH), the putative C-ring component YscQ, and the ruler component YscP, whereas wild-type YscD did not. These results suggest that substitutions in the L3 and L4 loops of YscD disrupted the dissociation of SycH

from YopH, leading to the accumulation of a large protein complex that stalled the T3S apparatus.

INTRODUCTION

The virulence of a wide variety of Gram-negative bacterial pathogens requires the transport of select proteins from the bacterial cytosol into host cells by the type III secretion (T3S) system (Cornelis, 2006; Ghosh, 2004). Such transported proteins have diverse and usually deleterious functions within host cells. Transport by the T3S system requires the action of ~20-25 proteins that assemble to form the injectisome, a macromolecular apparatus that spans the inner and outer membranes of the bacterial envelope and terminates with an extracellular appendage resembling a needle (Hodgkinson et al., 2009; Kimbrough and Miller, 2000; Schraidt and Marlovits, 2011). In the *Yersinia* T3S system, the inner membrane protein YscD (47 kDa) constitutes an essential component of the injectisome (Michiels et al., 1991; Plano and Straley, 1995).

YscD is composed of an N-terminal cytoplasmic domain, a single-pass membrane-spanning region, and a C-terminal periplasmic domain. The periplasmic domain of YscD interacts with the periplasmic domains of the outer membrane secretin YscC and the inner membrane lipoprotein YscJ (Ross and Plano, 2011). The complex composed of YscC, YscD, and YscJ appears to scaffold assembly of the *Yersinia* injectisome (Diepold et al., 2010; Koster et al., 1997). The stoichiometry of YscD in this complex is unknown, but equivalent complexes in *Salmonella* and *Shigella* suggest a ring-like assembly of 24 copies of YscD (Hodgkinson et al., 2009; Schraidt and Marlovits, 2011). The N-terminal

cytoplasmic domain of YscD (residues 1-121, ~13 kDa), called here YscDc, is predicted to have a forkhead-associated (FHA) fold and has been shown to be essential for T3S (Pallen et al., 2002; Ross and Plano, 2011). FHA domains are found in a large number of eukaryotic and prokaryotic proteins (Hofmann and Bucher, 1995), and while most FHA domains specify binding to phosphothreonine residues (Mahajan et al., 2008), a number have been identified to confer phosphorylation-independent interaction (Nott et al., 2009; Tong et al., 2010).

To provide guidance in understanding the role of YscD in T3S, we expressed, purified, and determined the X-ray crystal structure of YscDc. YscDc was found to be monomeric and not prone to oligomerization, and its structure confirmed the predicted FHA fold (Pallen et al., 2003), as has also been demonstrated recently by others (Lountos et al., 2012). Comparison with other FHA domain proteins, including MxiG, a YscD ortholog from *Shigella flexneri*, whose cytoplasmic domain was recently shown to have an FHA fold by nuclear magnetic resonance (NMR) and X-ray crystallographic techniques (Barison et al., 2012; McDowell et al., 2011), highlighted two loop regions as being potentially significant for function. Alanine substitutions at these two loops, L3 and L4, had no deleterious effects on protein structure or stability, but abrogated T3S in a dominant-negative manner. Proteins associated with YscD were identified by affinity purification coupled to liquid chromatography and mass spectrometry. Wild-type YscD was found to associate with YscJ (Michiels et al., 1991; Silva-

Herzog et al., 2008) and the effector YopH (Rosqvist et al., 1988). Notably, the L3 and L4 substitution mutants of YscD interacted with more YopH than did wild-type YscD. In addition, the specific chaperone of YopH, SycH (Woestyn et al., 1996), was found associated with the substitution mutants but not wild-type YscD, as were the ruler component YscP (Journet et al., 2003) and the putative C-ring component YscQ (Bzymek et al., 2012; Fields et al., 1994). These results indicate that the L3 and L4 loops are functionally essential. They also suggest that substitutions of these loops disrupted the dissociation of SycH from YopH, leading to the accumulation of a large protein complex that stalled the T3S system.

MATERIALS AND METHODS

Cloning and expression

The coding sequence of *yscD* was amplified by PCR from the pYV plasmid of *Y. pseudotuberculosis* 126 (Bölin et al., 1982). A PCR fragment encoding intact YscD was cloned into the pBAD expression vector (Invitrogen) to yield pBAD-yscD; this construct also included an N-terminal His-tag. A second PCR product encoding YscDc (residues 1-121) was cloned into the pET28b expression vector (Novagen), yielding pET28b-YscDc. This construct included an N-terminal His-tag followed by a PreScission protease cleavage site. Mutants of YscD were constructed by strand overlap extension PCR (Higuchi et al., 1988). The integrity of all constructs was verified by DNA sequencing.

Purification of YscDc

YscDc was expressed from pET28b-YscDc in *Escherichia coli* BL21 (DE3). Bacteria were grown at 37 ºC in lysogeny broth (LB) media supplemented with 50 mg/L kanamycin to an OD_{600} of 0.5, at which point expression was induced with 0.5 mM isopropyl β-D-1-thiogalactopyranoside. Bacteria were then grown for 16 h at 20 ºC, after which point they were harvested by centrifugation (5,800 x *g*, 10 min, 4º C). The bacterial pellet was resuspended in 1/100th volume of the original bacterial culture in buffer A (500 mM NaCl, 50 mM sodium phosphate buffer, pH 8.0, 10 mM β-mercaptoethanol (βME)) supplemented with

ethylene diamine tetraacetic acid (EDTA)-free protease cocktail inhibitor (one tablet per 2 L of original bacterial culture, Roche) and 20 μg/mL DNase (Sigma). Resuspended bacteria were lysed using an Emulsiflex-C5 (Avestin) homogenizer with three passes at 15,000 psi, and the lysate was clarified by centrifugation (14,000 x *g*, 10 min, 4 ºC). The supernatant was applied to a Ni^{2+}-nitrilotriacetic acid (NTA) agarose column (Sigma), the column was washed with 25 column volumes of buffer A containing 7 mM imidazole, and bound protein eluted from the column with three column volumes of buffer A containing 500 mM imidazole. The eluted fractions were concentrated by ultrafiltration using a YM-3 Centricon (Amicon), and further purified by size-exclusion chromatography (16/60 Superdex 200, GE Healthcare) in buffer B (50 mM NaCl, 10 mM HEPES, pH 7.5, and 10 mM βME). Purified YscDc was cleaved with a 50:1 YscDc:PreScission protease mass ratio in buffer B to remove the His-tag, and the cleaved sample was re-applied to a Ni^{2+}-NTA agarose column in buffer B. PreScission protease carried a His-tag and was thus bound to the Ni^{2+}-NTA column. Cleaved YscDc was isolated from the flow-through of the column, and concentrated by ultrafiltration using a YM-3 Centricon to 7.5 mg/mL; the concentration of YscDc was determined using a calculated ε_{280} of 12,490 $M^{-1}cm^{-1}$. In certain cases, the order of steps was varied, such that the size-exclusion chromatography step was carried out as the final step, following elution from the Ni^{2+}- NTA agarose column, cleavage with PreScission protease, re-application to the Ni^{2+}- NTA agarose column, and isolation of the flow-through from this column. No

difference in purity was observed by this alteration in the order of steps. Selenomethionine (SeMet) was incorporated into YscDc as described previously (Van Duyne et al., 1993), and SeMet-labeled YscDc was purified as above.

Crystallization, data collection, and structure determination

Crystals of unlabeled and SeMet-labeled YscDc were grown by the sitting-drop, vapor diffusion method at 20 ºC by mixing 0.2 μL of 7.5 mg/mL YscDc in buffer B with 0.3 μL of 3.5 M NaHCOO. The drop was dispensed by an Oryx8 crystallization robot into a CrystalClearDuo crystallization plate (Hampton), which contained 80 μL of 3.5 M NaHCOO in the well. Crystals were cryoprotected in 15% glycerol and 3.5 M NaHCOO, mounted in 50 μm loops (Hampton), and flash cooled in liquid N_2. Native diffraction data were collected from YscDc crystals and single wavelength anomalous dispersion (SAD) diffraction data from SeMet-labeled YscDc crystals at beamline 23 ID-B (Advanced Photon Source, Argonne National Laboratory) (Table 3.1).

Data from native and Se-Met crystals were indexed and scaled using HKL2000 (Otwinowski and Minor). Two molecules of YscDc were located in the asymmetric unit. Four SeMet sites (Met1 and Met50 from each chain) were located using the hybrid substructure search (HYSS) in the program Autosol of the Phenix suite, and phases were calculated and refined using Phenix (Adams et al., 2010). Automated model building was carried out using Phenix Autobuild, which produced a chain trace of residues 1-105. The model was then refined using

the native data set. A random 5% of reflections were omitted from the refinement for calculation of R_{free}. The model was adjusted manually based on inspection in COOT of σ_A-weighted 2mFo-DFc and mFo-DFc maps prior to subsequent cycles of refinement (Emsley and Cowtan, 2004). Each refinement cycle consisted of three rounds of bulk-solvent correction, anisotropic scaling, and refinement of atomic model parameters; default parameters with tight NCS restraints set at 0.2 were used. Waters were added in the later stages of refinement using PhenixRefine or were manually added into $\geq 3\sigma$ Fo-Fc density. The electron density for the main chain was unbroken and modeled from residues 1-108. The electron density of all side chains was visible, except for Glu54 in chains A and B. Structure validation was carried out using Molprobity (Table 3.1) (Chen et al., 2010).

Molecular figures were made with PyMol (http://pymol.sourceforge.net). Structure-based sequence alignments were generated using Expresso (Di Tommaso et al., 2011) and displayed using ESPript (Gouet et al., 2003). The electrostatic surface potential was calculated with the Adaptive Poisson-Boltzmann Solver (Baker et al., 2001) in PyMOL. Structural superpositions were calculated using FATCAT (Ye and Godzik, 2003) or Dali (Holm and Rosenström, 2010). The crystal structure and structure factors have been deposited with the Protein Data Bank (ID code 4D9V).

Generation of *Y. pseudotuberculosis* (*ΔyscD*)

The entirety of *yscD*, except for 15 bp at the 3' end, was substituted in-frame with *aph* (kanamycin resistance) by homologous recombination with a PCR fragment (Datsenko and Wanner, 2000). The 15 bp at the 3' end of *yscD* were left intact as they contain a predicted ribosome-binding site for *yscE*. The PCR fragment contained 500 bp of the pYV sequence upstream of *yscD*, followed by *aph*, the terminal 15 bp of *yscD*, and 500 bp of the pYV sequence downstream of *yscD*. Six hundred ng of this fragment were transformed by electroporation into competent *Y. pseudotuberculosis* harboring the plasmid pWL204 (Conchas and Carniel, 1990; Lathem et al., 2007). Electroporated bacteria were grown in brain heart infusion (BHI) medium at 26 ºC for 2 h, centrifuged (3,000 x *g*, 5 min, 25 °C), and the pellet was resuspended in BHI supplemented with 3 mM $CaCl_2$ and 50 mg/L kanamycin. Bacteria were grown further for 2 h at 26 °C in these conditions, and were transferred to BHI agar plates containing 3 mM $CaCl_2$ and 50 mg/L kanamycin. Plates were grown overnight at 26 °C. The integrity of the allelic replacement was verified by sequencing a PCR fragment resulting from primers that anneal 650 bp upstream and downstream of the *yscD* locus. To select for loss of the pWL204 plasmid, bacteria were grown on agar plates as above, but supplemented with 2% sucrose. Loss of pWL204 was confirmed by sensitivity to ampicillin. *Y. pseudotuberculosis* (*ΔyscD*) was complemented with wild-type or mutant *yscD* expressed from the pBAD plasmid, as described above.

Secretion Assay

Y. pseudotuberculosis was grown overnight at 28 ºC in BHI media with appropriate antibiotics and 2.5 mM $CaCl_2$. The overnight culture was diluted to an OD_{600} of 0.1 in 10 mL of BHI containing 10 mM ethylene glycol tetraacetic acid (EGTA), 10 mM $MgCl_2$, and appropriate antibiotics. In the case of *Y. pseudotuberculosis* harboring pBAD-yscD, cultures were supplemented with 0.002% arabinose once they reached an OD_{600} of 0.6 and shifted to 37 ºC once they reached an OD_{600} of 1.0; 0.002% arabinose was subsequently added every four hours during growth to account for the metabolic depletion of arabinose. Cultures were grown an additional 4 h.

To visualize secreted proteins, the bacterial supernatant was filtered (0.22 μm filter, Millipore), precipitated overnight by the addition of 10% trichloroacetic acid (TCA). Precipitated samples were centrifuged (5,000 x *g*, 5 min, 4 °C) and the pellet washed with ice-cold acetone. Pelleted proteins were air-dried, resuspended in SDS-PAGE sample buffer supplemented with 40 mM NaOH, boiled for 5 min, and separated by SDS-PAGE.

For Western blot analysis of expressed proteins, 3 mL of bacterial culture at an OD_{600} of 1.0 were harvested by centrifugation (3,800 x *g*, 5 min, 4 °C). Pelleted bacteria were resuspended in 30 μL SDS-PAGE sample buffer and lysed by boiling for 5 min. The sample was applied to SDS-PAGE for separation of proteins, and the gel was transferred to a PVDF membrane. The membrane was blocked for 1 hr at room temperature in 5% bovine serum albumin (BSA, Sigma-

Aldrich) in 150 mM NaCl, 50 mM Tris, pH 8.0, and 0.5% Tween 20 (TBST), washed once with TBST, and incubated for 16 hr at 4 °C with primary antibody (1:500 rabbit anti-YscD polyclonal antibodies) in 5% BSA in TBST. The primary antibodies were generated in rabbits using YscDc as an antigen (Cocalico Biologicals), and were purified by affinity chromatography using YscDc affixed to a solid matrix. Three washes of the membrane in TBST (each 15 min in duration) were carried out, and the membrane was then incubated with HRP-conjugated secondary anti-rabbit antibodies (1:2,000, Santa Cruz Biotechnology, Santa Cruz, CA) in 5% BSA in TBST for 30 min. Following three washes with TBST (each 20 min in duration), the membrane was developed using SuperSignal West Pico chemiluminescent substrate (Pierce) and visualized with a Bio-Rad ChemiDoc Imaging System.

As a loading control, RpoA was detected on the same membrane that had been probed for YscD. After probing for YscD as above, the membrane was stripped by incubation in 67% guanidine HCl (w/v), 50 μM EDTA, 50 mM glycine, pH 10.8, 2.5 mM KCl, and 1.4 mM βME for 10 min. The membrane was then blocked for 1 hr at room temperature in TBST containing 5% BSA, washed once with TBST, and incubated for 1 hr at 25 °C with primary antibody (1:1,000 mouse anti-RpoA monoclonal antibodies, Santa Cruz Biotechnology, Santa Cruz, CA) in TBST containing 5% BSA. Three washes of the membrane in TBST (each 10 min in duration) were carried out, and the membrane was then incubated with HRP-conjugated secondary anti-mouse antibodies (1:2,000, Santa Cruz

Biotechnology, Santa Cruz, CA) in TBST containing 5% BSA for 30 min. Following three washes with TBST (each 10 min in duration), the membrane was developed and visualized as above.

Circular dichroism

Circular dichroism spectra were collected for wild-type and mutant YscDc at 10 µM in 100 mM NaF, 10 mM potassium phosphate buffer, pH 7.6 on an Aviv 202 circular dichroism spectrometer using a 1 mm pathlength cuvette (holding 350 µL) (Hellma). For each sample, the average of three independent spectra recorded from 195 nm to 260 nm at 4 °C and 37 °C is reported. The scans were performed with 1 nm steps, and the CD signal at each wavelength was averaged for 5 seconds.

Identification of binding partners of YscD

Wild-type YscD and the L3 and L4 mutants were expressed from pBAD-YscD in *Y. pseudotuberculosis* (*ΔyscD*). Bacteria were grown as described above for the secretion assay, except that the media was BHI with appropriate antibiotics and 2.5 mM $CaCl_2$ throughout to suppress secretion. After 4 h growth of the culture at 37 °C, bacteria were harvested by centrifugation (5,800 x *g*, 10 min, 4º C). The bacterial pellet was resuspended in 1/10th volume of the original bacterial culture in buffer A (100 mM NaCl, 50 mM sodium phosphate buffer, pH 8.0, 10

mM βME) supplemented with EDTA-free protease cocktail inhibitor (Roche) (one tablet per 250 mL of original bacterial culture). Resuspended bacteria were lysed using an Emulsiflex-C5 (Avestin) homogenizer with three passes at 15,000 psi, and the lysate was clarified by centrifugation (14,000 x *g*, 10 min, 4 ºC). Bacterial membranes were pelleted by ultracentrifugation (95,000 x *g*, 4 h, 4°C), and solubilized in 1/100th volume of the original bacterial culture in buffer A containing 20 mM lauryldimethylamine oxide (LDAO). Forty percent of this sample was incubated with Ni^{2+}-NTA agarose beads (0.5 mL per mL of sample). The beads were washed with 10 bead volumes of buffer A containing 7 mM imidazole and 5 mM LDAO, and then washed five times with two bead volumes of buffer A alone to remove LDAO.

The protein-bead complexes were prepared for mass spectrometry as described previously (Guttman et al., 2009). They were diluted in TNE (50 mM Tris pH 8.0, 100 mM NaCl, 1 mM EDTA) buffer. RapiGest SF reagent (Waters Corp.) was added to the mix to a final concentration of 0.1% and samples were boiled for 5 min. Tris (2-carboxyethyl) phosphine (TCEP) was added to 1 mM final concentration and the samples were incubated at 37 °C for 30 min. The samples were then carboxymethylated with 0.5 mg/mL of iodoacetamide for 30 min at 37 °C, followed by neutralization with 2 mM final concentration of TCEP. Samples were digested with trypsin (1:50 trypsin:protein mass ratio) overnight at 37 °C. RapiGest was degraded and removed by treating the samples with 250 mM

HCl at 37 °C for 1 h, followed by centrifugation (15,800 x *g*, 30 min, 4 °C). The soluble fraction was then added to a new tube and the peptides were extracted and desalted using Aspire RP30 desalting columns (Thermo Scientific).

Trypsin-digested peptides were analyzed by high pressure liquid chromatography (HPLC) coupled with tandem mass spectroscopy (LC-MS/MS) using nanospray ionization, as previously described (McCormack et al., 1997) except for the following changes. The nanospray ionization experiments were performed using a QSTAR-Elite hybrid mass spectrometer (ABSCIEX) interfaced with nano-scale reversed-phase HPLC (Tempo) using a 10 cm-180 micron ID glass capillary packed with 5-µm C18 Zorbax^{TM} beads (Agilent Technologies, Santa Clara, CA). Peptides were eluted from the C18 column into the mass spectrometer using a linear gradient (5–60%) of acetonitrile (ACN) at a flow rate of 400 µL/min for 1 h. The buffers used to create the ACN gradient were: Buffer A (98% H_2O, 2% ACN, 0.2% formic acid, and 0.005% TFA) and buffer B (100% ACN, 0.2% formic acid, and 0.005% TFA). MS/MS data were acquired in a data-dependent manner in which the MS1 data was acquired at m/z of 400 to 1,800 Da and the MS/MS data was acquired from m/z of 50 to 2,000 Da. The collected data were analyzed using MASCOT® (Matrix Sciences) and Protein Pilot 4.0 (ABSCIEX) for peptide identifications and Peakview (ABSCIEX) for peak integration and quantification. A peak area of ~1.2 x 10^3 was estimated to be the detection limit. This estimate was based on integration of a peak near the noise

level; inspection showed that an intensity of ~30 was at the noise level, and the integrated peak had an intensity of 38.

RESULTS

YscDc has an FHA fold

YscDc was overexpressed in *E. coli*, purified to homogeneity, and crystallized. The crystal structure of YscDc was determined by single wavelength anomalous dispersion and refined to 2.52 Å resolution limit (Table S1). The structure revealed that YscDc has a typical FHA domain fold, characterized by a β-sandwich composed of 10 β-strands that form two sheets (Figure 3.1). The structure agrees in detail with that recently reported by others (rmsd 0.3 Å, 107 Cα) (Lountos et al., 2012). The two sheets, one of which is six-stranded (β2β1β10β9β7β8) and the other four-stranded (β4β3β5β6), pack against one another through hydrophobic side chains that form the hydrophobic core of the domain. All the strands are antiparallel, except for the short β4 strand, which runs parallel to the β3 strand. Along with the β4 strand, the β7, β8, and β9 strands are also especially short. The only helical portion of the domain consists of a short 3_{10}-helix between strands β1 and β2. The asymmetric unit of the crystal contains two copies of YscDc that are nearly identical (rmsd 0.25 Å, 108 Cα) and related by approximate two-fold symmetry. However, this association is unlikely to be biologically meaningful, as only ~560 $Å^2$ of total surface area are buried at the dimer interface. Consistent with this, YscDc was observed to run on a gel filtration column at the size indicative of a globular monomer (data not shown). The N-terminal residues of YscDc were well ordered, while the C-terminal

residues (109-121), which connect to the transmembrane region of YscD, were unstructured. This suggests that the cytoplasmic domain of YscD is flexibly tethered to the inner membrane, which would enable freedom in interactions with cytoplasmically exposed T3S components.

FHA domains are found in a variety of proteins across multiple kingdoms. The most similar structures to YscDc are the FHA domains of *Chlamydia trachomatis* CT664 (rmsd 2.0 Å, 96 Cα), *Mycobacterium tuberculosis* EmbR (rmsd 2.2 Å, 93 Cα), *M. tuberculosis* Rv0020c (rmsd 2.0 Å, 92 Cα), *H. sapiens* kinesin KIF13 (rmsd 2.1, 87 Cα), and *H. sapiens* Ki67 (rmsd 2.3 Å, 93 Cα) (Figure 3.1b) (Alderwick et al., 2006; Byeon et al., 2005; Pennell et al., 2010; Tong et al., 2010). However, YscDc has little sequence identity (average ~18 %) to these (Figure 3.1c) or other structurally characterized FHA domain proteins. Indeed, the identities of the side chains that make up the hydrophobic core in YscDc are not conserved in these other FHA domain proteins. However, there are several residues that are absolutely conserved in this set of proteins. These include Gly27 and His47 (Figure 3.1c): Gly27 initiates loop 3 (L3, the loop connecting the β3 and β4 strands) and His46, which faces inwards to make hydrogen bonds with main chains atoms of YscDc, terminates loop 4 (L4). L3 and L4 along with loop 6 have been shown to be crucial for target recognition in FHA domain proteins (Alderwick et al., 2006; Barthe et al., 2009; Huen et al., 2007; Kumeta et al., 2008).

YscDc lacks phosphothreonine-binding characteristics

Most but not all FHA domains specifically bind phosphothreonine residues. The interaction with phosphothreonine occurs primarily through a serine located on L4 that is three residues upstream of the conserved His (Figure 3.1c, red arrow), and secondarily through an arginine found in either L3 or L4. YscDc lacks the conserved Ser on L4 (in its place is Ala43) and has no arginine residues on either L3 or L4. Furthermore, in FHA domains that bind phosphothreonine residues, the surfaces of L3 and L4 are positively charged, while in YscDc the equivalent surface is negatively charged (Figure 3.2a). These pieces of evidence suggest that YscDc is unlikely to bind proteins in a phosphorylation-dependent manner. L3 and L4, however, may still be involved in protein-protein interactions, but in a phosphorylation-independent manner, as has been observed for the FHA domain of *H. sapiens* KIF13. L3 and L4 of KIF13, which lack the conserved Ser and Arg (Figure 3.1c) and have an uncharged electrostatic surface, have been observed to confer binding to the protein CENTA1 in a phosphorylation-independent manner (Tong et al., 2010).

The FHA domain of YscD has significant sequence similarity to orthologs within its own Ysc subfamily of T3S systems (Cornelis, 2006). These include *Aeromonas hydrophila* AscD, *Pseudomonas aeruginosa* PscD, and *Photorhabdus luminescens* SctD, whose predicted cytoplasmic domains have an average sequence identity of 44% with YscDc (Figure 3.2b). The hydrophobic core of YscDc (e.g., Leu49, Val51, Ile56, Leu58) is well conserved among these Ysc

subfamily members, indicative of the likely presence of FHA domains in these orthologs. Like YscD, these close family members are missing the Ser and Arg associated with phosphothreonine-binding, and thus the weight of evidence suggests that these Ysc subfamily orthologs are likely to interact with their partners in a phosphorylation-independent manner as well.

YscDc has more distant but recognizable sequence identity to the cytoplasmic domains of the well-studied YscD orthologs of the SPI-1 (*Salmonella enterica* PrgH, 17% identity) and SPI-2 (*Escherichia coli* EscD, 24% identity) subfamilies of the T3S system (Figure 3.2c) (Kimbrough and Miller, 2000; Kresse et al., 1998; Ogino et al., 2006; Schraidt and Marlovits, 2011; Spreter et al., 2009). This includes *Shigella flexneri* MxiG, a member of the SPI-1 subfamily. The structure of the cytoplasmic domain of MxiG (called here MxiGc) was recently shown by NMR and X-ray crystallographic techniques to consist of an FHA domain (Barison et al., 2012; McDowell et al., 2011). YscDc and MxiGc have 13% sequence identity and an rmsd of 3.08 Å between their two structures (86 Cα) (Figure 3.2d). MxiG lacks the conserved His, but has a Ser (S61) and Arg (R39) (Figure 3.2c, red arrowheads) that have been identified to be important for binding a threonine-phosphorylated peptide that corresponds to a sequence from the putative C-ring protein Spa33 (Barison et al., 2012; Morita-Ishihara et al., 2006). However, a different study using NMR titration reported no interaction between MxiGc and up to 50 mM phosphothreonine (McDowell et al., 2011).

Finally, it is worth noting that the sequences of YscD L3 and L4 are highly similar or nearly identical among orthologs in the Ysc subfamily, but quite dissimilar from PrgH, MxiG, and EscD (Figs. 3.2b, c). Consistent with this, L3 and L4 diverge the most structurally between YscDc and MxiGc (Figure 3.2d). Collectively, these observations suggest that interactions between YscDc and its partners are likely to occur at the L3 and L4 region, and further, that these interactions are likely to be conserved with members of the Ysc subfamily but not the SPI-1 or SPI-2 subfamilies.

L3 and L4 are functionally essential

To determine whether L3 and L4 are required for function, we substituted residues in these loops with alanines. Five sequential surface-exposed residues of L3 were substituted with alanines (Ser28, Asp29, Pro30, Leu31, and Gln32), as were four sequential surface-exposed residues of L4 (Asp39, Ser40, Glu41, and Ile42) (Figure 3.3a). In addition, single-site alanine substitution mutants were created in L4 at D39 and S40, and owing to the importance of serines in FHA domains for interactions, a single-site alanine substitution was also created at S38.

To assay the functional effects of these mutations, we created a strain of *Y. pseudotuberculosis* lacking *yscD*. As expected, wild-type *Y. pseudotuberculosis* secreted proteins in a low Ca^{2+}-dependent manner that is characteristic of T3S, whereas *Y. pseudotuberculosis* (*ΔyscD*) was deficient for T3S (Figure 3.3b) (Plano and Straley, 1995). Type III secretion was restored by wild-type *yscD*

(carrying an N-terminal His-tag), whose expression from a plasmid was induced by arabinose (Figure 3.3b), indicating that the deletion of *yscD* was nonpolar. The concentration of arabinose was empirically varied to mimic the level of expression of endogenous YscD, as determined by Western Blot using anti-YscD antibodies (Figure 3.3b). The Western Blot membrane was also probed with anti-RpoA antibodies, confirming the equal loading of samples. The alanine substitution mutants of YscD (carrying N-terminal His-tags) were next introduced into *Y. pseudotuberculosis* (*ΔyscD*). Both the L3 and the L4 multiple alanine substitutions were produced at levels equivalent to wild-type YscD, but were found to be deficient for T3S (Figure 3.3b). The single-site D39A and S40A substitution mutant appeared to be slightly attenuated for T3S, while S38A behaved like wild-type YscD for T3S. These single-site mutants were also produced at levels equivalent to wild-type YscD.

Because the L3 and L4 substitutions are located on surface loops of YscD, it seemed unlikely that substitutions of these loops would affect protein structure or stability. Nevertheless, we examined the physical consequences of the L3 and L4 substitutions. The substitutions were introduced into YscDc, and these mutant proteins were produced in *E. coli*, purified, and subjected to analysis by circular dichroism (CD) (Figure 3.3c). YscDc L3 and L4 were found to have CD spectra that were unchanged between 4° and 37 °C and similar to those of wild-type YscDc. Thus, we conclude that the alanine substitutions of L3 and L4 do not have deleterious effects on protein structure and stability.

Interactions of YscD with T3S components

To characterize the defects in T3S caused by the L3 and L4 alanine substitutions, we determined the identity of proteins that associate directly or indirectly with YscD. As above, wild-type *yscD* and the L3 and L4 substitution mutants (carrying His-tags) were expressed in *Y. pseudotuberculosis* (*ΔyscD*). Bacteria were grown under non-secreting conditions (i.e., high calcium concentration), and the membrane fraction was isolated from lysed bacteria and solubilized in detergent. Consistent with the observed stability of YscDc L3 and L4, both YscD L3 and L4 localized to the membrane fraction of *Y. pseudotuberculosis*, just as wild-type YscD did. YscD was captured from this fraction using Ni^{2+}-nitrilotriacetic acid (NTA) agarose beads, and the identities of proteins co-purifying with YscD were determined by high pressure liquid chromatography coupled with tandem mass spectroscopy from tryptic peptides. We also subjected *Y. pseudotuberculosis* (*ΔyscD*) to the same analysis to distinguish between specific and nonspecific interactions. Measurements were normalized based on two peptides from EF-Tu that were common to all of the samples (Table 3.2).

We found that wild-type YscD associated with YscJ, its expected partner, but also the effector protein YopH (Rosqvist et al., 1988) (Figure 3.4). No other associated proteins were identified for wild-type YscD (Ross and Plano, 2011). We expected the L3 and L4 substitution mutants to be defective for association, but surprisingly found both substitution mutants to have enhanced interactions

with YopH as compared to wild-type YscD. In addition, the specific chaperone of YopH, SycH (Woestyn et al., 1996), associated with the L3 and L4 substitution mutants, but not wild-type YscD. The lack of SycH was not due to the lower level of YopH associated with wild-type YscD. While the YscD L3 and L4 substitution mutants had ~4.7-fold more associated YopH than did wild-type YscD, they also had a level of SycH that was ~70-fold higher than the detection limit of the experiment (estimated at ~1.2 x 10^3 peak area). Thus, if SycH were associated with wild-type YscD (at the same level relative to YopH as for YscD L3 and L4), it would have been detectable (with an expected peak area of ~1.8 x 10^4).

The L3 and L4 substitutions maintained association with YscJ. The continued presence of YscJ suggests that the L3 and L4 mutants are proficient in assembly, consistent with their maintenance of protein structure and stability. In addition, the putative C-ring component YscQ (Bzymek et al., 2012; Fields et al., 1994) and the ruler component YscP (Journet et al., 2003) were observed to associate with the L3 and L4 substitution mutants but not wild-type YscD. These results indicate that the defect in secretion for the L3 and L4 substitution mutants was due to increased rather than decreased association between YscD and other T3S components.

The increased association of the L3 and L4 substitution mutants with T3S components raised the possibility that they may act as dominant negatives. To test this hypothesis, we expressed YscD L3 and L4 as well as wild-type YscD from the pBAD plasmid in a wild-type strain of *Y. pseudotuberculosis*. An increase in

the amount of YscD supplied by plasmid-encoded wild-type YscD had no significant effect on secretion (Figure 3.5). However, expression of YscD L3 and especially YscD L4 were found to suppress secretion (Figure 3.5). This dominant-negative behavior suggests that YscD L3 and L4 assemble in the membrane alongside wild-type YscD, and that their increased association with T3S components disables the function of wild-type YscD in secretion.

DISCUSSION

YscD and YscJ are predicted, based on analogy to the T3S systems of *Salmonella* and *Shigella* (Hodgkinson et al., 2009; Schraidt and Marlovits, 2011), to form a ring-like structure that consists of ~24 copies of each protein in the inner bacterial membrane. We found that the cytoplasmic domain of YscD, YscDc, exists as a monomer, with no higher-order structures being evident, even at the high protein concentrations of its crystalline form. This suggests that other portions of YscD are likely to mediate potential oligomerization. A 66-residue region at the very C-terminal periplasmic end of YscD appears to be the likely determinant (Ross and Plano, 2011). The 66-residue region interacts with the secretin YscC (Ross and Plano, 2011), a ring-shaped oligomer that appears to be the first component of the T3S apparatus to assemble (Diepold et al., 2010; Koster et al., 1997). Other portions of the YscD periplasmic region have been shown to be non-essential for T3S (Ross and Plano, 2011), namely the predicted phospholipid binding (BON) and the so-called ring-building domains, as has the specific sequence of the transmembrane domain (Ross and Plano, 2011).

The structure of YscDc confirmed that the cytoplasmic domain of YscD has an FHA fold (Pallen et al., 2002, 2003), as also has been demonstrated by others (Lountos et al., 2012). The FHA fold is strongly but not exclusively associated with phosphothreonine-binding (Hofmann and Bucher, 1995; Mahajan et al., 2008; Nott et al., 2009; Tong et al., 2010). While the details of

phosphothreonine-binding vary considerably among FHA domain proteins, most have in common the participation of a Ser that is three residues upstream of a conserved His on L4 and an Arg on L3 or L4. YscD has neither the Ser nor the Arg. Orthologs of YscD from the Ysc subgroup of the T3S system also lack the Ser and Arg associated with phosphothreonine-binding (Figure 3.2). Additionally, unlike the positively charged L3 and L4 of phosphothreonine-binding FHA domains, these loops in YscD are negatively charged. These observations suggest that YscD and its orthologs in the Ysc subfamily are unlikely to interact with partners in the phosphothreonine-dependent manner that is characteristic of FHA domains.

YscD has distant but recognizable sequence identity to orthologs in the SPI-1 and SPI-2 subfamilies. This includes the SPI-1 ortholog MxiG, whose cytoplasmic domain was shown to have an FHA fold (Barison et al., 2012; McDowell et al., 2011). L4 in MxiG lacks the conserved His but has two serines (S61 and S63), and L3 has an Arg (residue 39). The cytoplasmic domain of MxiG, MxiGc, was shown to bind a phosphothreonine-containing peptide whose sequence corresponds to the putative C-ring component Spa33. This interaction was seen to be phosphorylation-dependent, and MxiG R39 and S61 were found to be important for this interaction (Barison et al., 2012). MxiG and Spa33 have been previously shown to interact (Morita-Ishihara et al., 2006), but whether Spa33 is phosphorylated *in vivo* remains uncertain. MxiG R39 and S61 were also shown to have a role in type III secretion and epithelial cell invasion (Barison et

al., 2012). In contrast to these findings, a separate study found no evidence for interaction between 50 mM phosphothreonine and MxiGc, and an R39A/S61A/S63A triple alanine substitution mutant was observed to have no loss in type III secretion (McDowell et al., 2011). Thus, whether MxiG binds its partners in a phosphothreonine-dependent manner is currently controversial. The SPI-1 and SPI-2 orthologs PrgH and EscD, respectively, lack the conserved His, and while PrgH has a Ser in predicted L4, neither have arginines in predicted L3 or L4. This suggests that PrgH and EscD are likely to bind their partners in a phosphorylation-independent manner. One T3S ortholog, *C. trachomatis* CT664 from the *Chlamydiales* subfamily of the T3S system (Pallen et al., 2003), does have a typical phosphothreonine-binding motif in L3 and L4. CT664 has a Ser three residues upstream of the conserved His along with an Arg placed appropriately for phosphothreonine interaction (Figure 3.1c). The crystal structure of CT664 contains a phosphate bound at these residues, but no direct evidence exists yet for phosphothreonine interaction by CT664 or other *Chlamydiales* subfamily members.

While L3 and L4 in YscDc are unlikely to partake in phosphothreonine-dependent interactions, these same loops have been found in the FHA domain protein KIF13 to participate in phosphorylation-independent interaction (Tong et al., 2010). To determine whether L3 and L4 in YscD are required for function, we created single and multiple alanine substitutions in these loops. We found that multiple alanine substitutions of either L3 or L4 abrogated T3S, but had no

deleterious effects on protein structure or stability, as assessed by CD. We sought to understand the basis for the functional defects of the L3 and L4 substitution mutants by characterizing the proteins associated with YscD.

We detected an interaction between wild-type YscD and YscJ, which was expected (Ross and Plano, 2011). The YscD L3 and L4 mutants also interacted with YscJ, providing evidence that these mutant proteins assemble in the membrane like wild-type YscD. This conclusion was further supported by the dominant negative behavior of the L3 and L4 substitution mutants. They suppressed secretion by wild-type YscD, consistent with co-assembly of wild-type and mutant copies of YscD.

We also found an unexpected association between wild-type YscD and the effector YopH (Rosqvist et al., 1988). No other effectors were observed to associate with YscD. The action of YopH in host cells is nearly immediate (Andersson et al., 1999), and it is possible that the association between YopH and YscD provides YopH with precedence in the hierarchy of effector secretion. An even stronger association with YopH was observed for the YscD L3 and L4 substitution mutants. Notably, in addition to YopH, the YopH-specific chaperone SycH (Woestyn et al., 1996) was found associated with the YscD L3 and L4 substitution mutants but not with wild-type YscD.

It appears that dissociation of SycH from YopH is impaired in the YscD L3 and L4 mutants. This is unlikely to be a direct effect of YscD. Based on analogy to the *Salmonella* T3S (Akeda and Galán, 2005), it is likely that the

Yersinia T3S ATPase YscN is responsible for catalyzing the dissociation of SycH from YopH. Therefore, a plausible mechanism for the association of SycH with the YscD L3 and L4 substitution mutants is a defect in the recruitment of YscN by these mutant proteins. We did not observe an association between wild-type YscD and YscN, but this putative interaction is likely to be transient, breaking up after the release of SycH. Impaired dissociation of SycH from YopH would also provide an explanation for the pattern of additional T3S components associated with the YscD L3 and L4 substitution mutants. Among these components is YscQ, which forms the putative C-ring (Bzymek et al., 2012). YscQ was found associated with the L3 and L4 substitution mutants but not with wild-type YscD. YscQ may be recruited to YscD through SycH, as both the *Salmonella* and *Chlamydia* orthologs of YscQ, SpaO and CdsQ, respectively, are known to bind T3S chaperones (Lara-Tejero et al., 2011; Spaeth et al., 2009). The likely oligomeric nature of YscQ may provide the means by which additional copies of SycH-YopH associate with the YscD L3 and L4 mutants, explaining the increased quantity of YopH associated with these mutants. In addition, the ruler component YscP (Journet et al., 2003) was also found associated with the L3 and L4 substitution mutants but not with wild-type YscD. This interaction may also occur through YscQ, as YscP has been reported to interact with YscQ (Riordan et al., 2008). The overall picture that emerges is the presence of a large protein complex that is stably associated with the YscD L3 and L4 substitution mutants but missing for wild-type YscD. This protein complex appears to stall the T3S system

and prevent it from proceeding through the sequential steps required for protein export.

FIGURES AND TABLES

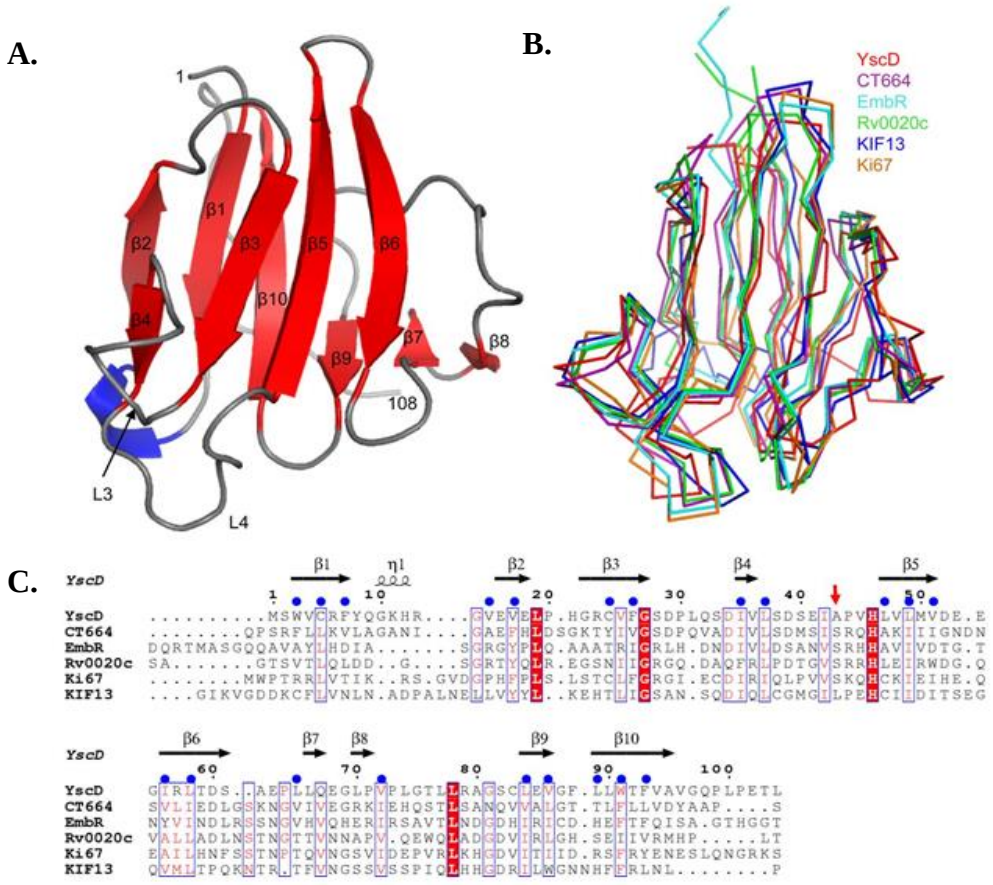

Figure 3.1 YscDc has an FHA fold.
A. Structure of YscDc (residues 1-108) in ribbon representation, with β-strands in red, coils in gray, and helices in blue. Loops L3 and L4 are indicated.
B. Structural superposition of YscDc with closely related structurally characterize FHA domains. YscDc is in red, CT664 (RSCB accession code 3GQS) purple, EmbR (2FEZ) cyan, Rv0020c (3PO8) green, KIF13 (3FM8) blue, and Ki67 (2AFF) orange. The proteins are shown as Cα traces.
C. Structure-based sequence alignment of the FHA domains shown in panel b. A red arrow denotes the position of the Ser in loop 4 that is conserved in phosphothreonine-binding FHA domains, and the blue circles denote core residues of YscDc. Secondary structure annotations at the top of the alignment are for YscDc.

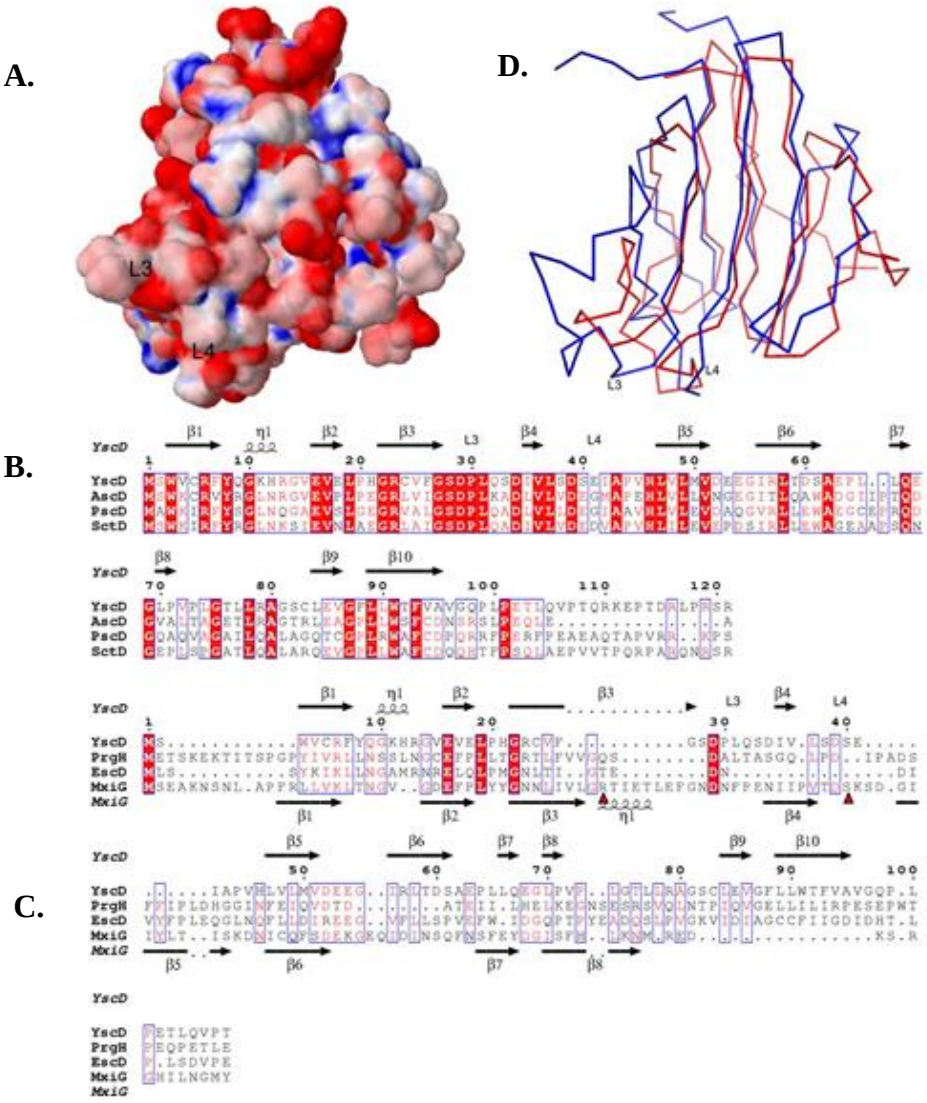

Figure 3.2 YscDc and T3S orthologs.
A. Electrostatic potential of YscDc mapped to its surface. Red is negative (-10 kT) and blue is positive (+10 kT).
B. Structure-based sequence alignments of YscD and Ysc subfamily members AscD, PscD, SctD. Secondary structure annotations at the top of the alignments are for YscDc.
C. Structure-based sequence alignments of YscD and T3S orthologs PrgH, EscD, and MxiG. Secondary structure annotations at the top of the alignments are for YscDc, and at the bottom for MxiG. Red arrowheads below MxiG denote MxiG R39 and S61.
D. Structural superposition of YscDc and the FHA domain of MxiG. YscDc is in red and MxiG (2XXS) in blue. The proteins are shown as Cα traces.

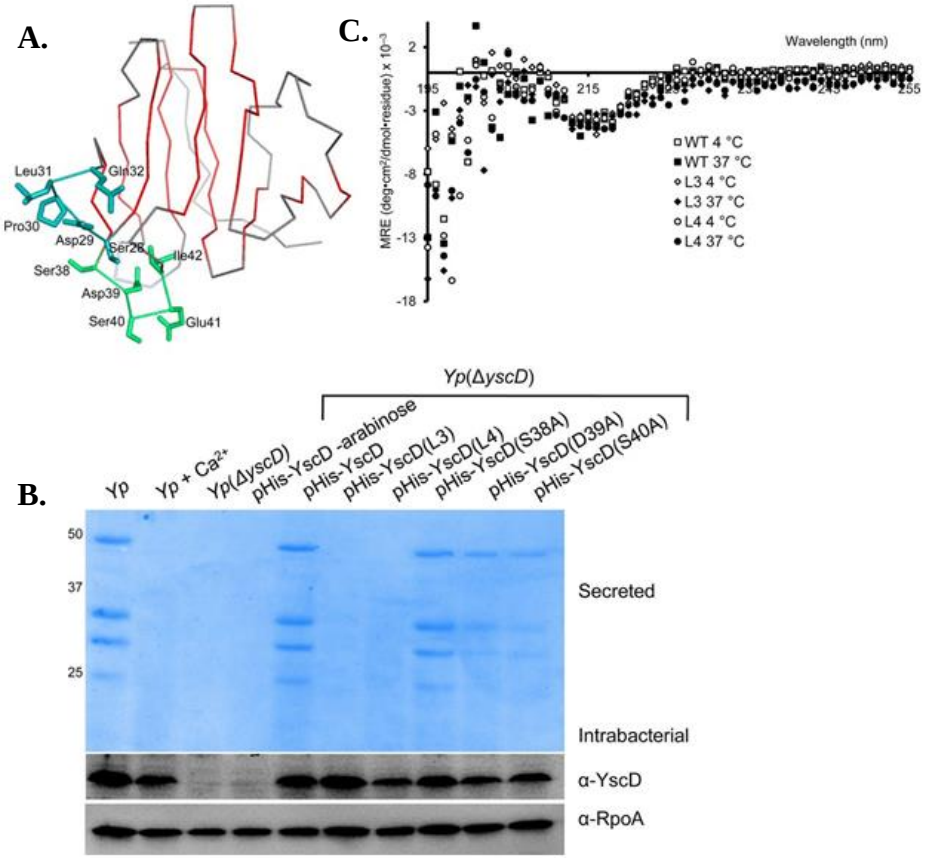

Figure 3.3 L3 and L4 mutants.
A. Positions of residues mutated in the L3 (blue) and L4 loops (green). YscDc is shown as a bonds trace, with β-strands in red and loops in gray.
B. Top panel, type III secretion as detected by SDS-PAGE of culture supernatants. *Y. pseudotuberculosis* (*ΔyscD*) was transformed with plasmids expressing wild-type (pHis-YscD) and mutant YscD (pHis-YscD(L3), pHis-YscD(L4), pHis-YscD(S38A), pHis-YscD(S39A), pHis-YscD(S40A)) under the inducible control of arabinose. *Yp* is wild-type *Y. pseudotuberculosis*; "+Ca^{2+}" indicates the presence of high calcium concentration, which suppresses T3S; "-arabinose" indicates lack of arabinose induction. The sizes of molecular mass standards in kDa are indicated at left. Middle panel, the level of intrabacterial YscD for each of the samples, as detected by an anti-YscD Western blot. Lower panel, the level of intrabacterial RpoA as a loading control, as detected by anti-RpoA blot.
C. Circular dichroism spectra of wild-type YscDc, YscDc(L3), and YscDc(L4) at 4 and 37 °C.

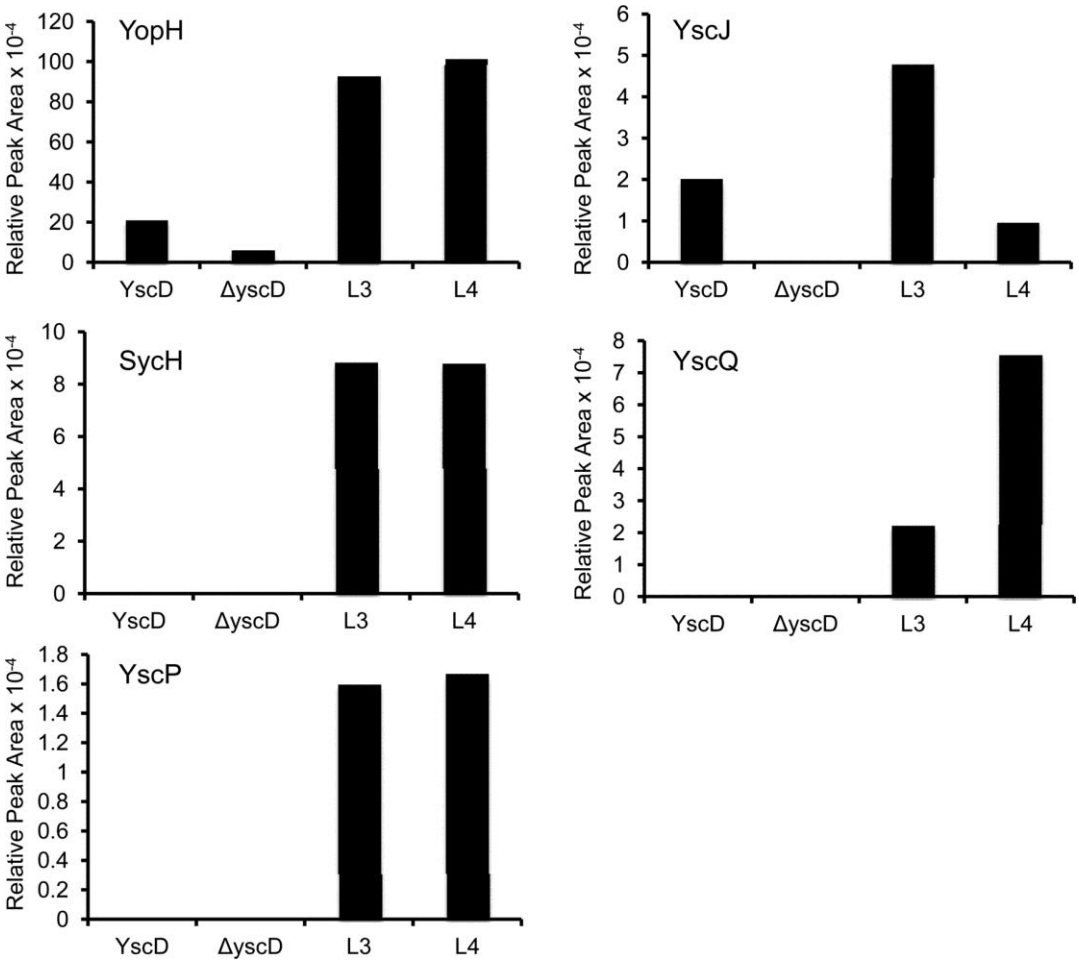

Figure 3.4 Proteins associated with YscD.
Proteins found associated (indicated at top left of each plot) with wild-type YscD, *ΔyscD* (lacking YscD and thus a specificity control), and the L3 and L4 substitutions mutants of YscD. Peak heights of peptides corresponding to these proteins are plotted relative to an internal standard, as identified by mass spectrometry (Table 3.2).

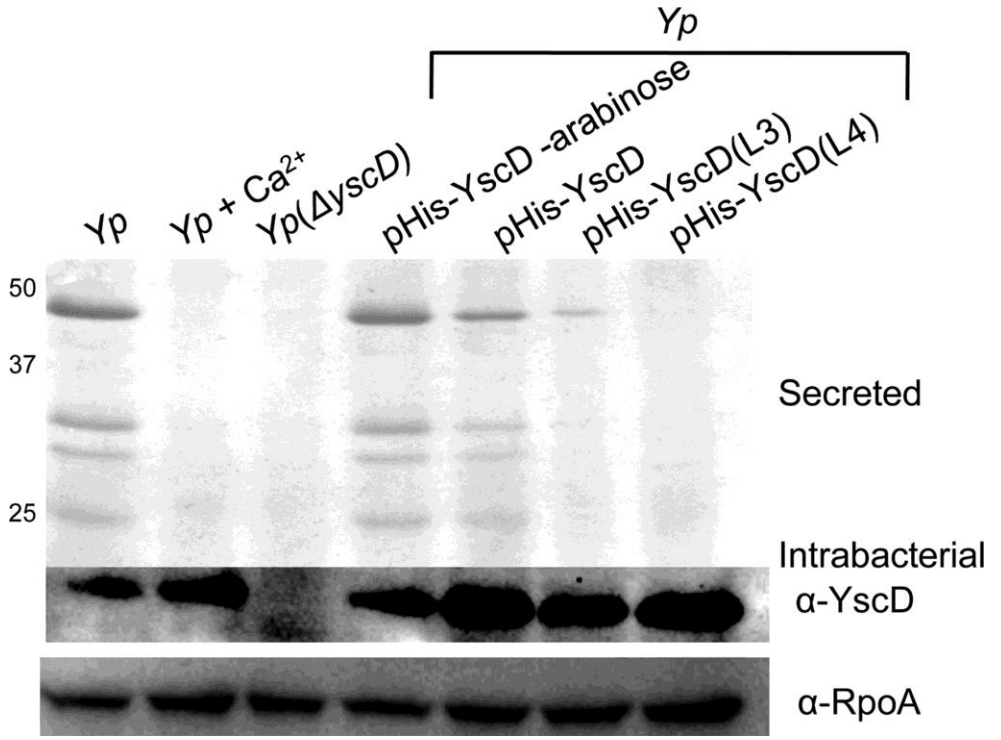

Figure 3.5 Dominant-negative effect of YscD L3 and L4.
Type III secretion detected by Coomassie-stained SDS-PAGE. The format is as in Figure 3.3b, with wild-type *Y. pseudotuberculosis* being transformed with plasmids expressing wild-type (pHis-YscD) and mutant YscD (pHis-YscD(L3), pHis-YscD(L4)) under the inducible control of arabinose.
sample and expressed as a percentage of YP126. Gray bars report standard errors of the mean.

Table 3.1 X-ray data collection and refinement statistics for YscDc.

	Native	SeMet
Data collection		
Space group	P432	P432
Cell dimensions *a* (Å)	117.1	116.8
Wavelength (Å)	0.97961	0.97949 (Peak)
Resolution (Å)*	50-2.50 (2.59-2.50)	41.29 -2.85 (2.90-2.85)
R_{merge} (%)	7.6 (57.8)	8.3 (37.4)
I/σ_I	46.8 (8.4)	39.9 (11.0)
Completeness (%)	99.9 (80.5)	99.3 (99.8)
Redundancy	41.5 (35.6)	24.6 (24.5)
Refinement		
Resolution (Å)	35.308-2.519 (2.651-2.519)	
No. reflections	9,819	
R_{work}/R_{free} (%)	20.4/25.7 (21.6/27.5)	
No. atoms	1,663	
Protein	1,647	
Water	16	
Mean B-factors (Å^2)		
Protein	49.4	
Water	45.8	
R.m.s. deviation		
Bond lengths (Å)	0.0089	
Bond angles (°)	1.315	
Validation		
Ramachandran		
favored	98.1%	
outliers	0%	
Clashscore	12.44 (91st percentile)	
Molprobity score	2.09 (94th percentile)	

*Data for highest resolution shell indicated in parenthesis.

Table 3.2 Mass spectrometry data

	Peptide	YscD	*ΔyscD*	L3	L4
EF Tu	IIELAGYLDSYIPEPER	1.932E+06	1.796E+06	2.205E+06	2.596E+06
	ELLSAYDFPGDDLPVVR	7.595E+05	8.189E+05	1.511E+06	1.757E+06
	average peak area	1.346E+06	1.307E+06	1.858E+06	2.177E+06
	correction factor	1.03	1.00	1.42	1.66
YopH	TPVLAVLASSSEIANQR	1.155E+05	2.830E+04	1.650E+06	1.865E+06
	ATAPSTVSPYGPEAR	3.068E+05	7.719E+04	9.788E+05	1.519E+06
	average peak area	2.111E+05	5.275E+04	1.314E+06	1.692E+06
	peak area/correction factor	2.051E+05	5.275E+04	9.248E+05	1.016E+06
SycH	ELVAFMR	0	0	1.993E+05	2.370E+05
	IWVVHLAPINEK	0	0	5.215E+04	5.568E+04
	average peak area	0	0	1.257E+05	1.463E+05
	peak area/correction factor	0	0	8.848E+04	8.788E+04
YscJ	EGNEMLALLR	2.075E+04	0	6.824E+04	1.588E+04
	peak area/correction factor	2.016E+04	0	4.801E+04	9.536E+03
YscQ	IPLPILISLR	0	0	3.135E+04	1.262E+05
	peak area/correction factor	0	0	2.206E+04	7.580E+04
YscP	ILAQGSYDLLER	0	0	2.273E+04	2.783E+04
	peak area/correction factor	0	0	1.600E+04	1.671E+04

ACKNOWLEDGEMENTS

This works was supported by NIH grant grant R01 AI061452 (P.G.)

We thank the staff at Beamline 23 ID-B for help in data collection.

The text of this chapter, in full, is a reprint of the material as it appears in the *Journal of Baceteriology*. The dissertation author was a co-primary author and the co-authors (Gamez A, Alayyoubi M, Ghassemian M, and Ghosh, P.) listed in this publication contributed to or supervised the research which forms the basis of this chapter.

REFERENCES

Adams, P.D., Afonine, P.V., Bunkóczi, G., Chen, V.B., Davis, I.W., Echols, N., Headd, J.J., Hung, L.-W., Kapral, G.J., Grosse-Kunstleve, R.W.. (2010). *PHENIX* : a comprehensive Python-based system for macromolecular structure solution. Acta Crystallogr. D Biol. Crystallogr. *66*, 213–221.

Akeda, Y., and Galán, J.E. (2005). Chaperone release and unfolding of substrates in type III secretion. Nature *437*, 911–915.

Alderwick, L.J., Molle, V., Kremer, L., Cozzone, A.J., Dafforn, T.R., Besra, G.S., and Fütterer, K. (2006). Molecular structure of EmbR, a response element of Ser/Thr kinase signaling in Mycobacterium tuberculosis. Proc. Natl. Acad. Sci. U. S. A. *103*, 2558–2563.

Andersson, K., Magnusson, K.E., Majeed, M., Stendahl, O., and Fällman, M. (1999). Yersinia pseudotuberculosis-induced calcium signaling in neutrophils is blocked by the virulence effector YopH. Infect. Immun. *67*, 2567–2574.

Baker, N.A., Sept, D., Joseph, S., Holst, M.J., and McCammon, J.A. (2001). Electrostatics of nanosystems: application to microtubules and the ribosome. Proc. Natl. Acad. Sci. U. S. A. *98*, 10037–10041.

Barison, N., Lambers, J., Hurwitz, R., and Kolbe, M. (2012). Interaction of MxiG with the cytosolic complex of the type III secretion system controls Shigella virulence. FASEB J. *26*, 1717–1726.

Barthe, P., Roumestand, C., Canova, M.J., Kremer, L., Hurard, C., Molle, V., and Cohen-Gonsaud, M. (2009). Dynamic and structural characterization of a bacterial FHA protein reveals a new autoinhibition mechanism. Struct. Lond. Engl. 1993 *17*, 568–578.

Bölin, I., Norlander, L., and Wolf-Watz, H. (1982). Temperature-inducible outer membrane protein of Yersinia pseudotuberculosis and Yersinia enterocolitica is associated with the virulence plasmid. Infect. Immun. *37*, 506–512.

Byeon, I.-J.L., Li, H., Song, H., Gronenborn, A.M., and Tsai, M.-D. (2005). Sequential phosphorylation and multisite interactions characterize specific target recognition by the FHA domain of Ki67. Nat. Struct. Mol. Biol. *12*, 987–993.

Bzymek, K.P., Hamaoka, B.Y., and Ghosh, P. (2012). Two translation products of Yersinia yscQ assemble to form a complex essential to type III secretion. Biochemistry (Mosc.) *51*, 1669–1677.

Chen, V.B., Arendall, W.B., 3rd, Headd, J.J., Keedy, D.A., Immormino, R.M., Kapral, G.J., Murray, L.W., Richardson, J.S., and Richardson, D.C. (2010). MolProbity: all-atom structure validation for macromolecular crystallography. Acta Crystallogr. D Biol. Crystallogr. *66*, 12–21.

Conchas, R.F., and Carniel, E. (1990). A highly efficient electroporation system for transformation of Yersinia. Gene *87*, 133–137.

Cornelis, G.R. (2006). The type III secretion injectisome. Nat. Rev. Microbiol. *4*, 811–825.

Datsenko, K.A., and Wanner, B.L. (2000). One-step inactivation of chromosomal genes in Escherichia coli K-12 using PCR products. Proc. Natl. Acad. Sci. U. S. A. *97*, 6640–6645.

Diepold, A., Amstutz, M., Abel, S., Sorg, I., Jenal, U., and Cornelis, G.R. (2010). Deciphering the assembly of the Yersinia type III secretion injectisome. EMBO J. *29*, 1928–1940.

Van Duyne, G.D., Standaert, R.F., Karplus, P.A., Schreiber, S.L., and Clardy, J. (1993). Atomic structures of the human immunophilin FKBP-12 complexes with FK506 and rapamycin. J. Mol. Biol. *229*, 105–124.

Emsley, P., and Cowtan, K. (2004). Coot: model-building tools for molecular graphics. Acta Crystallogr. D Biol. Crystallogr. *60*, 2126–2132.

Fields, K.A., Plano, G.V., and Straley, S.C. (1994). A low-Ca2+ response (LCR) secretion (ysc) locus lies within the lcrB region of the LCR plasmid in Yersinia pestis. J. Bacteriol. *176*, 569–579.

Ghosh, P. (2004). Process of Protein Transport by the Type III Secretion System. Microbiol. Mol. Biol. Rev. *68*, 771–795.

Gouet, P., Robert, X., and Courcelle, E. (2003). ESPript/ENDscript: Extracting and rendering sequence and 3D information from atomic structures of proteins. Nucleic Acids Res. *31*, 3320–3323.

Guttman, M., Betts, G.N., Barnes, H., Ghassemian, M., van der Geer, P., and Komives, E.A. (2009). Interactions of the NPXY microdomains of the low density lipoprotein receptor-related protein 1. Proteomics *9*, 5016–5028.

Higuchi, R., Krummel, B., and Saiki, R.K. (1988). A general method of in vitro preparation and specific mutagenesis of DNA fragments: study of protein and DNA interactions. Nucleic Acids Res. *16*, 7351–7367.

Hodgkinson, J.L., Horsley, A., Stabat, D., Simon, M., Johnson, S., da Fonseca, P.C.A., Morris, E.P., Wall, J.S., Lea, S.M., and Blocker, A.J. (2009). Three-dimensional reconstruction of the Shigella T3SS transmembrane regions reveals 12-fold symmetry and novel features throughout. Nat. Struct. Mol. Biol. *16*, 477–485.

Hofmann, K., and Bucher, P. (1995). The FHA domain: a putative nuclear signalling domain found in protein kinases and transcription factors. Trends Biochem. Sci. *20*, 347–349.

Holm, L., and Rosenström, P. (2010). Dali server: conservation mapping in 3D. Nucleic Acids Res. *38*, W545–549.

Huen, M.S.Y., Grant, R., Manke, I., Minn, K., Yu, X., Yaffe, M.B., and Chen, J. (2007). RNF8 transduces the DNA-damage signal via histone ubiquitylation and checkpoint protein assembly. Cell *131*, 901–914.

Journet, L., Agrain, C., Broz, P., and Cornelis, G.R. (2003). The needle length of bacterial injectisomes is determined by a molecular ruler. Science *302*, 1757–1760.

Kimbrough, T.G., and Miller, S.I. (2000). Contribution of Salmonella typhimurium type III secretion components to needle complex formation. Proc. Natl. Acad. Sci. U. S. A. *97*, 11008–11013.

Koster, M., Bitter, W., de Cock, H., Allaoui, A., Cornelis, G.R., and Tommassen, J. (1997). The outer membrane component, YscC, of the Yop secretion machinery of Yersinia enterocolitica forms a ring-shaped multimeric complex. Mol. Microbiol. *26*, 789–797.

Kresse, A.U., Schulze, K., Deibel, C., Ebel, F., Rohde, M., Chakraborty, T., and Guzmán, C.A. (1998). Pas, a novel protein required for protein secretion and attaching and effacing activities of enterohemorrhagic Escherichia coli. J. Bacteriol. *180*, 4370–4379.

Kumeta, H., Ogura, K., Adachi, S., Fujioka, Y., Tanuma, N., Tanuma, K., Kikuchi, K., and Inagaki, F. (2008). The NMR structure of the NIPP1 FHA domain. J. Biomol. NMR *40*, 219–224.

Lara-Tejero, M., Kato, J., Wagner, S., Liu, X., and Galán, J.E. (2011). A sorting platform determines the order of protein secretion in bacterial type III systems. Science *331*, 1188–1191.

Lathem, W.W., Price, P.A., Miller, V.L., and Goldman, W.E. (2007). A Plasminogen-Activating Protease Specifically Controls the Development of Primary Pneumonic Plague. Science *315*, 509–513.

Lountos, G.T., Tropea, J.E., and Waugh, D.S. (2012). Structure of the cytoplasmic domain of Yersinia pestis YscD, an essential component of the type III secretion system. Acta Crystallogr. D Biol. Crystallogr. *68*, 201–209.

Mahajan, A., Yuan, C., Lee, H., Chen, E.S.-W., Wu, P.-Y., and Tsai, M.-D. (2008). Structure and function of the phosphothreonine-specific FHA domain. Sci. Signal. *1*, re12.

McCormack, A.L., Schieltz, D.M., Goode, B., Yang, S., Barnes, G., Drubin, D., and Yates, J.R., 3rd (1997). Direct analysis and identification of proteins in mixtures by LC/MS/MS and database searching at the low-femtomole level. Anal. Chem. *69*, 767–776.

McDowell, M.A., Johnson, S., Deane, J.E., Cheung, M., Roehrich, A.D., Blocker, A.J., McDonnell, J.M., and Lea, S.M. (2011). Structural and functional studies on the N-terminal domain of the Shigella type III secretion protein MxiG. J. Biol. Chem. *286*, 30606–30614.

Michiels, T., Vanooteghem, J.C., Lambert de Rouvroit, C., China, B., Gustin, A., Boudry, P., and Cornelis, G.R. (1991). Analysis of virC, an operon involved in the secretion of Yop proteins by Yersinia enterocolitica. J. Bacteriol. *173*, 4994–5009.

Morita-Ishihara, T., Ogawa, M., Sagara, H., Yoshida, M., Katayama, E., and Sasakawa, C. (2006). Shigella Spa33 is an essential C-ring component of type III secretion machinery. J. Biol. Chem. *281*, 599–607.

Nott, T.J., Kelly, G., Stach, L., Li, J., Westcott, S., Patel, D., Hunt, D.M., Howell, S., Buxton, R.S., O'Hare, H.M.(2009). An intramolecular switch regulates phosphoindependent FHA domain interactions in Mycobacterium tuberculosis. Sci. Signal. *2*, ra12.

Ogino, T., Ohno, R., Sekiya, K., Kuwae, A., Matsuzawa, T., Nonaka, T., Fukuda, H., Imajoh-Ohmi, S., and Abe, A. (2006). Assembly of the type III secretion apparatus of enteropathogenic Escherichia coli. J. Bacteriol. *188*, 2801–2811.

Otwinowski, Z., and Minor, W. Processing of X-ray diffraction data collected in oscillation mode, Carter CW, Sweet RM, Macromolecular Crystallography, 1997, 307-326 (Academic Press, San Diego).

Pallen, M., Chaudhuri, R., and Khan, A. (2002). Bacterial FHA domains: neglected players in the phospho-threonine signalling game? Trends Microbiol. *10*, 556–563.

Pallen, M.J., Chaudhuri, R.R., and Henderson, I.R. (2003). Genomic analysis of secretion systems. Curr. Opin. Microbiol. *6*, 519–527.

Pennell, S., Westcott, S., Ortiz-Lombardía, M., Patel, D., Li, J., Nott, T.J., Mohammed, D., Buxton, R.S., Yaffe, M.B., Verma, C. (2010). Structural and functional analysis of phosphothreonine-dependent FHA domain interactions. Struct. Lond. Engl. 1993 *18*, 1587–1595.

Plano, G.V., and Straley, S.C. (1995). Mutations in yscC, yscD, and yscG prevent high-level expression and secretion of V antigen and Yops in Yersinia pestis. J. Bacteriol. *177*, 3843–3854.

Riordan, K.E., Sorg, J.A., Berube, B.J., and Schneewind, O. (2008). Impassable YscP substrates and their impact on the Yersinia enterocolitica type III secretion pathway. J. Bacteriol. *190*, 6204–6216.

Rosqvist, R., Bölin, I., and Wolf-Watz, H. (1988). Inhibition of phagocytosis in Yersinia pseudotuberculosis: a virulence plasmid-encoded ability involving the Yop2b protein. Infect. Immun. *56*, 2139–2143.

Ross, J.A., and Plano, G.V. (2011). A C-terminal region of Yersinia pestis YscD binds the outer membrane secretin YscC. J. Bacteriol. *193*, 2276–2289.

Schraidt, O., and Marlovits, T.C. (2011). Three-dimensional model of Salmonella's needle complex at subnanometer resolution. Science *331*, 1192–1195.

Silva-Herzog, E., Ferracci, F., Jackson, M.W., Joseph, S.S., and Plano, G.V. (2008). Membrane localization and topology of the Yersinia pestis YscJ lipoprotein. Microbiol. Read. Engl. *154*, 593–607.

Spaeth, K.E., Chen, Y.-S., and Valdivia, R.H. (2009). The Chlamydia type III secretion system C-ring engages a chaperone-effector protein complex. PLoS Pathog. *5*, e1000579.

Spreter, T., Yip, C.K., Sanowar, S., André, I., Kimbrough, T.G., Vuckovic, M., Pfuetzner, R.A., Deng, W., Yu, A.C., Finlay, B.B. (2009). A conserved structural motif mediates formation of the periplasmic rings in the type III secretion system. Nat. Struct. Mol. Biol. *16*, 468–476.

Di Tommaso, P., Moretti, S., Xenarios, I., Orobitg, M., Montanyola, A., Chang, J.-M., Taly, J.-F., and Notredame, C. (2011). T-Coffee: a web server for the multiple sequence alignment of protein and RNA sequences using structural information and homology extension. Nucleic Acids Res. *39*, W13–17.

Tong, Y., Tempel, W., Wang, H., Yamada, K., Shen, L., Senisterra, G.A., MacKenzie, F., Chishti, A.H., and Park, H.-W. (2010). Phosphorylation-independent dual-site binding of the FHA domain of KIF13 mediates phosphoinositide transport via centaurin alpha1. Proc. Natl. Acad. Sci. U. S. A. *107*, 20346–20351.

Woestyn, S., Sory, M.P., Boland, A., Lequenne, O., and Cornelis, G.R. (1996). The cytosolic SycE and SycH chaperones of Yersinia protect the region of YopE and YopH involved in translocation across eukaryotic cell membranes. Mol. Microbiol. *20*, 1261–1271.

Ye, Y., and Godzik, A. (2003). Flexible structure alignment by chaining aligned fragment pairs allowing twists. Bioinforma. Oxf. Engl. *19 Suppl 2*, ii246–255.

Chapter 4:

Functionally essential interaction between *Yersinia* YscO and the T3S4 domain of YscP

ABSTRACT

The type III secretion (T3S) system is essential to the virulence of a large number of gram-negative bacterial pathogens, including *Yersinia*. YscO is required for T3S in *Yersinia* and is known to interact with several other T3S proteins, including the chaperone SycD and the needle length regulator YscP. To define which interactions of YscO are required for T3S, we pursued model-guided mutagenesis: three conserved and surface-exposed regions of modeled YscO were targeted for multiple alanine substitutions. Most of the mutations abrogated T3S and did so in a recessive manner, consistent with a loss of function. Both functional and nonfunctional YscO mutant proteins interacted with SycD, indicating that the mutations had not affected protein stability. Likewise, both functional and nonfunctional versions of YscO were exclusively intrabacterial. Functional and nonfunctional versions of YscO were, however, distinguishable with respect to interaction with YscP. This interaction was observed only for wild-type YscO and a T3S-proficient mutant of YscO, but not for the several T3S-deficient YscO mutants of YscO. Evidence is presented that the YscO-YscP interaction is direct, and that the type III secretion substrate specificity switch (T3S4) domain of YscP is sufficient for this interaction. These results provide evidence that the interaction of YscO with YscP, and in particular the T3S4 domain of YscP, is essential to type III secretion.

INTRODUCTION

Gram-negative bacterial pathogens utilize a variety of mechanisms to survive and reproduce within their hosts. One of the most common involves the translocation of specific bacterial proteins directly from the bacterial cytosol into the cytosol of host cells by means of the type III secretion (T3S) system (Büttner, 2012; Cornelis, 2006). Such transported proteins generally have deleterious and, in many cases, toxic effects on host cells. The T3S system is conserved in *Salmonella, Shigella,* and *Yersinia* spp. among other gram-negative bacteria, and is related evolutionarily to the bacterial flagellum (Büttner, 2012; Cornelis, 2006). Of the ~20-25 proteins that comprise the T3S system, ~8-10 of these are dually conserved in the T3S and flagellar systems (Büttner, 2012). These dually conserved proteins localize to the inner bacterial membrane, either as integral membrane or peripheral membrane-associated proteins that constitute the basal body of the T3S system.

Yersinia YscO (154 residues, 19 kDa) is one such dually conserved protein (Payne and Straley, 1998). This small peripheral membrane-associated protein localizes to the inner bacterial membrane and the cytosol (Payne and Straley, 1998). YscO has also been reported to be secreted by *Y. pestis* and *enterocolitica* (Diepold et al., 2012; Payne and Straley, 1998). While YscO is essential for type III secretion (Payne and Straley, 1998), the basis for its essentiality is unknown. Several *Yersinia* T3S proteins have been shown to

interact with YscO. Among these is SycD (Evans and Hughes, 2009), which is a chaperone for the T3S translocon proteins YopB and YopD (Neyt and Cornelis, 1999). This interaction was detected through a co-purification assay using *E. coli* lysates containing SycD and a GST-YscO fusion protein. The same experiment showed that SycT, a chaperone for the translocated protein YopT, also binds YscO, albeit with lower apparent affinity (Evans and Hughes, 2009). The interactions of YscO with these T3S chaperones mirrors interactions observed for FliJ (147 residues, 17 kDa), which is the flagellar ortholog of YscO as defined by synteny and common predicted physical properties. FliJ associates with the flagellar chaperones FlgN and FliT (Evans et al., 2006), and notably, these associations occur only when these chaperones are free. These results suggest that FliJ may function by capturing released chaperones for further cycles of binding to cognate targets (Evans et al., 2006).

The *Yersinia* protein YscP also interacts with YscO (Riordan et al., 2008). YscP acts as a molecular ruler and sets the precise length of the extracellular needle-like structure of the T3S apparatus (Journet et al., 2003). The interaction between YscP and YscO was detected in *Y. enterocolitica* using a YscP-GST fusion protein that blocks the T3S system (Riordan et al., 2008). Several proteins co-purified with this blocking YscP-GST protein, including YscO and also YscN (the T3S ATPase) (Woestyn et al., 1994), YscL (the negative regulator of YscN) (Blaylock et al., 2006), and YscQ (the putative C-ring component) (Bzymek et al., 2012). Further evidence for a physical interaction between YscO and YscP comes

from the observation that the inhibition of type III secretion due to overexpression of YscP can be relieved by overexpression of YscO (Payne and Straley, 1999). Additionally, the *Chlamydia trachomatis* ortholog of YscO, CT670, has been seen to interact with the *C. trachomatis* ortholog of YscP, CT671, as determined through bacterial two-hybrid and co-purification assays in *E. coli* (Lorenzini et al., 2010).

The structures of the YscO orthologs *C. trachomatis* CT670 (Lorenzini et al., 2010) and *Salmonella* FliJ (Ibuki et al., 2011) have been determined and reveal simple α-helical coiled-coil hairpins. We used this information to model the structure of YscO and carry out model-guided mutagenesis. We identified three regions in the model that are conserved and surface-exposed. Multiple alanine-substitution mutagenesis was carried out in these regions, and most of the mutations were found to abrogate T3S. These mutations were recessive to wild-type, consistent with a loss of function. Both functional and nonfunctional YscO mutant proteins were found intrabacterially but not in the secreted fraction. This was also the case for wild-type YscO, in contrast to data reported for *Y. pestis* and *enterocolitica* (Diepold et al., 2012; Payne and Straley, 1998). Likewise, both functional and nonfunctional YscO mutant proteins interacted with SycD, suggesting that the mutations had not affected the structure or stability of YscO. The functional and nonfunctional YscO mutant proteins were, however, distinguishable with respect to interaction with YscP. Only wild-type YscO and a T3S-proficient mutant of YscO interacted with YscP, while none of the T3S-

deficient mutants of YscO did so. Evidence is presented that this interaction was direct, and that the ~100 C-terminal residues of YscP, which form the type III secretion substrate specificity switch (T3S4) domain of YscP, were sufficient for this interaction. The YscP T3S4 domain is so-named because its loss affects both the secretion of the early T3S substrate YscF, which polymerizes into the needle-like structure, and later substrates, such as the Yop effector proteins (Agrain et al., 2005). Overall, our results provide evidence that the interaction of YscO with YscP, and in particular the T3S4 domain of YscP, is essential to type III secretion.

MATERIALS AND METHODS

Generation of YscO model

A model of YscO was generated with Swiss-Model (Arnold et al., 2006) using the YscO ortholog CT670 as a template (PDB 3K29) (Lorenzini et al., 2010). The molecular model in Figure 1 was generated with PyMol (http://www.pymol.org). Sequences were aligned with ClustalW2 (Larkin et al., 2007) and depicted with EsPript (Gouet et al., 2003). COILS (Lupas et al., 1991) was used to predict coiled-coil heptad positions.

Construction of *Y. pseudotuberculosis (ΔyscO::aph)*

Homologous recombination was used to replace *yscO* with *aph*, which confers resistance to kanamycin. A PCR fragment encoding 500 basepairs (bp) of the pYV sequence upstream of *yscO*, followed by *aph* and 500 bp of the pYV sequence downstream of *yscO* was generated. The PCR product was co-electroporated with pWL204 (Lathem et al., 2007), which encodes the *red* recombinase genes and the levansucrase gene *sacB* (for sucrose counter selection), into competent *Y. pseudotuberculosis*. Bacteria were grown for 2 h in bovine heart infusion (BHI) media, and transformants were selected by plating on BHI containing 2.5 mM $CaCl_2$, 50 μg/mL kanamycin, and 5% arabinose; arabinose was included to induce the expression of the *red* recombinase genes. Transformants were plated on the above media supplemented with 10% sucrose in

order to select for the loss of pWL204. This loss was confirmed by the sensitivity of colonies to 30 μg/mL ampicillin. The proper substitution of *yscO* by *aph* was confirmed by sequencing 500 bp upstream and downstream of *aph*.

Complementation of *Y. pseudotuberculosis (ΔyscO::aph)*

Wild-type and mutant *yscO* alleles, which were generated by the QuikChange method (Agilent), were cloned into the arabinose-inducible pBAD vector. These constructs included an N-terminal Strep-tag (WSHPQFEK) for purposes of detection. The resulting plasmids were electroporated into *Y. pseudotuberculosis* (wild-type as well as *ΔyscO::aph*), and transformants were selected by growing on BHI containing 2.5 mM $CaCl_2$ and 30 μg/mL ampicillin.

To assay secretion, *Y. pseudotuberculosis* strains were cultured by shaking overnight at 26 ºC in 5 mL BHI with antibiotics as appropriate (kanamycin 50 μg/mL or ampicillin 30 μg/mL). A 1:20 dilution was made into fresh BHI containing 10 mM $MgCl_2$ and 10 mM ethylene glycol tetraacetic acid (EGTA), and the cultures were grown with shaking for two hours at 26 ºC. For strains expressing *yscO* from the pBAD vector, 0.1% arabinose was added as well. In some samples, 2.5 mM $CaCl_2$ was added in place of 10 mM $MgCl_2$ and 10 mM EGTA in order to verify that the secretion was type III. Cultures were grown at 26 ºC to an OD_{600} of 1.0, and then shifted to 37 ºC, at which time an additional 0.1% arabinose was added to strains carrying pBAD vectors. Cultures were then grown for an additional 3 h at 37 ºC. The concentration of bacteria was normalized to an

OD_{600} of 1.0 using BHI prior to separation of bacteria from the culture medium by centrifugation (4 ºC, 10 min, 3000 x *g*). The supernatant was put through a 0.22 μm filter, after which point cold trichloroacetic acid (TCA) was added to a final concentration of 10%. The samples were incubated on ice for 1 h and then pelleted by centrifugation (4 ºC, 15 min, 20,000 x *g*). The pellet was washed three times with cold acetone, resolubilized in 2x SDS-PAGE sample buffer, and boiled. Samples were resolved by Coomassie-stained 12.5% SDS-PAGE.

Western blots

Samples were resolved by 12.5-15% SDS-PAGE, and transferred to a polyvinylidene fluoride membrane (Millipore). Membranes were blocked with 20 mL of 5% milk in TBS (150 mM NaCl, 50 mM Tris, pH 8.0) for 1 hr at 26 ºC. HRP-conjugated anti-Strep Tag II monoclonal antibody (1:1000, EMD), anti-YopE polyclonal antibodies (1:1000, a gift from J. Bliska), anti-YscO polyclonal antibodies (MIPA65, 1:1000, a gift from G. Cornelis) (Diepold et al., 2012), or anti-YscP polyclonal antibodies (MIPA57, 1:1000, a gift from G. Cornelis) (Diepold et al., 2012) in 5% milk in TBS were incubated with membranes for 16 h at 4 ºC. Samples for binding assays were treated similarly, except for an additional incubation for 1 hr at 25 ºC with anti-His rabbit polyclonal antibodies (1:1000, Santa Cruz) in 5% milk in TBS. Membranes were then washed 3x with 20 mL TBS with 0.5% Tween (TBST), and incubated with HRP-conjugated goat anti-rabbit antibodies (1:5000, Santa Cruz Biotechnology) in 5% milk in TBS for

30 min at 25 ºC. Membranes were once again washed 3x with 20 mL TBST. For detection, SuperSignal West Chemiluminescent Substrate was used according to the manufacturer's instructions (Thermo).

In cases in which the membrane was stripped for probing with a different primary antibody, the membrane was incubated in 67% (w/v) guanidine HCl, 50 µM ethylene diamine tetraacetic acid (EDTA), 50 mM glycine, pH 10.8, 2.5 mM KCl, and 1.4 mM β-mercaptoethanol (β-ME) for 10 min. The membrane was then blocked and probed as above, or in the case of probing for RpoA as a loading control, the following protocol was followed. The membrane was blocked for 1 h at room temperature in TBST containing 5% BSA, washed once with TBST, and incubated for 1 h at 25 °C with primary antibody (1:1,000 mouse anti-RpoA monoclonal antibodies; Santa Cruz Biotechnology) in TBST containing 5% BSA. Three washes of the membrane in TBST (each 10 min in duration) were carried out, and the membrane was then incubated with HRP-conjugated secondary anti-mouse polyclonal antibodies (1:2,000; Santa Cruz Biotechnology) in TBST containing 5% BSA for 30 min. Following three washes with TBST (each 10 min in duration), the membrane was developed and visualized as described above.

Preparation of His-SycD, YscP-His, and His-YscP T3S4

Y. pseudotuberculosis SycD, YscP, and YscP T3S4 (residues 341-440) were cloned into pET-28b (Novagen) with an N-terminal His-tag (SycD and YscP T3S4) or C-terminal His-tag (YscP) and transformed into *Escherichia coli* BL21

(DE3). Bacteria were grown at 37 °C in Luria Broth media with 30 μg/mL kanamycin to an OD_{600} of 0.6, at which time expression was induced with 1 mM isopropyl β-D-1-thiogalactopyranoside and the bacteria were grown for 16 h further at 20 °C. Bacteria were harvested by centrifugation (4 °C, 15 min, 3000 x *g*) and resuspended in (12.5 mL per L of bacterial culture) lysis buffer (150 mM [for His-SycD] or 500 mM [for YscP-His and His-YscP T3S4] NaCl, 50 mM sodium phosphate buffer, pH 8, and 5 mM [for His-SycD] or 10 mM [for YscP-His] β-ME supplemented with protease inhibitor cocktail (1 Complete tablet per 50 mL lysis buffer, Roche). Bacteria were lysed by four passages through a high pressure homogenizer (Emulsiflex-C5, Avestin) and centrifuged (4 ºC, 30 min, 20,000 x *g*) to remove cell debris. The supernatant, which contained His-SycD, YscP-His, or His-YscP T3S4, was applied to a Ni^{2+}-NTA column equilibrated with lysis buffer containing 20 mM imidazole. After 10 column volume washes with this buffer, proteins were eluted in 5 column volumes of lysis buffer containing 250 mM (His-SycD) or 500 mM imidazole (YscP-His and His-YscP T3S4). Fractions containing His-SycD, YscP-His, or His-YscP T3S4 as visualized by Coomassie-stained 15% SDS-PAGE, were pooled and dialyzed into lysis buffer. The proteins were then concentrated by ultrafiltration (YM-3K, Pall) and further purified by size exclusion chromatography (Sephadex 200, GE Healthcare) in lysis buffer. His-SycD, YscP-His, and His-YscP T3S4 were concentrated to 45, 25, and 20 mg/mL, respectively, by ultrafiltration (YM-3K, Amicon). Concentrations of these proteins was determined using calculated

molar ε_{280} of 10,720 $M^{-1}cm^{-1}$ for SycD-His, 25,470 $M^{-1}cm^{-1}$ for YscP-His, and 16,244 $M^{-1}cm^{-1}$ for His-YscP T3S4.

Purification of Strep-YscO

Y. pseudotuberculosis (Δ*yscO::aph*) complemented with *yscO* containing a Strep-tag was grown at 28 ºC to an OD_{600} of 0.6, induced with 2.0% arabinose, and grown further for 4 h. Bacteria were then harvested by centrifugation (4 ºC, 15 min, 3,000 x *g*), solubilized in buffer A (300 mM NaCl, 50 mM Tris, pH 8, 1 mM EDTA, and 5 mM β-ME), and lysed by sonication. The lysate was centrifuged (4 ºC, 20 min, 20,000 x *g*) to remove insoluble material. The supernatant was incubated at 4 °C for 16 h with 1 mL Strep-Tactin beads (IBA) that had been pre-equilibrated with buffer A. The beads were then washed with 20 column volumes of buffer A, followed by centrifugation (26 ºC, 30 s, 3,000 x *g*). Strep-YscO was then eluted from the beads using buffer A containing 2.5mM desthiobiotin. Eluted fractions containing YscO, as visualized by Coomassie-stained 15% SDS-PAGE, were pooled and concentrated by ultrafiltration (YM-3K, Amicon).

Binding Assays

Y. pseudotuberculosis (Δ*yscO::aph*) complemented with various alleles of *yscO* was grown at 28 ºC to an OD_{600} of 0.6, induced with 0.1% arabinose, and grown further for 4 h. Bacteria were then harvested by centrifugation (4 ºC, 15

min, 3,000 x *g*), solubilized in buffer A (300 mM NaCl, 50 mM Tris, pH 8, 1 mM EDTA, and 5 mM β-ME), and lysed by sonication. The lysate was centrifuged (4 ºC, 20 min, 20,000 x *g*) to remove insoluble material. The supernatant was incubated at 4 °C for 16 h with 100 µL Strep-Tactin beads (IBA) that had been pre-equilibrated with buffer A. The beads were then washed 2-3x with 200 µL of buffer A, with a centrifugation step (26 ºC, 30 s, 3,000 x *g*) between each wash. His-SycD (3 µM), YscP-His (1 µM), or His-YscP T3S4 (5 µM) was incubated with the beads in 200 µL of buffer A supplemented with 0.1% Triton for 1 h at 4 ºC, followed by five washes of the beads with the same buffer; each wash was followed by a centrifugation step (26 ºC, 30 s, 3,000 x *g*). The beads were then boiled in 2x SDS-PAGE sample buffer, and the samples were analyzed by Western blotting.

For the YscO-YscP binding assay using purified components, YscP-His was incubated at 4 °C with 50 µL Ni^{2+}-NTA beads (Sigma) for 1 h, which had been equilibrated with binding buffer (300mM NaCl, 50 mM sodium phosphate, pH 8, 10 mM imidazole, and 10 mM βME). Strep-YscO was incubated with the resin in 100 µL binding buffer for 1 h at 4 ºC, followed by five washes of 200 µL each of the beads with the same buffer; each wash was followed by a centrifugation step (4 ºC, 30 sec, 3,000 x *g*). The beads were then incubated with binding buffer containing 500 mM imidazole for 10 min followed by centrifugation (26 ºC, 30 sec, 3,000 x *g*). The eluted fraction along with other fractions were visualized by Coomassie-stained 15% SDS-PAGE.

RESULTS

Mutagenesis of conserved surface-exposed patches

Sequence and structural analyses indicate that YscO is likely to form an α-helical coiled-coil hairpin structure that closely resembles the structures of the YscO orthologs *C. trachomatis* CT670 (14) and *Salmonella* FliJ (Ibuki et al., 2011). Based on this, we generated a structural model for YscO using Swiss-Model (Arnold et al., 2006), and identified residues that are predicted to be solvent exposed and are also conserved within the YscO family of proteins (Fig. 1). We targeted three conserved solvent-exposed patches, called highly conserved regions (HCR) 1, 2, and 3, for alanine substitutions. HCRs 1 and 3 flank one another on the coiled coil and are distal to HCR2, which lies at the predicted hairpin turn. Four residues were substituted with alanines at each of the HCRs: Arg12 (predicted to occupy the *g* position of the heptad repeat), Arg15 (*c*), Glu17 (*e*), and Lys18 (*f*) for HCR1; Gln73 (*e*), Arg74 (*f*), Arg80 (*e*), and Glu81 (*f*) for HCR2; and Arg115 (*b*), Lys120 (*g*), Phe121 (*c*), and Leu124 (*f*) for HCR3. For HCR1, we also constructed a mutant having only the last three residues substituted with alanines (i.e., all but Arg12); this mutant was designated HCR1.3.

Type III secretion

To determine if these mutations had affected T3S, we first created a *Y. pseudotuberculosis* strain lacking *yscO* through replacement of this gene with

aph. Consistent with prior results, the deletion of *yscO* led to loss of secretion (3) (Fig. 2a). By comparison, wild-type *Y. pseudotuberculosis* secreted proteins in a calcium-dependent manner (i.e., at low but not high calcium concentration), which is diagnostic of T3S in *Yersinia*. The deletion of *yscO* was found to be non-polar, as *yscO* expressed inducibly from the *araC* promoter of a pBAD plasmid rescued T3S (Fig. 2a). This was shown to be a specific effect, as T3S was not rescued in the absence of arabinose induction of *yscO*. The induced expression of YscO was verified through Western blot detection of a Strep-tag included with pBAD-borne *yscO*. The α subunit of RNA polymerase (RpoA) was used as a loading control for this experiment, as its expression is independent of the T3S. The *yscO* HCR mutants were introduced into *Y. pseudotuberculosis* (*ΔyscO::aph*) on the pBAD plasmid, and their ability to complement T3S was evaluated. While *yscO* HCR1.3 was fully functional in rescuing T3S, none of the other mutants restored function. Each of the substitution mutants produced quantities of YscO equivalent to that of pBAD-borne wild-type YscO, as detected by Western blot. These results indicate that the defects in T3S of the *yscO* HCR1, 2, and 3 substitution mutants are not due to changes in expression level. It is worth noting that the functional HCR1.3 substitution mutant differs from the nonfunctional HCR1 substitution mutant by a single residue, Arg12. These results thus highlight a critical role for Arg12 in T3S function, along with the surface patches encompassed by HCR2 and 3.

We further characterized the loss of T3S in *yscO* HCR1, 2, and 3 by determining whether these were dominant or recessive with respect to endogenous, wild-type *yscO*. The *yscO* HCR mutants were inducibly expressed in wild-type *Y. pseudotuberculosis*, and their effect on T3S was evaluated. We found that the *yscO* HCR mutants were recessive, as T3S was maintained for all the mutants (Fig. 2b). These data are consistent with the substitutions in HCR1, 2, and 3 resulting in a loss of function.

YscO has been reported to be secreted by *Y. pestis* and *Y. enterocolitica* (Diepold et al., 2012; Payne and Straley, 1998). We wondered whether the loss of T3S in *yscO* HCR1, 2, and 3 resulted from a defect in YscO secretion. Since these mutations led to a loss of secretion, we expressed them in wild-type *Y. pseudotuberculosis* and asked whether the mutant YscO proteins were present in the type III secreted fraction, as detected via their Strep-tag. Surprisingly, while the mutant YscO proteins were evident in the intrabacterial fraction, they were not evident in the secreted fraction (Fig. 3). This included both functional (i.e., YscO HCR1.3) and nonfunctional (i.e., YscO HCR1, 2, and 3) mutants. Type III secretion was confirmed to have occurred in these strains, as YopE was detected in the secreted fraction by Western blot using anti-YopE antibodies. As expected, YopE was also found in the intrabacterial fraction.

Due to the discrepancy between these results showing that YscO is not secreted and prior results showing that it is (Diepold et al., 2012; Payne and Straley, 1998), we next examined secretion of endogenous YscO by *Y.*

pseudotuberculosis. For this, we used polyclonal anti-YscO antibodies, which had been used previously for detection of *Y. entercolitica* YscO (Diepold et al., 2012). Strep-tagged YscO purified from *Y. pseudotuberculosis* was used as a positive control for these experiments. The polyclonal anti-YscO antibodies were cross-reactive, but we were able to detect YscO in the intrabacterial fraction at its correct molecular mass; this protein was not present in *Y. pseudotuberculosis* (*ΔyscO::aph*) (Fig. 3). However, as above, YscO was not evident in the type III secreted fraction, which was confirmed to contain YopE. Likewise, YscO was not detected in the secreted fraction of *Y. pseudotuberculosis* complemented with any of the *yscO* HCR mutants. We draw the conclusion from this experiment that YscO is not secreted by *Y. pseudotuberculosis* and further that secretion of YscO is not required for type III secretion. At present, it is not clear why there is a discrepancy with prior results (3, 4). However, the more important point for this study is that the T3S-proficient *yscO* HCR1.3 mutant was indistinguishable from the T3S-deficient *yscO* HCR1, 2, and 3 mutants with regard to YscO secretion.

Interaction with SycD

To identify the mechanistic basis for the defects in HCR1, 2, and 3, we examined interactions between YscO and the chaperone SycD. YscO produced recombinantly in *E. coli* was found to form insoluble inclusion bodies that were recalcitrant to refolding (data not shown). Therefore, YscO was obtained from *Y. pseudotuberculosis* for this experiment. We applied lysates of *Y.*

pseudotuberculosis that had been induced for expression of Strep-tagged YscO to Strep-Tactin beads, which were then washed to remove nonspecifically bound proteins. To these beads, we then added His-tagged SycD that had been expressed in *E. coli* and purified by metal chelation chromatography. The Strep-Tactin beads were once again washed to eliminate nonspecific binding, and proteins remaining bound to the beads were co-precipitated and visualized by Western blot. We probed the Western blot membrane simultaneously with anti-His and anti-Strep tag antibodies to visualize both YscO and SycD. In agreement with a previous report (Evans and Hughes, 2009), we found that wild-type YscO interacted with SycD (Fig. 4). This was a specific effect as no binding of His-tagged SycD to the Strep-Tactin beads occurred in the absence of Strep-tagged YscO being induced. Notably, all of the YscO substitution mutants, both functional (i.e., HCR1.3) and nonfunctional (i.e., HCR1, 2, and 3), were observed to bind SycD (Fig. 4). The maintenance of SycD interaction for these YscO alanine-substitution mutants attests to the structural integrity and stability of these proteins. These results also indicate that the defects in T3S for the HCR1, 2, and 3 mutants are not attributable to interaction with SycD.

Interaction with YscP

We next examined the interaction of YscO with YscP, in the same manner as above using His-tagged YscP which had been expressed in *E. coli* and purified. We found that YscP was sensitive to proteolytic degradation, resulting in two to

three prominent degradation products along with intact YscP, as detected by Western blot (Fig. 5). Intact YscP and all its visible degradation products were found to interact with wild-type YscO (Fig. 5). Most important, while the functional HCR1.3 substitution mutant interacted with YscP, the nonfunctional HCR1, 2, and 3 substitution mutants did not interact with YscP. These results indicate that the defects in T3S for the HCR1, 2, and 3 are attributable to the loss of interaction with YscP.

Since these experiments were carried out with YscP produced in *E. coli*, we turned to *Y. pseudotuberculosis* to verify the interaction between YscO and YscP. We induced expression of pBAD-encoded wild-type YscO or YscO HCR1 in *Y. pseudotuberculosis* (*ΔyscO::aph*), and carried out a co-precipitation assay using Strep-Tactin beads (Fig. 6a). We probed for the presence of YscP in the co-precipitated fraction using anti-YscP antibodies. YscP was observed to interact with wild-type YscO but not YscO HCR1, confirming the results presented above.

We next asked whether the interaction between YscO and YscP was direct. For this, sufficient quantities of *Y. pseudotuberculosis* Strep-YscO were purified to be visualized by Coomassie stained SDS-PAGE. To this was added purified YscP-His produced in *E. coli*, and the interaction between these two proteins was assayed by a Ni^{2+}-NTA coprecipitation assay (Fig. 6b). While there were some impurities (and truncation products in the case of YscP) that co-purified with YscO and YscP, these two proteins were the dominant species and

found to interact specifically. This result provides strong evidence that the interaction between YscO and YscP is direct.

As the data in Figure 5 showed that YscO bound the smallest YscP degradation product visible, we asked whether there were domains of YscP that were sufficient for interaction with YscO. Since the His-tag on YscP was at its C-terminus, we concentrated on the C-terminal T3S4 domain of YscP (residues 341-440). As above, the YscP T3S4 domain was expressed as a His-tagged protein in *E. coli*, purified, and incubated with lysates of *Y. pseudotuberculosis.* Similarly to intact YscP, only wild-type YscO and the functional HCR1.3 mutant interacted with the YscP TS34 domain, while the nonfunctional HCR1, 2, and 3 mutants showed no interaction (Fig. 7).

Collectively, these results indicate that the interaction between YscO and YscP is required for T3S, and that the T3S4 domain of YscP is sufficient for this interaction.

DISCUSSION

We have used model-guided mutagenesis to characterize the interactions of YscO with SycD and YscP. YscO is predicted to have a simple α-helical coiled-coil hairpin structure, as seen in its orthologs *Chlamydia* CT670 (Lorenzini et al., 2010) and *Salmonella* FliJ (Ibuki et al., 2011). The hairpin structure in FliJ has been noted to resemble part of the γ subunit of F_oF_1-ATP synthase (Ibuki et al., 2011). In accordance with this structural similarity, FliJ was shown to promote hexameric ring assembly of the flagellar ATPase FliI by inserting into the center of the FliI ring (Ibuki et al., 2011), just as the γ subunit does in the F_oF_1-ATP synthase. However, YscO is dissimilar from FliJ with respect to this function. YscO has been shown to be dispensable for the assembly of the *Yersinia* T3S ATPase YscN, as judged by the formation of fluorescent foci by an EGFP-YscN fusion protein in *Y. enterocolitica* regardless of the presence of YscO (Diepold et al., 2012).

The structural model of YscO made it possible to identify residues that are likely to be conserved and exposed to the surface for interaction with binding partners. We identified three conserved and exposed regions (i.e., HCR1, 2, and 3) and subjected these to multiple alanine substitution mutagenesis. These regions, in the case of HCR1 and HCR3, were near the base of the hairpin or, in the case of HCR2, near the turn of the hairpin. Four alanine substitutions each were created in HCR1, 2, and 3. An additional mutant, HCR1.3, was constructed

that contained only three of the four substitutions of HCR1. The HCR1.3 mutant was highly useful for comparison, as it was unaffected for type III secretion. In contrast, HCR1, 2, and 3 were deficient for type III secretion. In all cases, equivalent levels of YscO were evident, indicating that the defects in HCR1, 2, and 3 were not due to changes in expression level. These three T3S-deficient mutants were recessive to wild-type *yscO*, consistent with a loss of function.

In contrast to prior reports that indicated that YscO is itself secreted by *Y. pestis* and *entercolitica* (Diepold et al., 2012; Payne and Straley, 1998), we did not detect secretion of YscO by *Y. pseudotuberculosis*. This was the case even though we used the same antibodies as had been used for *Y. entercolitica* YscO (98% sequence identity between *Y. pseudotuberculosis* and *enterocolitica* YscO) (Diepold et al., 2012). The basis for this difference is not clear at present. We note that no functional significance has been attributed to the secretion of YscO, but the more important point for this study is that the functional and nonfunctional versions of YscO were indistinguishable with respect to YscO secretion.

We examined whether the T3S defects of the YscO HCR mutants were attributable to defects in interactions of YscO with SycD and YscP. We found that all the YscO mutants bound recombinant SycD, regardless of whether these mutants were competent for type III secretion. The maintenance of interaction with SycD suggests that the alanine substitutions affected neither the structure nor stability of YscO. These results also suggest that portions of YscO outside of HCR1, 2, and 3 are responsible for binding SycD. Because of all the YscO

mutants bind SycD, these data do not address whether the interaction between YscO and SycD is functionally important; this issue awaits further experimentation.

In contrast to the results with SycD, we found that interactions of YscO with YscP strictly correlated with type III secretion. Wild-type and HCR1.3 YscO, which were competent for type III secretion, bound recombinant YscP, but HCR1, 2, and 3, which were incompetent for type III secretion, did not. This YscO-YscP interaction was confirmed in *Y. pseudotuberculosis*, and experiments using purified components provided evidence that the interaction was direct. We noticed that YscP was prone to proteolytic digestion during purification, and that the smallest visible fragment of C-terminally His-tagged YscP bound YscO. This suggested that the C-terminal T3S4 domain of YscP may be sufficient to bind YscO. We carried out interaction experiments with recombinant YscP T3S4, and verified that the YscP T3S4 domain is sufficient to interact with YscO. YscO Arg12 appears to be critical to this interaction, as this residue is the only difference between YscO HCR1.3, which binds the YscP T3S4 domain, and HCR1, which does not.

What role might the interaction between YscO and YscP play in type III secretion? One possibility is suggested by the observation that YscO interacts with YscU, a transmembrane protein that is involved in controlling the substrate specificity of type III secretion (Allaoui et al., 1994; Edqvist et al., 2003). YscO was found to co-purify in *Y. enterocolitica* with a GST fusion to the cytoplasmic

domain of YscU (Riordan and Schneewind, 2008). The cytoplasmic domain of YscU undergoes autoproteolytic cleavage (Riordan and Schneewind, 2008; Sorg et al., 2007), and the interaction with YscO was best in a mutant of the C-terminal domain of YscU (G270N) that is incapable of undergoing this cleavage. This suggests that YscO associates with YscU prior to its autocleavage. As noted above, YscP is also involved in controlling substrate specificity (Edqvist et al., 2003). While an interaction between YscP and YscU has not been observed, it is noteworthy that the phenotype resulting from loss of *yscP* is suppressed by a mutation in the cytoplasmic domain of YscU (Edqvist et al., 2003). Thus, these results along with our observations raise the possibility that YscO functions as a bridge between the secretion specificity controlling proteins YscP and YscU. With the evidence presented here that the interaction between YscO and the YscP T3S4 domain is essential to type III secretion, this and other possibilities can be tested in greater details.

FIGURES AND TABLES

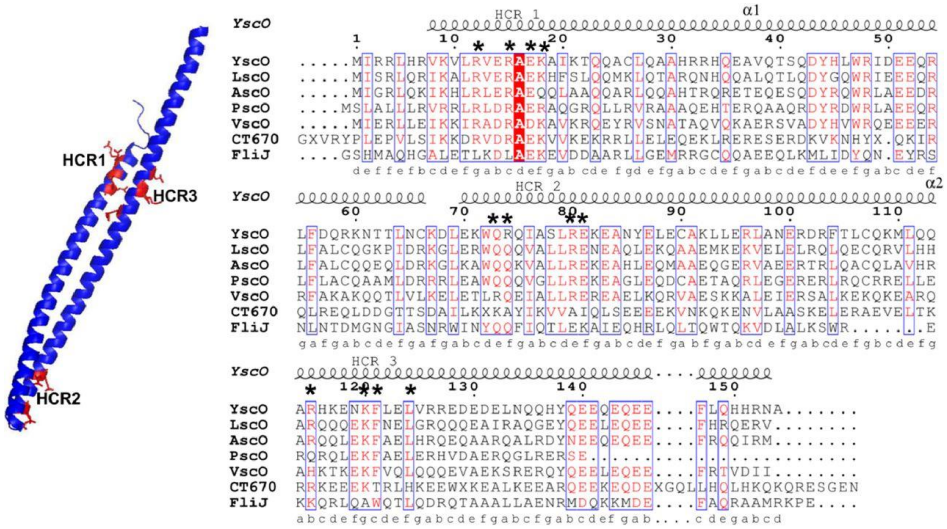

Figure 4.1 Model of YscO.
Left, a model of YscO shown in ribbon representation. The locations of HCR1, 2, and 3 are in red, with residues targeted for mutagenesis shown in bonds representation. Right, multiple sequence alignment of *Y. pseudotuberculosis* YscO, *Photorhabdus luminescens* LscO, *Aeromonas hydrophila* AscO, *Vibrio alginolyticus* VscO, *Pseudomonas aeruginosa* PscO, *C. trachomatis* CT670, and *Salmonella* FliJ. The secondary structure shown above the sequences corresponds to the model of YscO, and the letters below the sequences correspond to heptad register positions predicted for YscO. The stars indicate alanine-substituted residues.

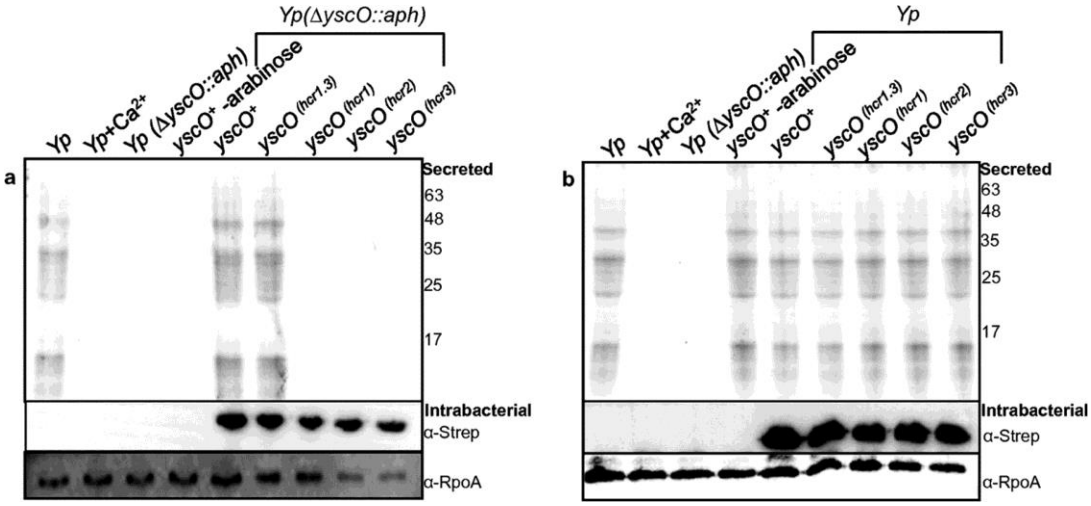

Figure 4.2 Type III secretion.
A. Top, proteins secreted into the extracellular media through the T3S system by wild-type *Y. pseudotuberculosis* (Yp); wild-type *Y. pseudotuberculosis* in high calcium concentration (Yp+Ca^{2+}); *Y. pseudotuberculosis* (Δ*yscO::aph*); *Y. pseudotuberculosis* (Δ*yscO::aph*) transformed with a plasmid encoding inducible wild-type *yscO*, without induction (*yscO*$^{+}$ -arabinose) or with induction (*yscO*$^{+}$) of *yscO* expression; and *Y. pseudotuberculosis* (Δ*yscO::aph*) transformed with pBAD encoding inducible *yscO* HCR1.3, 1, 2, or 3 (all induced). Proteins were detected by Coomassie-stained SDS-PAGE. Molecular mass markers are indicated at right. Middle, expression level of intrabacterial, plasmid-encoded Strep-tagged YscO, as visualized by Western blot using an anti-Strep Tag antibody. Bottom, expression level of intrabacterial RpoA, which served as a loading control, as visualized by Western blot using anti-RpoA antibodies.
B. Same as in panel **a**, except plasmid-encoded *yscO* was introduced into wild-type *Y. pseudotuberculosis*

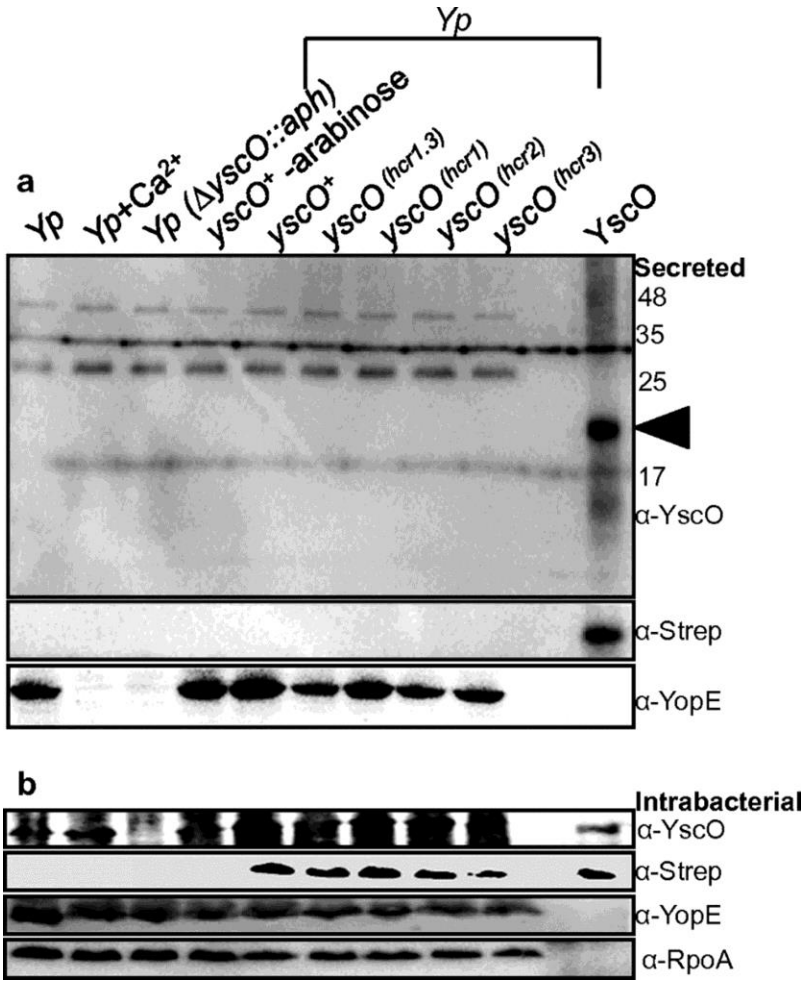

Figure 4.3 Intrabacterial localization of YscO.
a. Samples shown in Figure 2b were analyzed by Western blot using anti-YscO (top), anti-Strep tag (middle), and anti-YopE (lower) antibodies. The last lane, which is separated from the others by an empty lane, contains purified Strep-YscO, whose position is indicated by the arrowhead. Molecular mass markers are indicated at right.
b. Intrabacterial expression levels of proteins analyzed in panel **a** using anti-YscO, anti-Strep tag, and anti-YopE antibodies. Additionally, the intrabacterial expression level of RpoA was detected with anti-RpoA antibodies as a loading control.and when it is activated, as the peak of the activity curve is normally distributed, as described in the methods.

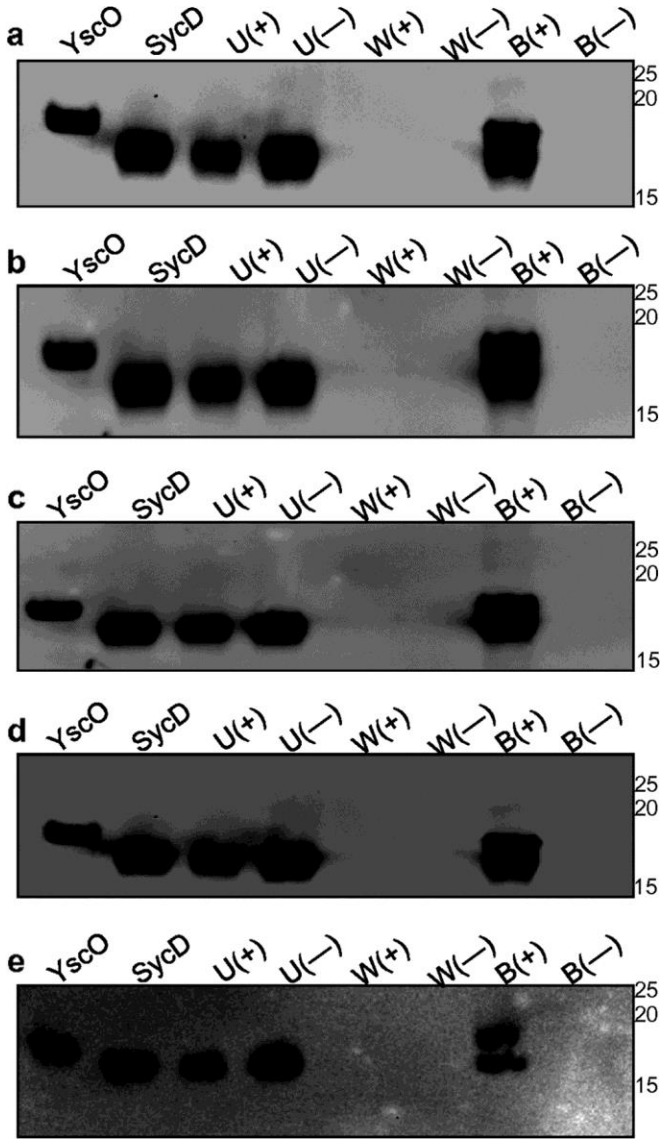

Figure 4.4 Interaction between YscO and SycD.
Lysates from *Y. pseudotuberculosis* that were induced ('+') or uninduced ('—') for expression of Strep-tagged (**a**) wild-type YscO, **(b**) YscO HCR1.3, (**c**) YscO HCR1, (**d**) YscO HCR2, or (**e**) YscO HCR3 were applied to StrepTactin beads, and purified His-tagged SycD was added to this. After washing the StrepTactin beads, proteins remaining bound to the beads were analyzed by Western blot using anti-Strep tag and anti-His tag antibodies simultaneously. The first two lanes show the input levels of YscO and SycD in the experiment. 'U' signifies the unbound fraction, 'W' the final wash fraction, and 'B' the bound fraction

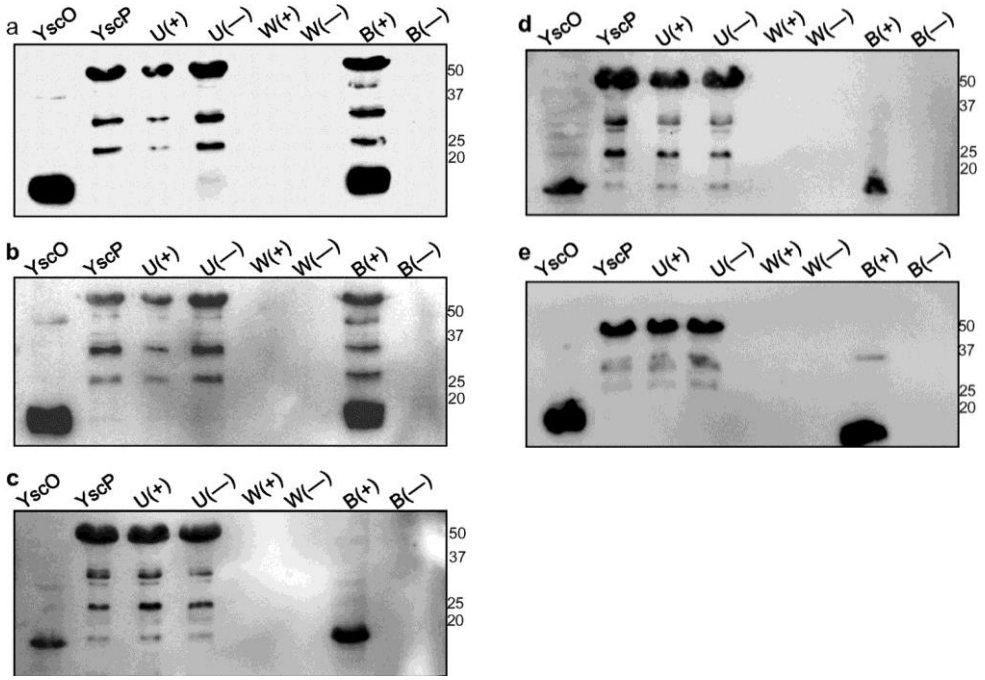

Figure 4.5 Interaction between YscO and YscP.
The format is the same as in Figure 4.4, except that His-tagged YscP was used instead of His-tagged SycD.

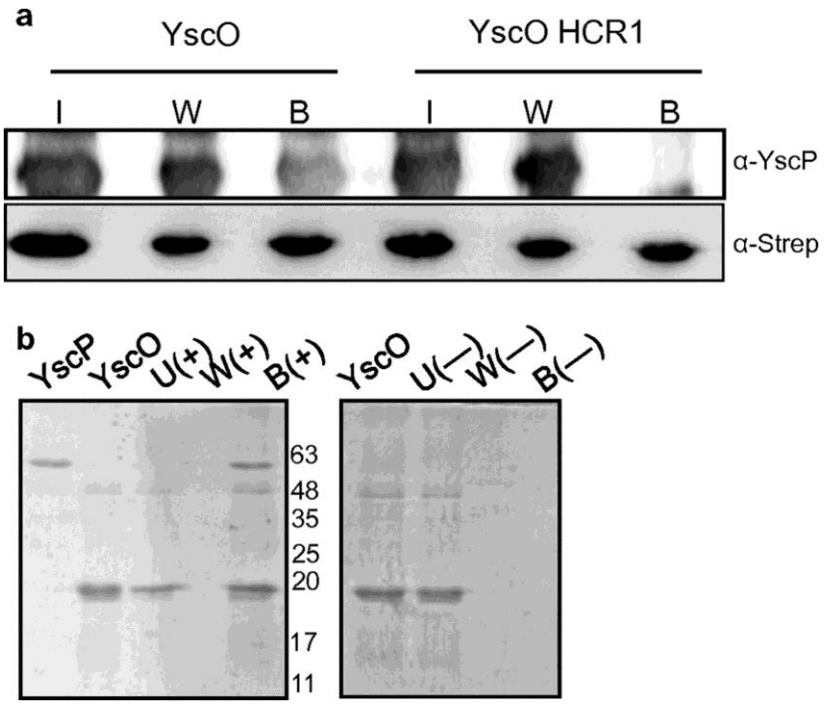

Figure 4.6 YscO-YscP interaction in *Yersinia* and the interaction detected by Coomassie staining.

a. Lysates from *Y. pseudotuberculosis* that were induced for expression of Strep-tagged wild-type YscO (left) or nonfunctional YscO HCR1 (right) were applied to StrepTactin beads. After washing the StrepTactin beads, proteins remaining bound to the beads were analyzed by Western blot using anti-YscP and anti-Strep tag antibodies. 'I' signifies the input, 'W' the final wash fraction, and 'B' the bound fraction.

b. Purified His-tagged YscP was applied to Ni-NTA beads and purified Strep-tagged YscO was added to this (+). To serve as a negative control (—) purified Strep-tagged YscO was added to Ni-NTA beads alone. After washing the beads, proteins were eluted from the beads and visualized by Coomassie-stained 12.5% SDS-PAGE. The "YscP" and "YscO" lanes indicate the input levels of each protein used in the experiment. 'U' signifies the unbound fraction, 'W' the final wash fraction, and 'B' the bound fraction. The two panels are from the same gel. Molecular mass markers are indicated between the two panels.

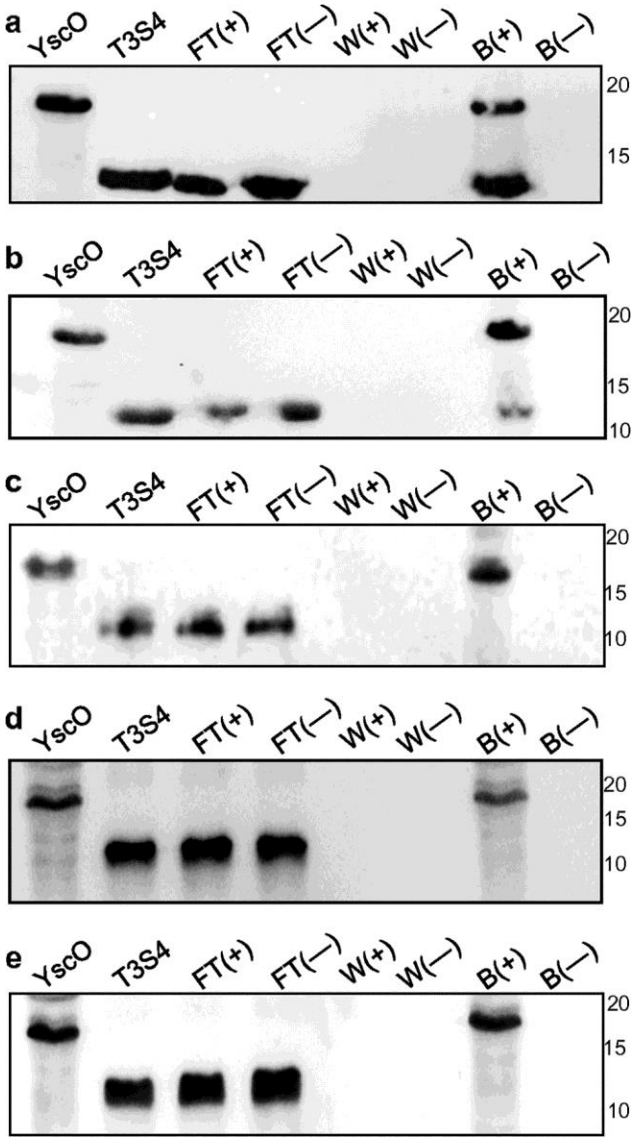

Figure 4.7 Interaction between YscO and the YscP T3S4 domain.
The format is the same as in Figure 4.4, except that the His-tagged T3S4 domain of YscP was used instead of His-tagged SycD.

ACKNOWLEDGEMENTS

This work was supported by NIH grant R01 AI061452 (PG).

The text of this chapter, in full, is a reprint of the material as it appears in the *Journal of Bacteriology*. The dissertation author was the primary researcher and/or author and the co-author (P. Ghosh) listed in this publication contributed to or supervised the research which forms the basis of this chapter.

REFERENCES

Agrain, C., Callebaut, I., Journet, L., Sorg, I., Paroz, C., Mota, L.J., and Cornelis, G.R. (2005). Characterization of a Type III secretion substrate specificity switch (T3S4) domain in YscP from Yersinia enterocolitica. Mol. Microbiol. *56*, 54–67.

Allaoui, A., Woestyn, S., Sluiters, C., and Cornelis, G.R. (1994). YscU, a Yersinia enterocolitica inner membrane protein involved in Yop secretion. J. Bacteriol. *176*, 4534–4542.

Arnold, K., Bordoli, L., Kopp, J., and Schwede, T. (2006). The SWISS-MODEL workspace: a web-based environment for protein structure homology modelling. Bioinforma. Oxf. Engl. *22*, 195–201.

Blaylock, B., Riordan, K.E., Missiakas, D.M., and Schneewind, O. (2006). Characterization of the Yersinia enterocolitica Type III Secretion ATPase YscN and Its Regulator, YscL. J. Bacteriol. *188*, 3525–3534.

Büttner, D. (2012). Protein export according to schedule: architecture, assembly, and regulation of type III secretion systems from plant- and animal-pathogenic bacteria. Microbiol. Mol. Biol. Rev. MMBR *76*, 262–310.

Bzymek, K.P., Hamaoka, B.Y., and Ghosh, P. (2012). Two translation products of Yersinia yscQ assemble to form a complex essential to type III secretion. Biochemistry (Mosc.) *51*, 1669–1677.

Cornelis, G.R. (2006). The type III secretion injectisome. Nat. Rev. Microbiol. *4*, 811–825.

Diepold, A., Wiesand, U., Amstutz, M., and Cornelis, G.R. (2012). Assembly of the Yersinia injectisome: the missing pieces. Mol. Microbiol. *85*, 878–892.

Edqvist, P.J., Olsson, J., Lavander, M., Sundberg, L., Forsberg, A., Wolf-Watz, H., and Lloyd, S.A. (2003). YscP and YscU regulate substrate specificity of the Yersinia type III secretion system. J. Bacteriol. *185*, 2259–2266.

Evans, L.D.B., and Hughes, C. (2009). Selective binding of virulence type III export chaperones by FliJ escort orthologues InvI and YscO. FEMS Microbiol. Lett. *293*, 292–297.

Evans, L.D.B., Stafford, G.P., Ahmed, S., Fraser, G.M., and Hughes, C. (2006). An escort mechanism for cycling of export chaperones during flagellum assembly. Proc. Natl. Acad. Sci. U. S. A. *103*, 17474–17479.

Gouet, P., Robert, X., and Courcelle, E. (2003). ESPript/ENDscript: Extracting and rendering sequence and 3D information from atomic structures of proteins. Nucleic Acids Res. *31*, 3320–3323.

Ibuki, T., Imada, K., Minamino, T., Kato, T., Miyata, T., and Namba, K. (2011). Common architecture of the flagellar type III protein export apparatus and F- and V-type ATPases. Nat. Struct. Mol. Biol. *18*, 277–282.

Journet, L., Agrain, C., Broz, P., and Cornelis, G.R. (2003). The needle length of bacterial injectisomes is determined by a molecular ruler. Science *302*, 1757–1760.

Larkin, M.A., Blackshields, G., Brown, N.P., Chenna, R., McGettigan, P.A., McWilliam, H., Valentin, F., Wallace, I.M., Wilm, A., Lopez, R.., Thompson, JD., Gibson, TJ., Higgins, DG. (2007). Clustal W and Clustal X version 2.0. Bioinforma. Oxf. Engl. *23*, 2947–2948.

Lathem, W.W., Price, P.A., Miller, V.L., and Goldman, W.E. (2007). A Plasminogen-Activating Protease Specifically Controls the Development of Primary Pneumonic Plague. Science *315*, 509–513.

Lorenzini, E., Singer, A., Singh, B., Lam, R., Skarina, T., Chirgadze, N.Y., Savchenko, A., and Gupta, R.S. (2010). Structure and protein-protein interaction studies on Chlamydia trachomatis protein CT670 (YscO Homolog). J. Bacteriol. *192*, 2746–2756.

Lupas, A., Van Dyke, M., and Stock, J. (1991). Predicting coiled coils from protein sequences. Science *252*, 1162–1164.

Neyt, C., and Cornelis, G.R. (1999). Role of SycD, the chaperone of the Yersinia Yop translocators YopB and YopD. Mol. Microbiol. *31*, 143–156.

Payne, P.L., and Straley, S.C. (1998). YscO of Yersinia pestis is a mobile core component of the Yop secretion system. J. Bacteriol. *180*, 3882–3890.

Payne, P.L., and Straley, S.C. (1999). YscP of Yersinia pestis is a secreted component of the Yop secretion system. J. Bacteriol. *181*, 2852–2862.

Riordan, K.E., and Schneewind, O. (2008). YscU cleavage and the assembly of Yersinia type III secretion machine complexes. Mol. Microbiol. *68*, 1485–1501.

Riordan, K.E., Sorg, J.A., Berube, B.J., and Schneewind, O. (2008). Impassable YscP substrates and their impact on the Yersinia enterocolitica type III secretion pathway. J. Bacteriol. *190*, 6204–6216.

Sorg, I., Wagner, S., Amstutz, M., Müller, S.A., Broz, P., Lussi, Y., Engel, A., and Cornelis, G.R. (2007). YscU recognizes translocators as export substrates of the Yersinia injectisome. EMBO J. *26*, 3015–3024.

Woestyn, S., Allaoui, A., Wattiau, P., and Cornelis, G.R. (1994). YscN, the putative energizer of the Yersinia Yop secretion machinery. J. Bacteriol. *176*, 1561–1569.

Chapter 5:

Construction of a vector to identify binding partners to the 5' secretion signal of YopE using reverse-CLIP and RaPID techniques

ABSTRACT

Many gram-negative bacteria are able to subvert the host immune response by employing the type III secretion system. *Yersinia* spp. secrete Yops (*Yersinia* outer proteins) via the type III pathway in response to environmental cues. One of the fundamental and unsolved problems in the T3S system is how the secretion signals in these Yops are recognized. In this chapter, I constructed two vectors to identify potential binding partners to the 5' secretion signal of *yopE* mRNA using reverse-CLIP and RaPID techniques. These two techniques use RNA aptamers fused to the 5' mRNA signal sequence of *yopE* and utilized the high affinity of streptavidin as a means of affinity purifying components associated with 5' signal. The RaPID technique was found to be a more promising option than the reverse-CLIP technique. The next steps for progress with the RaPID technique are to ensure that sufficient mRNA is being purified for mass spectrometric characterization as well as determining optimal UV crosslinking conditions.

INTRODUCTION

Two secretion signals are present in most effectors. The first is a 5'/N-terminal signal, which is present in all effectors and has been shown to be sufficient for secretion into the media, and in some effectors, translocation into host cells. The designation for the 5'/N-terminal signal originates from the fact that evidence exists that the signal resides in the first ~15 codons of the mRNA encoding the effector (Anderson and Schneewind, 1997) , and evidence also exists that the signal resides in the N-terminal ~15 amino acid residues of the effector (Lloyd et al., 2001). These two scenarios are not exclusionary. The second signal is downstream of the N-terminal signal and is responsible for binding a T3S chaperone. This signal is present only in some effectors, and in those effectors, has been shown to be required for translocation (Sorg et al., 2005). The effector YopE has been well studied and contains both a 5'/N-terminal signal and a chaperone-binding signal (Anderson and Schneewind, 1997; Lloyd et al., 2001).

The strongest evidence for the 5’ mRNA signal model is that synonymous changes to the mRNA have been shown to abrogate secretion. However, other synonymous changes to the mRNA have been shown to be tolerated (Ramamurthi and Schneewind, 2005). These two different signals may both be utilized, but at different times of infection.

A major impediment to understanding how the 5'/N-terminal signal functions is the lack of identified receptors. No common amino acid or peptide sequence could be identified among the secretion signals. Systematic mutagenesis of the secretion signal yielded mutants defective in Yop translocation; however, no point mutants could be identified that specifically abolished secretion. Previous studies have shown mutations that completely altered the peptide sequences of these signals also failed to prevent secretion.

This chapter is focused on the 5' mRNA signal, and uses the effector YopE as the subject of study. I wanted to develop a construct I could use to identify potential receptors for the 5' signal through *in vivo* crosslinking coupled with mass spectrometry. Two different small RNA tags, or aptamers, were fused to the 5' mRNA signal sequence of *yopE*. Both aptamers take advantage of the high affinity binding of streptavidin. The first is the S1 RNA aptamer, which binds streptavidin directly (Srisawat and Engelke, 2001).

The S1 aptamer was originally developed by Srisawat and Engelke (2001) to isolate the RPR1 RNA subunit of yeast RNaseP. Srisawat and Engelke used SELEX (systematic evolution of ligands by exponential enrichment) and *in vitro* selection to isolate a streptavidin-binding aptamer from a random RNA library (Srisawat and Engelke, 2001). The minimal S1 motif is comprised of a 44-nucleotide (nt)-long structured RNA containing two double-stranded (ds) RNA helices, a 13-nt internal loop between the two helices and a 9-nt terminal loop (Figure 5.1A) (Srisawat and Engelke, 2002). I tested a variety of constructs using

different lengths of the *S1* aptamer ranging from the minimal motif of 44 nucleotides ($S1_{1\text{-}44}$) (Figure 5.1A) to the full length of 165 nucleotides ($S1_{1\text{-}165}$), and fused these to the first 45 coding nucleotides of *yopE* ($yopE_{1\text{-}45}$). Additionally I also included linker regions (GG or GAG) of different lengths between the first 15 codons of YopE and the *S1* aptamer. I determined that while the full-length *S1* aptamer of 165 nucleotides was sufficient for binding streptavidin using *in vitro* transcribed RNA, it was not sufficient for binding streptavidin in the presence of *Yersinia* lysates.

The second aptamer is the bacteriophage-derived MS2 aptamer (Figure 5.1B), which binds the coat protein MS2CP and is used in RNA-binding protein purification and identification (RaPID) technique (Slobodin and Gerst, 2011). RaPID has previously been used in mammalian and yeast systems to identify RNA-interacting proteins by either RNA-binding proteins (RBPs) or proteins involved in ribonucleoprotein (RNP) complexes through crosslinking coupled with mass spectrometry. The RaPID method uses the high affinity interaction between the MS2 aptamer and the MS2CP (K_d = 3nM) as a means of capturing mRNA. The MS2CP portion occurs as an MS2CP-GFP-SBP tripartite fusion protein in the RaPID construct. The MS2CP portion of this fusion protein would interact with an mRNA containing the MS2 aptamer. The GFP portion of the fusion protein is included for potential visualization and analysis by Western blot. The streptavidin binding protein (SBP) tag is included for its high affinity to streptavidin (K_d = 2.5 nM) for purification from cell lysates (Keefe et al., 2001).

In sum, the logic behind this construct is that it would enable purification of an mRNA that contained both the YopE 5' signal and the MS2 aptamer. This mRNA would presumably bind the MS2CP-GFP-SBP fusion protein *in vivo*, and the entire complex containing the mRNA and fusion protein would be isolated after lysis through affinity between SBP and immobilized streptavidin.

I constructed a bicistronic vector containing *yopE*$_{1\text{-}45}$*-MS2* aptamer and MS2CP-GFP-SBP fusion protein for simultaneous expression. Here I show I was able to express and purify MS2CP-GFP-SBP with *yopE*$_{1\text{-}45}$*-MS2*. Quantification of the mRNA that is produced and purified as well as optimization of UV crosslinking conditions are future steps for progress with the RaPID technique for identification of binding partners of the YopE 5' signal.

MATERIALS AND METHODS

Cloning of *yopE* mRNA constructs for reverse-CLIP and RaPID techniques

In the case of the reverse-CLIP technique (Ule et al., 2005) with the *yopE-S1* aptamer tag serving as the target, the first 15 codons (or first 45 coding nucleotides) of *yopE* (*yopE*$_{1-45}$) fused to nucleotides 1-165 of the *S1* tag (*S1*$_{1-165}$) (Srisawat and Engelke, 2002) or just nucleotides 1-165 of the *S1* tag were inserted into the arabinose-inducible pBAD vector using sequence and ligase independent cloning (SLIC) (Li and Elledge, 2012). In the case of the RaPID technique (Slobodin and Gerst, 2011) with the first 15 codons of *yopE* (*yopE*$_{1-45}$) serving as a target, a construct (a generous gift from the Gerst lab) encoding the *MS2* coat protein (MS2CP) fused to GFP and a streptavidin binding peptide (SBP) tag of 38 amino acids (MDEKTTGWRGGHVVEGLAGELEQLRARLEHHPQGQREP) was cloned into the arabinose-inducible pBAD vector. In order to achieve simultaneous expression of the *yopE-MS2* RNA and the MS2CP-GFP-SBP protein, a bicistron was introduced into the pBAD vector. For this, a second ribosome binding site was inserted upstream of the coding sequence for MS2CP-GFP-SBP using the QuikChange method (Agilent). A PCR product was generated containing the first 45 nucleotides of *yopE* and *MS2* aptamer. This PCR product was then cloned into the bicistronic pBAD vector containing MS2CP-GFP-SBP using the SLIC method.

The serotype III *Yersinia pseudotuberculosis* strain 126 (*ΔyopE::aph*), in which *yopE* is replaced by *aph*, has been described previously (Rodgers et al., 2010). The constructs for either reverse-CLIP or RaPID techniques were electroporated into *Y. pseudotuberculosis* (*ΔyopE::aph*) strain (Conchas and Carniel, 1990), and transformants were selected by growing on BHI containing 2.5 mM $CaCl_2$, 30 μg/mL kanamycin, and 30 μg/mL ampicillin.

Expression and purification of *yopE* mRNA for reverse-CLIP and RaPID techniques

Y. pseudotuberclosis strains were cultured while shaking overnight at 26 °C in 5 ml BHI containing 2.5 mM $CaCl_2$ and antibiotics as appropriate (50 μg/ml kanamycin or 30 μg/ml ampicillin). A 1:20 dilution of the overnight culture was made into fresh media, and the resulting cultures were grown at 26 °C while shaking to an optical density at 600 nm (OD_{600}) of 0.6, and then induced with 1% arabinose; a fresh aliquot of 1% arabinose was added every 2 h following induction. Cultures were grown for an additional 3 h, harvested (4 °C, 10 min, 3,000 × g), and re-suspended (1 mL per 10 mL of bacterial culture) in either buffer A for *yopE*$_{1\text{-}45}$-*S1*$_{1\text{-}165}$ (50 mM HEPES [pH 7.4], 10 mM $MgCl_2$, 100 mM NaCl, 1 mM DTT, and 10% glycerol) or buffer B for *yopE*$_{1\text{-}45}$-*MS2*-MS2CP-GFP-SBP (50 mM Tris, pH 8, 150 mM NaCl, 1% Triton-X 100, 10 mM $MgCl_2$, 1 mM DTT). Bacteria were lysed by sonication and centrifuged (4 °C, 15 min, 20,000 × g) to remove cell debris. The supernatant, which contained either *yopE*$_{1\text{-}45}$-*S1*$_{1\text{-}}$

$_{165}$or *yopE*$_{1-45}$-*MS2*-MS2CP-GFP-SBP, was applied to streptavidin resin (1μL resin per mL of bacterial culture) (Thermo) for 1 h at 26 °C (*yopE*$_{1-45}$-*S1*$_{1-165}$) or 16 h at 4 °C (*yopE*$_{1-45}$-*MS2*-MS2CP-GFP-SBP). After 4 resin bed volume washes with Buffer A or B, for *yopE-S1* or *yopE*$_{1-45}$-*MS2*-MS2CP-GFP-SBP, respectively, samples were eluted in 8 M urea. In some experiments, supernatants containing *yopE*$_{1-45}$-*S1*$_{1-165}$ were supplemented with *in vitro* transcribed and purified *yopE*$_{1-45}$-*S1*$_{1-165}$. The presence of either *yopE*$_{1-45}$-*S1*$_{1-165}$ or *yopE*$_{1-45}$-*MS2* RNA was verified by reverse-transcription polymerase chain reaction (RT-PCR) using iSCRIPT cDNA synthesis kit (Bio-Rad) for cDNA library synthesis and insert specific primers (IDT).

Crosslinking experiments

Bacteria were re-suspended after harvesting by centrifugation (4 °C, 10 min, 3,000 × g) in RNA*later*®**,** and irradiated three times on ice with a 10 s pulse of 100–400 mJ/cm^2 ultraviolet light (~15 cm distance from UV source) using a Stratalinker (Stratagene model 2400). After irradiation cells were pelleted by centrifugation (4 °C, 10 min, 3,000 × g), and re-suspended in Buffer B and purified as above.

***In vitro* transcription experiments**

RNA was synthesized by *in vitro* transcription using T7 RNA polymerase. Three different sorts of DNA templates were used. The first sort of template was

a series of PCR products (Table 1) carrying a T7 polymerase promoter and sequences encoding various lengths of *yopE* and S_1 aptamer. Additionally, the vector pRS315-S1-RPRI (a generous gift from D. Engelke), which contains the full length *S1-RPR1* aptamer, $yopE_{1\text{-}45}$-$S1_{1\text{-}165}$ and the T7 polymerase promoter served as templates. The vector was linearized downstream of the S_1 aptamer using *AvrII* restriction digestion in order to carry out runoff transcription. Transcription reactions were performed overnight at 37 °C using 20 μg/ml of linearized vector, 0.5 mM of each nucleoside triphosphate (Promega), and 1 mg/ml of T7 RNA polymerase in T7 buffer (25 mM $MgCl_2$, 5 mM dithiothreitol (DTT), 2 mM spermidine, 40 mM Tris, pH 7.5). The reaction was then treated with 20 U/ml of RNase-free DNase (Promega) for 4 hr at 37 °C. The reaction was extracted with an equal volume of phenol:chloroform:isoamyl alcohol (25:24:1 v/v). Ammonium acetate, pH 5.5, was added to the aqueous phase to a final concentration of 3 M, after which 2.5 volumes of 100% ethanol were added. The sample was incubated at −80 °C for 1 hr and then precipitated by centrifugation (30 min, 15,800 × g, 4 °C). The pellet, which contained the RNA, was washed with 1 ml cold 70% ethanol, air dried for 10 min at room temperature, and re-solubilized in RNase-free sterile water. The purity of the samples was determined by the A_{260}:A_{280} ratio as well as by ethidium bromide-stained agarose gels.

Western Blots

Samples were resolved by 12.5-15% SDS-PAGE, and transferred to a polyvinylidene fluoride membrane (Millipore). Membranes were blocked with 20 mL of 5% milk in TBS (150 mM NaCl, 50 mM Tris, pH 8.0) for 1 hr at 26 ºC followed by incubation with anti-GFP polyclonal antibody (1:1000, Santa Cruz Biotechnology), in 5% milk in TBS for 16 h at 4 ºC. Membranes were then washed 3x with 20 mL TBS with 0.5% Tween (TBST), and incubated with HRP-conjugated goat anti-rabbit antibodies (1:5000, Santa Cruz Biotechnology) in 5% milk in TBS for 30 min at 25 ºC. Membranes were once again washed 3x with 20 mL TBST. For detection, SuperSignal West Chemiluminescent Substrate was used according to the manufacturer's instructions (Thermo).

RESULTS

YopE fused to the S1 aptamer does not bind streptavidin in the presence of *Yersinia* lysates

I used the first 15 codons of YopE as a target to study potential binding partners for the 5' signal through *in vivo* crosslinking coupled with mass spectrometry. I tested two RNA aptamers that bind streptavidin (Slobodin and Gerst, 2011; Srisawat and Engelke, 2002) to identity components associated with the 5’ mRNA type III secretion signal of *yopE*.

The first aptamer I developed for fusion to *yopE* mRNA is the *S1* RNA aptamer, which binds streptavidin directly (Figure 5.1). I made a series of PCR products consisting of the T7 polymerase promoter sequence followed by the first 15 codons of *yopE* fused to various lengths of the *S1*aptamer tag to serve as a template for *in vitro* transcription (Table 5.1). I also inserted linkers between $yopE_{1\text{-}45}$ and the *S1*aptamer tag for the same purpose (Table 5.1). I then used these transcribed RNA for co-precipitation assays to determine which fusion construct was optimal for binding streptavidin (Table 5.1 and data not shown). I found $yopE_{1\text{-}45}$-$S1_{1\text{-}165}$ to be the only construct to bind streptavidin (Figure 5.2A).

To determine if $yopE_{1\text{-}45}$-$S1_{165}$ RNA would bind streptavidin resin in the presence of *Yersinia* lysates, I expressed the RNA under the control of the arabinose-inducible promoter found in the pBAD vector in *Y. pseudotuberculosis* 126 *ΔyopE* (Rodgers et al., 2010). I verified that the $yopE_{1\text{-}45}$-$S1_{1\text{-}165}$ RNA was

expressed by running reverse transcription polymerase chain reaction (RT-PCR) on total RNA preparations of the cell lysates using primers specific for *yopE*$_{1-45}$-*S1*$_{165}$. However, I found that *yopE*$_{1-45}$-*S1*$_{165}$ in the presence of *Yersinia* lysates was unable to bind streptavidin (Figure 5.2A). As I did not see any binding, I attempted supplementing *Yersinia* lysates with purified *yopE*$_{1-45}$-*S1*$_{1-165}$ *and* testing streptavidin binding (Figure 5.3). Again, I did not see any binding of *yopE*$_{1-45}$-*S1*$_{165}$ to streptavidin even with these supplemented samples. As a positive control, I used the full length *S1* tag fused to the RPR1 subunit of RNase P, *S1RPR1*, which has previously been used to isolate the RPR1 subunit of RNase P from yeast lysates (Walker et al., 2008). I did not see binding of *S1RPR1* in the presence of *Yersinia* lysates, indicating the lysate composition may not suitable for the *S1* aptamer.

The second construct I tested made use of the RaPID technique, which makes use of the MS2 aptamer. This aptamer interacts with the MS2 coat protein (MS2CP), which was provided as a tripartite MS2CP-GFP-SBP fusion protein. The last part of this fusion, the streptavidin binding peptide, binds streptavidin with high affinity (Slobodin and Gerst, 2011). I first inserted the coding sequence for the MS2CP-GFP-SBP fusion protein into a pBAD vector. I then introduced a second ribosome binding site upstream of the MS2CP-GFP-SBP fusion in order to construct a bicistron. Finally I inserted the first 45 nucleotides of *yopE* fused to the MS2 aptamer sequence downstream of the first ribosome binding site. With this bicistronic construct, I co-expressed *yopE*$_{1-45}$-*MS2* and MS2CP-GFP-SBP in

Y. pseudotuberculosis 126 (*ΔyopE*) (Rodgers et al., 2010). I found that the MS2CP-GFP-SBP protein bound streptavidin resin and co-purified the *yopE*$_{1-45}$-*MS2* RNA (Figure 5.4). As I was able to purify *yopE*$_{1-45}$-*MS2* and MS2CP-GFP-SBP, I attempted UV crosslinking prior to purification to capture binding partners to the 5' secretion signal of YopE. I first tested four separate UV crosslinking irradiation conditions (Figure 5.5) and found that irradiating the cells with three pulses of 400 mJ/cm^2 had the highest amount of crosslinking, as visualized by the disappearance of lower molecular weight proteins and formation of gel-impermeant high molecular weight products (Figure 5.5). I applied this crosslinking condition to the purification of *yopE*$_{1-45}$-*MS2* and MS2CP-GFP-SBP, but did not see binding of MS2-GFP-SBP to streptavidin (data not shown). Thus, further optimization of crosslinking conditions is required to find one that enables purification.

DISCUSSION

In this study I sought to find a method to identify proteins that bind to the 5' secretion signal of the effector YopE. I first attempted the reverse-CLIP method using the *S1* aptamer. The only *in vitro* transcribed *yopE-S1* fusion that bound streptavidin, $yopE_{1\text{-}45}S1_{1\text{-}165}$, did not bind streptavidin resin in the presence of *Yersinia* lysates. There are a few possibilities why I may not have seen binding of $yopE_{1\text{-}45}$-$S1_{1\text{-}165}$ to streptavidin in the presence of *Yersinia* lysates. One possibility is that the lysate composition is different from the *in vitro* transcription buffer composition and this may have inhibited binding. Another possibility is that the lysate contains RNases that may have digested the $yopE_{1\text{-}45}$-$S1_{165}$ sufficiently such that binding to streptavidin was not detected. The *S1* aptamer also requires proper folding in the context of *in vivo* synthesis and perhaps in the presence of *Yersinia* it did not fold properly and thus did not bind streptavidin.

A direction for the future is a modification to the *S1* RNA aptamer referred to as *S1m* aptamer, which has recently been published which is a more stable and constrained form of *S1* RNA aptamer with an extended basal stem formed by strand complementarity (Leppek and Stoecklin, 2014). *S1m* was further optimized by introducing multiple copies of the *S1m* aptamer in order to increase binding efficiency through a synergistic effect. This 4-fold repeat or 4x*S1m* was found to be more efficient in streptavidin binding than the RaPID technique (Leppek and Stoecklin, 2014). This 4x*S1m* aptamer could be investigated further

to determine whether the reverse-CLIP technique provides a viable option for identifying binding partners of the YopE 5’ signal.

In the case of RaPID technique, I was able to find a construct that was expressed and capable of being purified through affinity for MS2CP-GFP-SBP. As in the reverse-CLIP technique, one of the main issues is the quantity of RNA, in this case *yopE*$_{1\text{-}45}$*-MS2,* present during the purification. The next steps in using the RaPID technique for determining binding partners for the 5’ secretion signal of YopE is the quantification of *yopE*$_{1\text{-}45}$*-MS2* during purification of MS2CP-GFP-SBP and introducing UV crosslinking perhaps at a lower irradiation level than I tested.

FIGURES AND TABLES

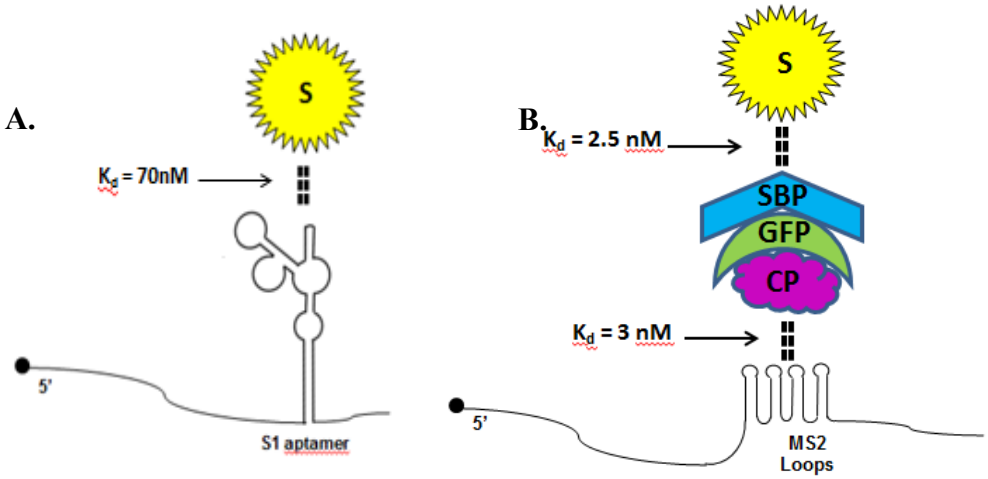

Figure 5.1 RNA aptamers used in this study.
A. Schematic of the reverse-CLIP method using the *S1* aptamer to bind streptavidin (yellow) and the affinity of the interaction is indicated.
B. Schematic of the RaPID technique (as adapted from Slobodin and Gerst, 2010) employing MS2 aptamer and interacts with the target protein MS2CP (fuchsia) which is fused to GFP (green) and SBP (blue) and through SBP interacts with streptavidin (yellow). The affinities of both of these interactions are indicated.

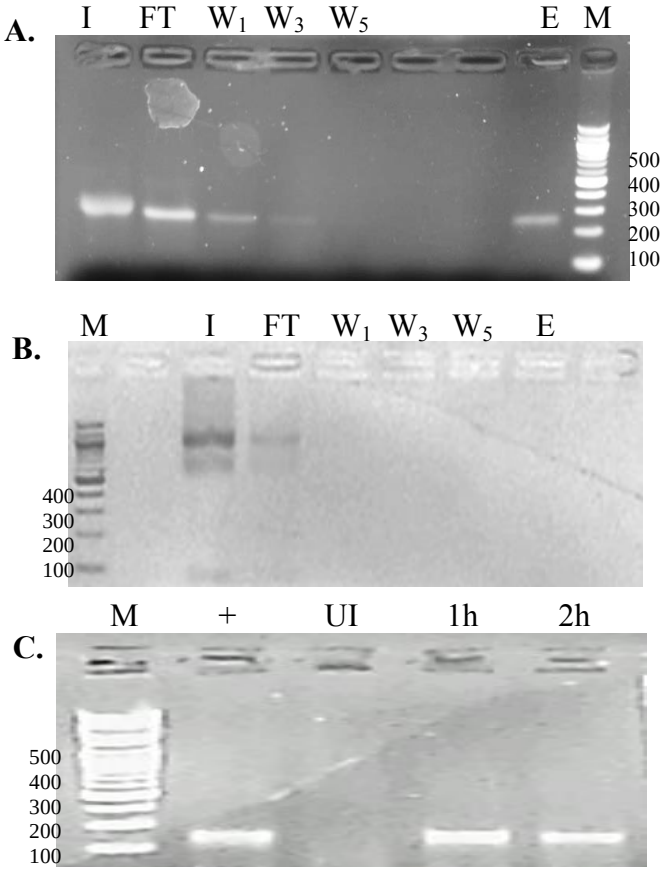

Figure 5.2 Binding of the *S1* aptamer fused to 5' secretion signal of YopE.
A. Purification of *in vitro* transcribed $yopE_{1\text{-}45}$-$S1_{1\text{-}165}$ where "M", "I", "FT", "W", and "E" denote marker, input, flow through, washes, and elution respectively.
B Purification of $yopE_{1\text{-}45}$-$S1_{1\text{-}165}$ from *Yersinia* lysates where "M", "I", "FT", "W", and "E" denote marker, input, flow through, washes, and elution respectively.
C. RT-PCR for $yopE_{1\text{-}45}$-$S1_{1\text{-}165}$ where "+" indicates *in vitro* transcribed $yopE_{1\text{-}45}$-$S1_{1\text{-}165}$ RNA as template and "UI", "1h", and "2h" indicates RNA prepared from *Yersinia* induced for 0, 1, and 2h as templates.
B. Same as in panel a, except plasmid-encoded *yscO* was introduced into wild-type *Y. pseudotuberculosis*

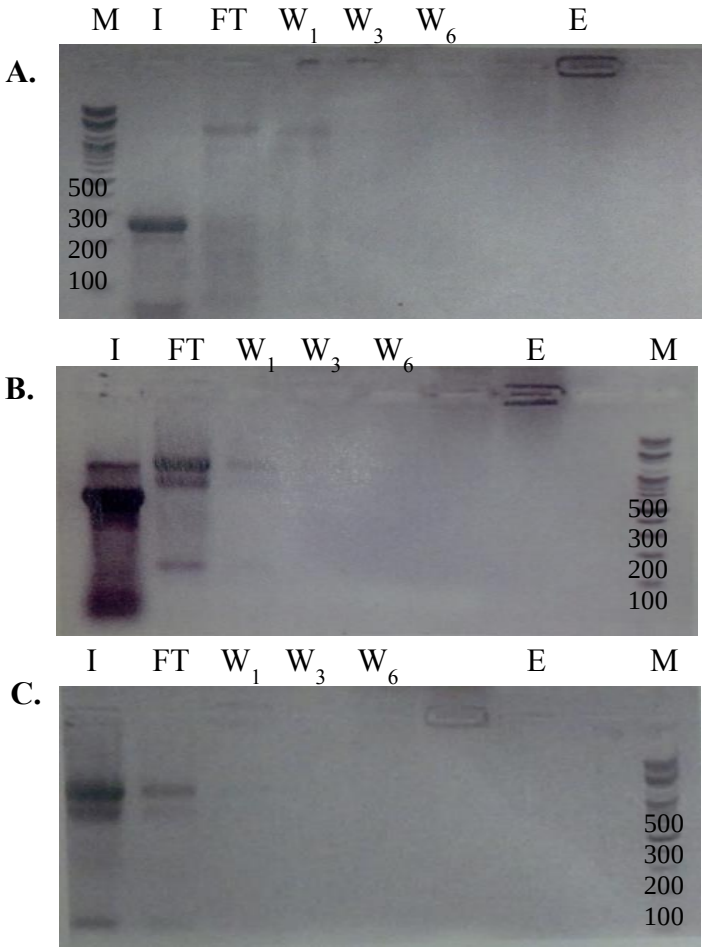

Figure 5.3 Purification of *yopE*$_{1-45}$ – *S1*$_{1-165}$ from *Yersinia* lysates.
Purification of *yopE*$_{1-45}$-*S1*$_{1-165}$ either supplemented with *in vitro* transcribed *yopE*$_{1-45}$-*S1*$_{1-165}$ (panel A), *in vitro* transcribed (panel B), or no supplemented RNA (panel C) where "M", "I", "FT", "W", and "E" denote maker, input, flow through, wash, and elution respectively.

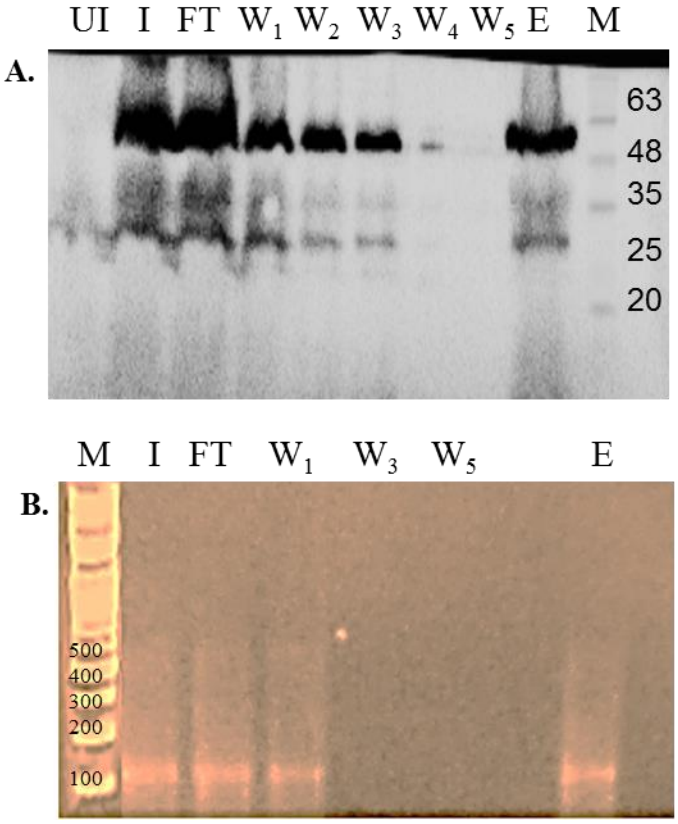

Figure 5.4 Purification of *yopE*$_{1-45}$*-MS2* and MS2CP-GFP-SBP .
A. anti-GFP Western blot for MS2CP-GFP-SBP where "M", "I", "FT", "W", and "E" denote marker, input, flow through, wash, and elution respectively. MS2CP-GFP-SBP is indicated by arrow.
B. RT-PCR for *yopE*$_{1-45}$*-MS2* using total RNA preparations of samples in panel A as template.

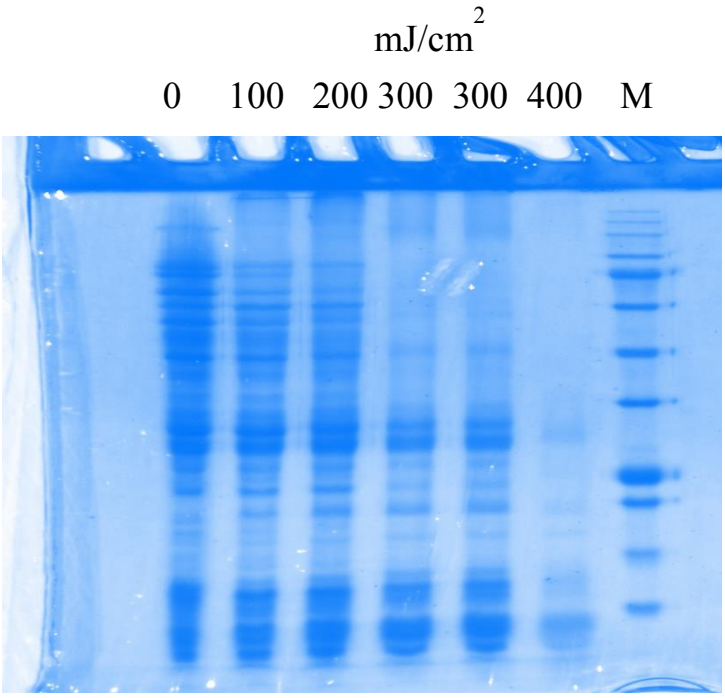

Figure 5.5 UV Crosslinking of *Yersinia pseudotuberculosis (ΔyopE)* expressing *yopE$_{1-45}$-MS2* and MS2CP-GFP-SBP.
Samples were irradiated three times on ice with a 10 s pulse of 100–400 mJ/cm^2 ultraviolet light (~15 cm distance from UV source) using a Stratalinker (Stratagene model 2400). "M" denotes marker.

Table 5.1 *yopE-S1* fusion constructs binding to streptavidin.

Construct	Binding to streptavidin
$yopE_{1\text{-}45nt}$:$S1_{1\text{-}42nt}$:$yopE_{46\text{-}72nt}$	-
$yopE_{1\text{-}45nt}$:GG:$S1_{1\text{-}42nt}$:$yopE_{46\text{-}72nt}$	-
$yopE_{\text{-}45nt}$:GAG:$S1_{1\text{-}42nt}$:$yopE_{46\text{-}72nt}$	-
$yopE_{\text{-}45nt}$:$S1_{1\text{-}69nt}$	-
$yopE_{\text{-}45nt}$:$S1_{1\text{-}69nt}$:$yopE_{46\text{-}72nt}$	-
$yopE_{\text{-}45nt}$:$S1_{1\text{-}165nt}$	+

ACKNOWLEDGEMENTS

This research was funded with NIH grant R01 AI061452 (PG).

REFERENCES

Anderson, D.M., and Schneewind, O. (1997). A mRNA signal for the type III secretion of Yop proteins by Yersinia enterocolitica. Science *278*, 1140–1143.

Conchas, R.F., and Carniel, E. (1990). A highly efficient electroporation system for transformation of Yersinia. Gene *87*, 133–137.

Keefe, A.D., Wilson, D.S., Seelig, B., and Szostak, J.W. (2001). One-step purification of recombinant proteins using a nanomolar-affinity streptavidin-binding peptide, the SBP-Tag. Protein Expr. Purif. *23*, 440–446.

Leppek, K., and Stoecklin, G. (2014). An optimized streptavidin-binding RNA aptamer for purification of ribonucleoprotein complexes identifies novel ARE-binding proteins. Nucleic Acids Res. *42*, e13–e13.

Li, M.Z., and Elledge, S.J. (2012). SLIC: a method for sequence- and ligation-independent cloning. Methods Mol. Biol. *852*, 51–59.

Lloyd, S.A., Norman, M., Rosqvist, R., and Wolf-Watz, H. (2001). Yersinia YopE is targeted for type III secretion by N-terminal, not mRNA, signals. Mol. Microbiol. *39*, 520–531.

Ramamurthi, K.S., and Schneewind, O. (2005). A synonymous mutation in Yersinia enterocolitica yopE affects the function of the YopE type III secretion signal. J. Bacteriol. *187*, 707–715.

Rodgers, L., Mukerjea, R., Birtalan, S., Friedberg, D., and Ghosh, P. (2010). A solvent-exposed patch in chaperone-bound YopE is required for translocation by the type III secretion system. J. Bacteriol. *192*, 3114–3122.

Slobodin, B., and Gerst, J.E. (2010). A novel mRNA affinity purification technique for the identification of interacting proteins and transcripts in ribonucleoprotein complexes. RNA *16*, 2277–2290.

Slobodin, B., and Gerst, J.E. (2011). RaPID: an aptamer-based mRNA affinity purification technique for the identification of RNA and protein factors present in ribonucleoprotein complexes. Methods Mol. Biol. Clifton NJ *714*, 387–406.

Sorg, J.A., Miller, N.C., and Schneewind, O. (2005). Substrate recognition of type III secretion machines –testing the RNA signal hypothesis. Cell. Microbiol. *7*, 1217–1225.

Srisawat, C., and Engelke, D.R. (2001). Streptavidin aptamers: affinity tags for the study of RNAs and ribonucleoproteins. RNA N. Y. N *7*, 632–641.

Srisawat, C., and Engelke, D.R. (2002). RNA affinity tags for purification of RNAs and ribonucleoprotein complexes. Methods San Diego Calif *26*, 156–161.

Walker, S.C., Scott, F.H., Srisawat, C., and Engelke, D.R. (2008). RNA Affinity Tags for the Rapid Purification and Investigation of RNAs and RNA-Protein Complexes. Methods Mol. Biol. Clifton NJ *488*, 23–40.

Ule, J., Jensen, K., Mele, A., and Darnell, R.B. (2005). CLIP: a method for identifying protein-RNA interaction sites in living cells. Methods *37*, 376–386.

Chapter 6:

Identification of binding partners to the secretion and translocation signals of the T3S effector YopE

ABSTRACT

Yersinia spp. as well as many other gram-negative bacteria utilize the type III secretion (T3S) system to transport effectors into the host cell. These effectors are targeted for export by the T3S by distinct signals within the bacterium to distinguish between export substrates and the many other proteins present within the bacterium. One targeting signal, referred to as the secretion or 5'/N-terminal signal consists of the first 15 effector codons or amino acids of the individual secreted effector. In some effectors, a second signal is hypothesized to form when specific chaperone proteins associate with their cognate effectors. In this chapter I present results of analyzing potential binding partners to these signals, encompassed by the first 80 amino acids of the *Yersinia* effector YopE ($YopE_{1-80}$) through affinity purification coupled with mass spectrometry. I found that the inner rod protein YscI and the ATPase regulator YscL selectively were bound by wild-type $YopE_{1-80}$ and a non-translocating mutant $3\text{-}Ala_{1-80}$ whereas the T3S gate-keeper YopN was selectively bound by $3\text{-}Ala_{1-80}$.

INTRODUCTION

The type III secretion (T3S) system is employed by many gram-negative bacteria and uses a needle-like protein complex that spans both bacterial inner and outer bacterial membranes as well as the host plasma membrane to translocate effector proteins into host cells (Galán and Wolf-Watz, 2006; Ghosh, 2004). These effectors in *Yersinia* are referred to as *Yersinia* outer proteins, or Yops, and are directly injected into the host cell to disrupt the host immune response (Cornelis, 2006). T3S occurs in an ordered fashion with needle components being secreted first and then translocater Yops followed by effector Yops (Cornelis, 2006; Galán and Wolf-Watz, 2006; Ghosh, 2004). The needle component YscF as well as the inner rod protein YscI, have been implicated in this substrate switching (Wood et al., 2008). This ordered fashion of T3S has been shown to be under the control of distinct signals and Yops haves secretion signals that target them for secretion and/or translocation. One signal is the 5'/N-terminal secretion signal and is present in all effectors (Anderson and Schneewind, 1997; Lloyd et al., 2001). Some effectors, however, are hypothesized to have a second translocation signal which is formed upon the association of Yops with their associated chaperone proteins within the bacterium (Cheng et al., 1997). These chaperones comprise a large family where individual chaperones bind and function in the translocation of a single or a few effectors. Additionally, even though these chaperone proteins have a limited sequence identity to one another

(≤ 20%), their effector binding is well conserved (Birtalan and Ghosh, 2001; Birtalan et al., 2002; Büttner et al., 2005; van Eerde et al., 2004; Lilic et al., 2006; Locher et al., 2005; Luo et al., 2001; Phan et al.; Schubot et al., 2005; Singer et al., 2004; Stebbins and Galán, 2001). T3S chaperones bind specifically to their cognate effectors within a ~25–100-residue chaperone-binding region, referred to as the effector chaperone binding (Cb) region (Birtalan et al., 2002; Lilic et al., 2006; Phan et al.; Schubot et al., 2005; Stebbins and Galán, 2001). The chaperone-effector complex is proposed to constitute a signal that is recognized by a bacterial component required for type III secretion (Rodgers et al., 2010).

SycE-YopE is a particularly well-studied chaperone-effector pair of the T3S system. Previous studies have shown that the translocation of YopE requires SycE, and that the chaperone-effector complex may contain the signal for this translocation (Cheng et al., 1997). Biochemical and crystallographic data for the *Yersinia* SycE-YopE chaperone-effector complex show that chaperone action is isolated to only the Cb region of YopE and SycE does not interact with or affect any other regions of YopE (Birtalan et al., 2002; Lilic et al., 2006). Moreover, NMR studies of the N-terminal 100 residues of YopE, which includes the Cb region have shown that YopE is flexible and disordered in the absence of SycE and binding of the chaperone to effector causes a disorder-to-order transition in the Cb region of YopE(Rodgers et al., 2008). This effect is localized to the Cb region with no change to the other regions of YopE. Residues were identified in the Cb region of YopE which disrupt translocation of the effector but do not

abrogate steady state expression/secretion of YopE, binding to SycE, and stability in mammalian cells (Rodgers et al., 2010). These two mutants, termed 3-Ala (V23A/E25A/S32A) and 5-Ala (V23A/E25A/S27A/R29A/S32A) contained alanine substitutions of residues in solvent-exposed patches of the chaperone-bound Cb region of YopE. These mutant proteins, which were functionally equivalent to one another and did not translocate but were equivalent to wild-type YopE in all other aspects of YopE function (Rodgers et al., 2010). These studies indicate that the chaperone-effector pair may form a three-dimensional targeting signal in the Cb region of the effector.

In this chapter I present possible binding partners to the first 80 amino acids, which encompass the effector T3S secretion and translocation signals by means of streptavidin affinity purification coupled with tandem mass spectrometry. The constructs used in this study were $YopE_{1-80}$-SBP-His, 3-Ala_{1-80}-SBP-His, and SBP-His. $YopE_{1-80}$-SBP-His and Ala_{1-80}-SBP-His consist of the first 80 amino acids of YopE (with alanine substituted residues for the 3-Ala mutant) fused to a 38 amino acid streptavidin binding peptide (SBP) tag, for binding streptavidin and a his tag for detection purposes. SBP-His served as a control to eliminate proteins which interacted with the SBP-His portion or non-specifically with the resin. I expressed and purified $YopE_{1-80}$-SBP-His, 3-Ala_{1-80}-SBP-His, and SBP-His from *Yersinia pseudotuberculosis* (*ΔyopE*) under secreting conditions. In collaboration with Jason Liang and Huilin Zhou of the University of California, San Diego, I used hydrophilic-interaction chromatography (HILIC) and tandem

mass spectrometry to identify binding partners to $YopE_{1-80}$. In addition to SycE, I found two T3S components which associated specifically with $YopE_{1-80}$ and 3-Ala_{1-80} under secreting conditions. These two components are the inner rod protein YscI and the ATPase regulator YscL. Additionally I found the T3S gate-keeper, YopN associated with 3-Ala_{1-80} but not $YopE_{1-80}$ under secreting conditions.

MATERIALS AND METHODS

Cloning of *ΔyopE, yopE$_{1-80}$-sbp-his, 3-ala$_{1-80}$-sbp-his, and sbp-his*

The serotype III *Yersinia pseudotuberculosis* strain 126 (*ΔyopE::aph*), in which *yopE* is replaced by *aph*, has been described previously (Rodgers et al., 2010). The *yopE$_{1-80}$-sbp-his, 3-ala$_{1-80}$-sbp-his,* and *sbp-his* constructs were all cloned into the pBAD vector. Both *yopE$_{1-80}$-sbp-his* and *3-ala$_{1-80}$-sbp-his* encode the first 80 amino acids of YopE fused to a streptavidin binding peptide tag (SBP) of 38 amino acids (MDEKTTGWRGGHVVEGLAGELEQLRARLEHHPQGQR-EP) and a His tag, and have been described previously (Ku, 2013). The *sbp-his* construct was derived from *yopE$_{1-80}$-sbp-his* by the QuikChange method (Agilent). These constructs were electroporated into the *Y. pseudotuberculosis* 126 (*ΔyopE*) strain (Conchas and Carniel, 1990), and transformants were selected by growing on BHI containing 2.5 mM $CaCl_2$, 30 μg/mL kanamycin, and 30 μg/mL ampicillin.

Expression and purification of YopE$_{1-80}$-SBP-His, 3-Ala$_{1-80}$-SBP-His, and SBP-His

Y. pseudotuberclosis strains were cultured while shaking overnight at 26 °C in 5 mL BHI containing 2.5 mM $CaCl_2$ and antibiotics as appropriate (50 μg/mL kanamycin or 30 μg/mL ampicillin). A 1:20 dilution of the overnight culture was made into fresh media and the resulting cultures were grown at 26 °C

while shaking to an optical density at 600 nm (OD_{600}) of 0.6, and then induced with 1% arabinose; a fresh aliquot of 1% arabinose was added every 2 h following induction. Cultures were grown for an additional 3 h, harvested (4 °C, 10 min, 3,000 × g), and re-suspended (1 mL per 10mL of bacterial culture) in buffer A (PBS containing 0.5-1% Triton-X 100). Bacteria were lysed by sonication and centrifuged (4 °C, 15 min, 20,000 × g) to remove cell debris. The supernatant, was applied to streptavidin resin (0.3 mL resin per L cell culture) (Thermo) for 16 h at 4 °C. After washing (3-30 resin bed volume) with buffer A, samples were eluted with 8 M urea.

Secretion Assays

To test for secretion, *Y. pseudotuberculosis* strains were cultured by shaking overnight at 26 °C in 5 mL BHI with antibiotics as appropriate (50 μg/mL kanamycin or 30 μg/mL ampicillin). A 1:20 dilution was made into fresh BHI containing 10 mM $MgCl_2$ and 10 mM ethylene glycol tetraacetic acid (EGTA), and the cultures were grown with shaking for 2 h at 26°C. Arabinose at 0.1% concentration was added to each sample. In some samples, 2.5 mM $CaCl_2$ was added in place of 10 mM $MgCl_2$ and 10 mM EGTA in order to verify that the secretion was type III. Cultures were grown at 26 °C to an optical density at 600 nm (OD_{600}) of 1.0 and then shifted to 37 °C, at which time an additional 0.1% arabinose was added. Cultures were then grown with shaking for 3 h further at 37°C. The concentration of bacteria was normalized to an OD_{600} of 1.0 using BHI

prior to separation of bacteria from the culture medium by centrifugation (4 °C, 10 min, 3,000 × g). The supernatant was put through a 0.22-μm-pore-size filter, after which point cold trichloroacetic acid (TCA) was added to a final concentration of 10%. The samples were incubated on ice for 1 h and then pelleted by centrifugation (4 °C, 15 min, 20,000 × g). The pellet was washed three times with cold acetone, resolubilized in 2× Tris-tricine PAGE sample buffer, and boiled. Samples were resolved by 16.5% Tris-tricine PAGE gel and analyzed by Western Blot (see below).

Silver Staining

Samples were resolved by 4-20% gradient gel (Bio-Rad), which was then incubated in fixing solution (30% ethanol, 10% acetic acid) for 30 min. The gel was then washed 3 times with 30 mL of H_2O and incubated in sensitizer solution (0.02% sodium thiosulfate). Following sensitization, the gel was incubated in silver staining solution (0.2% silver nitrate) for 25 min and then developing solution (3% sodium carbonate, 0.185% formaldehyde, 0.0004% sodium thiosulfate) for 10-15 min (Blum et al., 1987).

Western Blot

Samples were resolved by a 16.5% Tris-tricine gel and transferred to a polyvinylidene fluoride membrane (Millipore). The membrane was blocked with 20 mL of 5% milk in TBS (150 mM NaCl, 50 mM Tris [pH 8.0]) for 1 h at 26 °C.

Horseradish peroxidase (HRP)-conjugated anti-His monoclonal antibody (1:1,000; Santa Cruz Biotechnology) in TBS containing 5% milk was incubated with the membrane for 16 h at 4 °C. The membrane was then washed 3 times with 20 mL TBS containing 0.5% Tween (TBST) followed by 3 washes with TBST (20 mL per wash). For detection, SuperSignal West chemiluminescent substrate was used according to the manufacturer's instructions (Thermo Fisher Scientific).

Formaldehyde Crosslinking

After harvesting (4 °C, 10 min, 3,000 × g), cells were washed once with 10 mL of PBS and re-suspended in 1 mL of PBS. Varying concentrations of formaldehyde (0.5-4%) were added to the cells to determine optimal crosslinking conditions. The crosslinking reaction was quenched by adding 2.5 M glycine to a final concentration of 0.125 M. Cells were then collected and washed with PBS (4 °C) and samples were resolved by 12.5-15% SDS-PAGE and stained with Coommassie® Blue (Life Technologies) (Chowdhury et al., 2009).

Sample Preparation for Mass Spectrometry

Proteins bound to streptavidin beads were eluted by incubating in 8 M urea, PBS, pH 8.0 for 20 min at 25 ºC. The resulting slurry was centrifuged (5 min, 12,000 x g, 4 ºC), and the supernatant was collected and prepared for analysis by mass spectrometry. Samples were reduced by the addition of 15 mM dithiothreitol (DTT) for 30 min at 42 ºC and alkylated with 30 mM iodoacetamide

for 30 min at 25 ºC. The samples were then trypsinized (0.5 μg per 200 μL trypsin, Promega) for 16 h at 37 ºC. Following trypsin digestion, peptides were desalted using a C18 SepPak, and dried in silanized glass vials under vacuum followed by resuspension in 80% acetonitrile/20% water. Samples were injected into a TSK gel Amide-80 column (1 mm × 15 cm, 5 μm; Tosoh, Grove City, OH), and separated by HILIC fractionation as previously described (Albuquerque et al., 2008). Samples were then analyzed using a LTQ tandem mass spectrometer (Thermo Fisher Scientific, San Jose, CA).

Data Analysis Method for Large-scale MS Screens

Raw MS/MS spectra were searched by SEQUEST on a Sorcerer system using a composite *Yersinia pseudotuberculosis* serotype I protein database from the UniProt Knowledge base (http://uniprot.org). The following search parameters were used: semi-tryptic, mass tolerance of 1.2 Da for precursor ions, and static modification of 57.021465 Da for alkylated cysteine residues.

RESULTS

Type III secretion of YopE$_{1-80}$-SBP-His and 3-Ala$_{1-80}$-SBP-His

To determine if the fusion constructs YopE$_{1-80}$-SBP-His and 3-Ala$_{1-80}$-SBP-His would be secreted into the extracellular medium in a calcium-dependent manner, which is a diagnostic of the *Y. pseudotuberculosis* T3S system, I expressed these constructs under the control of the arabinose-inducible promoter found in the pBAD vector in *Y. pseudotuberculosis* 126 (*ΔyopE*) (Rodgers et al., 2010). Consistent with full length YopE, these truncated constructs were secreted by the *Yersinia pseudotuberculosis* T3S system (Figure 6.1). This effect was confirmed to be T3S as in the presence of Ca^{2+} there was no YopE$_{1-80}$-SBP-His or 3-Ala$_{1-80}$-SBP-His in the extracellular medium (Figure 6.1). The control SBP-His, as expected, was not secreted by *Yersinia pseudotuberculosis* T3S (Figure 6.1).

Binding partners of the *Yersinia* T3S have been identified using LC MS/MS

I attempted tandem mass spectrometry to identify binding partners to YopE$_{1-80}$-SBP-His and 3-Ala$_{1-80}$-SBP-His. I expressed and purified YopE$_{1-80}$-SBP-His,3-Ala$_{1-80}$-SBP-His, and SBP-His along with binding partners using streptavidin affinity achieved through the SBP tag (Figure 6.2a). I verified YopE$_{1-80}$-SBP-His, 3-Ala$_{1-80}$-SBP-His, and SBP-His capture by performing western blots on the elutions using anti-His tag antibodies (Figure 6.2b). In order to obtain a sensitive level of detection from the mass spectrometer as well as remove

detergent from samples, I used hydrophilic interaction chromatography (HILIC) (Albuquerque et al., 2008). This method of chromatography depends on the interaction of hydrophilic and charged amino acid residues via hydrogen bonding and ionic interactions with the resin. HILIC has been shown to provide a much better mass spectrometry signal than reverse phase liquid chromatography (RPLC) in samples containing detergent and membrane associated proteins (Buszewski and Noga, 2012). HILIC fractions were applied to a LTQ tandem mass spectrometer and resulting MS/MS raw data were searched against the entire *Yersinia* genome. Peptides were considered valid if they met established score values which used the following criteria: the peptide was a semi-tryptic peptide (showed cleavage at a lysine or arginine), had a trans proteomic pipeline (TPP) probability score above 0.8, contained a static mass modification of 57.021465 Da for alkylated cysteine residues, and contained a mass tolerance of 1.2 Da (Chen et al., 2010; Deutsch et al., 2010; James, 2001; Kapp et al., 2003). Additionally, peptides of interest were further validated by examination of individual spectra and identification of at least three tandem b/y ions as well as attributing any discrepancies from the theoretical spectra to either gain or loss of water (Figure 6.3). One other diagnostic was used when the peptide contained a proline. The proline in the peptide must have the highest y ion signal of the peptide (Figure 6.3). Due to the fact the raw data was searched against the entire *Yersinia pseudotuberculosis* serotype I database, proteins that bound to SBP-His also appeared in the comprehensive list of interacting peptides with $YopE_{1\text{-}80}$-SBP-His.

Many of these were general cell division, housekeeping, or ribosomal proteins (Table 6.1). I did find the most abundant peptides for $YopE_{1-80}$-SBP-His and 3-Ala_{1-80}-SBP-His came from, as expected, SycE. There were approximately 30 individual unique peptides of SycE with approximately 80% coverage of the protein. Additionally, many of the peptides from SycE appeared in consecutive HILIC fractions with multiple copies of the same peptide of SycE appearing in the same fraction (data not shown). This indicated that SycE was so abundant it was detected multiple times. In addition to SycE, I identified YscI, the inner rod protein as binding selectively to wild-type $YopE_{1-80}$ and 3-Ala_{1-80}-SBP-His but not with the negative control SBP-His (Table 6.2). I also found that YscL, the T3S ATPase regulator protein, associated with wild-type $YopE_{1-80}$ and 3-Ala_{1-80} mutant but not SBP-His (Table 6.2). In addition, the so-called gate-keeper of secretion, YopN, selectively associated with 3-Ala_{1-80} but not with $YopE_{1-80}$ and SBP-His (Table 6.3).

DISCUSSION

In this chapter I sought to find potential binding partners for the T3S secretion and translocation signals of the effector YopE through affinity purification coupled with mass spectrometry. I examined $YopE_{1-80}$ and while SycE was the most abundant interaction with $YopE_{1-80}$ I did find two T3S components that associated with wild-type YopE and 3-Ala mutant but not with the SBP-His. These two T3S components are YscI, which is the inner rod protein of the T3S system andYscL, which is the T3S ATPase regulator protein.

The T3S system is energized by ATP and so the T3S ATPase, YscN, is a critical component of the T3S in *Yersinia*. YscN is predicted to reside at the interface of the T3S apparatus and the bacterial cytoplasm and may be tethered to the membrane by its regulator YscL (Blaylock et al., 2006). Previous studies have shown that YscL and YscN interact with each other, and the overexpression of a glutathione *S*-transferase-YscL fusion abolishes secretion and down-regulates the expression of the secretion apparatus components (Blaylock et al., 2006). Additionally, it has been demonstrated that YscL is a potent inhibitor of YscN activity (Blaylock et al., 2006). YscN likely plays a central role in recognition and initiation of secretion of type III substrates, and homologues of YscN in other T3S systems have been shown to interact with chaperone-effector complexes (Lorenz and Büttner, 2009; Stone et al., 2008; Yoshida et al., 2014). However, previous interaction studies have not shown a direct binding interaction between*Yersinia*

YscN and the chaperone-effector pair of SycE-YopE (Rodgers et al., 2010). Similarly I did not find association between YscN and $YopE_{1-80}$ or $3\text{-}Ala_{1-80}$ (Table 6.2). I did, however, find the regulator of YscN, YscL, associated with both $YopE_{1-80}$ and $3\text{-}Ala_{1-80}$. This leads to the hypothesis that the interaction between YscN and the secretion/translocation signals of effectors may occur through interactions with the regulator protein YscL. As this association of YscL to $YopE_{1-80}$ and $3\text{-}Ala_{1-80}$ was seen under secreting conditions, it will be interesting to do this same analysis under non-secreting conditions to observe any possible changes prior to the initiation of type III secretion.

YscL has also been shown to bind YscU, which has a cytoplasmic domain involved in substrate switching (Riordan and Schneewind, 2008). This cytoplasmic domain auto-cleaves, and mutations which inhibit auto-cleavage of the cytoplasmic domain do not bind YscL and, in turn, caused a critical defect in promoting secretion (Riordan and Schneewind, 2008). This may be why YscL associates with the late effectors $YopE_{1-80}$ and $3\text{-}Ala_{1-80}$ mutant.

YscI has been shown to play a critical role in substrate specificity switching (Wood et al., 2008). YscI has been shown to interact with the molecular ruler of the T3S system, YscP, and the inner membrane protein, YscU, to switch the substrate specificity of the T3S system and enable Yop export once the needle attains its proper length. Similar to the needle component YscF, YscI is secreted by the type III secretion system (Journet et al., 2003; Wood et al., 2008). Furthermore, point mutations of YscI have been shown to secrete substantial

amounts of Yops but exhibit severe defects in needle formation. It is hypothesized that formation of the inner rod, not the needle, may be critical for substrate specificity switching and that YscP with YscU exert their effects on substrate export by controlling the secretion of YscI (Wood et al., 2008). This may be why I did not find YscF associated with $YopE_{1-80}$ or 3-Ala_{1-80}, but did detect YscI. It also indicates I may have captured $YopE_{1-80}$ during its movement through the needle. This interaction needs to be verified by a direct binding study with purified $YopE_{1-80}$ and 3-Ala_{1-80} and purified YscI or by western analysis using YscI antibodies.

Interestingly, I did find one T3S component which associated with the 3-Ala_{1-80} mutant and did not bind wild type $YopE_{1-80}$. This component is the gate-keeper for effector secretion, YopN, which is a secreted and translocated protein of the T3S system. YopN is a component of the YopN/SycN/YscB/TyeA complex of proteins that are targeted to the T3S apparatus and prevent Yop secretion until a secretion-triggering signal is encountered (Day and Plano, 1998; Ferracci et al., 2005). Furthermore, proteins belonging to YopN/MxiC/InvE family of proteins are present in essentially all T3SSs and function to prevent effector protein secretion prior to receiving a secretion activation signal (Pallen et al., 2005). As 3-Ala_{1-80} does not translocate, it is quite interesting that YopN associated with it since the YopN/SycN/YscB/TyeA complex is thought to function as a molecular plug or gatekeeper. This gatekeeper functions to control the access of T3S effectors and translocators to the T3S apparatus (Cheng et al., 2001; Day et al.,

2003). This interaction needs to be verified through a direct binding assay using purified components or by western analysis.

Assembly of the T3S apparatus requires the participation of approximately 20-25 *Yersinia* secretion (Ysc) protein. YscL regulates YscN and may tether it to the base of the T3S apparatus so it is primed and ready for secretion of substrates (Blaylock et al., 2006). This apparatus initially secretes YscI and YscF that assemble into an inner rod-like structure and an extracellular needle-like structure, respectively (Edqvist et al., 2003; Wood et al., 2008). Through the action of YscP, the molecular ruler of the T3S directs a YscU-dependent substrate specificity switch from early substrates (YscF, YscI, and YscP) to late substrates consisting of translocators/effectors when the needle reaches the proper length (Agrain et al., 2005; Journet et al., 2003; Sorg et al., 2007; Wood et al., 2008). YscU additionally interacts with the putative sorting platform for substrate export YscK-YscL-YscQ complex. A complex composed of the YopN, SycN, YscB, and TyeA proteins is then targeted to the injectisome and prevents Yop secretion until a secretion triggering signal is encountered (Day and Plano, 1998; Ferracci et al., 2005). Through affinity purification coupled with mass spectrometry I have begun to identify binding partners to the translocation signal of YopE. Further experiments are required to identify the importance of SycE in any of these binding interactions by using a *ΔsycEΔyopE* background to express and purify wild type $YopE_{1\text{-}80}$-SBP-His and 3-$Ala_{1\text{-}80}$-SBP-His. Additionally, this technique

can be applied to non-secreting conditions to find what changes occur during the activation of the T3S system in *Yersinia.*

FIGURES AND TABLES

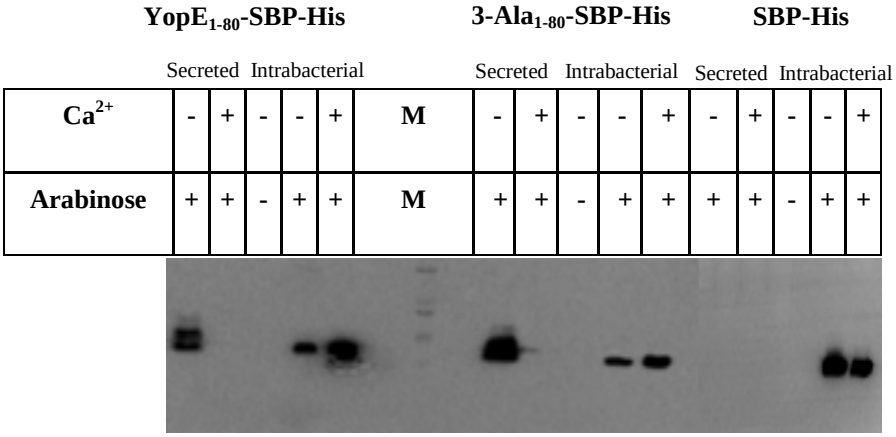

Figure 6.1 Type III secretion of YopE$_{1-80}$-SBP-His and 3-Ala$_{1-80}$-SBP-His are by *Yersinia* T3S.
Anti-His Western blot to detect YopE$_{1-80}$-SBP-His (left), 3-Ala$_{1-80}$-SBP-His (middle), an SBP-His secreted into the extracellular medium as well as intrabacterial expression by *Y. pseudotuberculosis (ΔyopE::aph)* transformed with pBAD encoding inducible wild-type (*yopE$_{1-80}$-sbp-his*), mutant (*3-ala$_{1-80}$-sbp-his)* or *(sbp-his)* with (+) or without induction (-) by arabinose as well as in the presence (+) and absence (-) of calcium (Ca^{2+}) as indicated. "M" denotes marker.

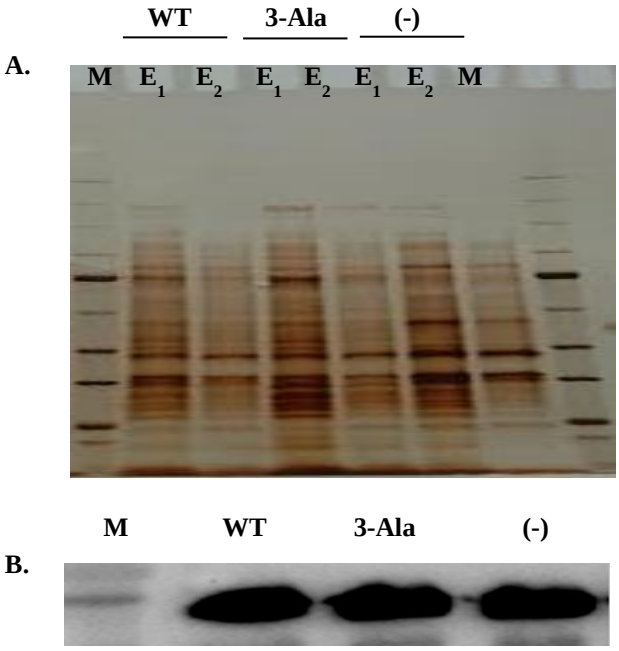

Figure 6.2 Purification of YopE$_{1-80}$-SBP-His, 3-Ala$_{1-80}$-SBP-His, and SBP-His under secreting conditions.

A. Silver Stain of streptavidin affinity purification for YopE$_{1-80}$-SBP-His (WT), 3-Ala$_{1-80}$-SBP-His (3-Ala), and SBP-His (-) where "M and "E" denote marker and elution respectively.

B. Anti-His Western blot of pooled elutions from panel A where WT, 3-Ala, and (-) denote YopE$_{1-80}$-SBP-His, 3-Ala$_{1-80}$-SBP-His, and SBP-His respectively.

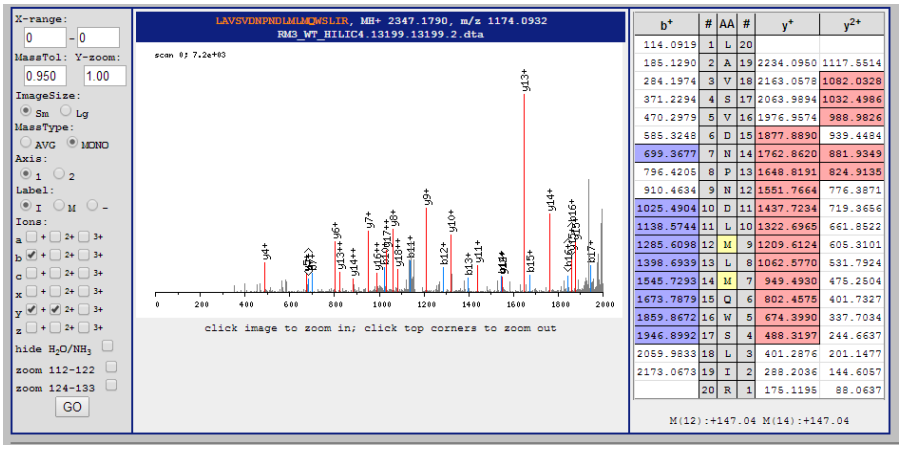

b+	#	AA	#	y+	y2+
114.0919	1	L	20		
185.1290	2	A	19	2234.0950	1117.5514
284.1974	3	V	18	2163.0578	1082.0328
371.2294	4	S	17	2063.9894	1032.4986
470.2979	5	V	16	1976.9574	988.9826
585.3248	6	D	15	1877.8890	939.4484
699.3677	7	N	14	1762.8620	881.9349
796.4205	8	P	13	1648.8191	824.9135
910.4634	9	N	12	1551.7664	776.3871
1025.4904	10	D	11	1437.7234	719.3656
1138.5744	11	L	10	1322.6965	661.8522
1285.6098	12	M	9	1209.6124	605.3101
1398.6939	13	L	8	1062.5770	531.7924
1545.7293	14	M	7	949.4930	475.2504
1673.7879	15	Q	6	802.4575	401.7327
1859.8672	16	W	5	674.3990	337.7034
1946.8992	17	S	4	488.3197	244.6637
2059.9833	18	L	3	401.2876	201.1477
2173.0673	19	I	2	288.2036	144.6057
	20	R	1	175.1195	88.0637

Figure 6.3 Validation of peptide of YscI in YopE$_{1-80}$-SBP-His elution
MS spectrum of a valid peptide as it is a semi-tryptic peptide and contains at least three consecutive b or y ions as well as mass differences of peaks are verified to be due to gain and/or loss of water. Additionally, the largest y ion signal is due to the proline present in the peptide.

Table 6.1 Proteins which associate with $YopE_{1-80}$ and $3\text{-}Ala_{1-80}$ as identified by mass spectrometry under secreting conditions.
Proteins were identified by mass spectrometry from *Yersinia pseudotuberculosis* which co-purified with wild-type $YopE_{1-80}$ and the mutant $3Ala_{1-80}$ on streptavidin beads. Proteins which bound streptavidin binding peptide-His fusion tag (SBP-His) were excluded from this list.

Accession Number	Name	Function
YP_072175.1	30S ribosomal protein S19	Protein S19 forms a complex with S13 that binds the 16S ribosomal RNA
YP_069946.1	3-phosphoshikimate 1-carboxyvinyltransferase	Aromatic amino acid biosynthesis
YP_069831.1	50S ribosomal protein L25	Part of the 50S ribosomal rRNA/L5/L18/L25 sub-complex
YP_070622.1	protein oppA precursor	ABC transporter and periplasmic oligopeptide-binding
YP_068854.1	Acetyl-coenzyme A synthetase	Catalyzes the conversion of acetate into acetyl-CoA and enables the cell to use acetate during aerobic growth to generate energy via TCA cycle
YP_070090.1	ATP phosphoribosyltransferase	Catalyzes the condensation of ATP and 5-phosphoribose 1-diphosphate to form N'-(5'-phosphoribosyl)-ATP
YP_068647.1	ATP-dependent protease subunit HslV	Protease subunit of a proteasome-like degradation complex hypothesized to be a general protein degrading machinery
YP_069352.1	Catalase-peroxidase	Bifunctional enzyme with both catalase and broad-spectrum peroxidase activity
YP_069234.1	Cell division protein ftsZ	Protein essential to the cell-division process
YP_071096.1	NADH-quinone oxidoreductase subunit B	NDH-1 shuttles electrons from NADH, via FMN and iron-sulfur (Fe-S) centers, to quinones in respiratory chain
YP_070834.1	Putative phosphoenolpyruvate synthase regulatory protein	Bifunctional serine/threonine kinase and phosphorylase involved in the regulation of the phosphoenolpyruvate synthase by catalyzing its phosphor/dephosphor-ylation
YP_072380.1	Small heat shock protein IbpA	Associates with aggregated proteins, together with IbpB, to stabilize and protect them from irreversible denaturation and extensive proteolysis during heat shock and oxidative stress
YP_072451.1	tRNA uridine 5-carboxymethylaminomethyl modification enzyme MnmG	NAD-binding protein involved in the addition of a carboxymethylaminomethyl (cmnm) group at the wobble position (U34) of certain tRNAs

Table 6.1 Proteins which associate with $YopE_{1-80}$ and $3\text{-}Ala_{1-80}$ as identified by mass spectrometry under secreting conditions.
Proteins were identified by mass spectrometry from *Yersinia pseudotuberculosis* which co-purified with wild-type $YopE_{1-80}$ and the mutant $3Ala_{1-80}$ on streptavidin beads. Proteins which bound streptavidin binding peptide-His fusion tag (SBP-His) were excluded from this list. (Table 6.1 continued).

YP_069631.1	UPF0250 protein YPTB1093	Belongs to the UPF205 family of proteins
YP_068494.1	Yop proteins translocation protein I, YscI	Inner rod protein of the *Yersinia* T3S involved in translocation of Yop proteins
YP_068497.1	Yop proteins translocation protein L, YscL	Protein required for the export process of the Yop proteins and is the regulator protein for the T3S ATPase, YscN
YP_068435.1	YopE chaperone, SycE	The chaperone to the T3S effector YopE

Table 6.2 Proteins which associate with $YopE_{1-80}$ specifically as identified by mass spectrometry under secreting conditions.
Proteins were identified by mass spectrometry from *Yersinia pseudotuberculosis* which co-purified with wild-type $YopE_{1-80}$ on streptavidin beads. Proteins which bound streptavidin binding peptide-His fusion tag (SBP-His) or the mutant 3-Ala_{1-80} (3-Ala_{1-80}SBP-His) were excluded from this list.

Accession Number	Name	Function
YP_068495.1	Yop proteins translocation lipoprotein J, YscJ	Protein required for the export process of the Yop proteins as member of the injectisome complex of proteins in the *Yersinia* T3S
YP_071279.1	Putative ABC transporter, periplasmmic iron binding protein precursor	362 amino acid protein and a putative ABC transporter, periplasmmic iron binding protein precursor
YP_069351.1	Putative cytochrome b(562) precursor	127 amino acid protein and a putative cytochrome b(562) precursor

Table 6.3 Proteins which associates specifically with 3-Ala_{1-80} as identified by mass spectrometry under secreting conditions.
Proteins were identified by mass spectrometry from *Yersinia pseudotuberculosis* which co-purified with wild-type 3-Ala_{1-80} on streptavidin beads. Proteins which bound streptavidin binding peptide-His fusion tag (SBP-His) or wildtype $YopE_{1-80}$ ($YopE_{1-80}$SBP-His) were excluded from this list.

Accession Number	Name	Function
YP_068474.1	Periplasmic nitrate reductase	Catalytic subunit of the periplasmic nitrate reductase (NAP)
YP_071267.1	Outer membrane protein YopN	Gate-keeper of the *Yersinia* T3S and plays a major role in regulation of translocation of Yops

ACKNOWLEDGEMENTS

This research was funded with NIH grant R01 AI061452 (PG).

REFERENCES

Agrain, C., Callebaut, I., Journet, L., Sorg, I., Paroz, C., Mota, L.J., and Cornelis, G.R. (2005). Characterization of a Type III secretion substrate specificity switch (T3S4) domain in YscP from Yersinia enterocolitica. Mol. Microbiol. *56*, 54–67.

Albuquerque, C.P., Smolka, M.B., Payne, S.H., Bafna, V., Eng, J., and Zhou, H. (2008). A Multidimensional Chromatography Technology for In-depth Phosphoproteome Analysis. Mol. Cell. Proteomics *7*, 1389–1396.

Anderson, D.M., and Schneewind, O. (1997). A mRNA signal for the type III secretion of Yop proteins by Yersinia enterocolitica. Science *278*, 1140–1143.

Birtalan, S., and Ghosh, P. (2001). Structure of the Yersinia type III secretory system chaperone SycE. Nat. Struct. Biol. *8*, 974–978.

Birtalan, S.C., Phillips, R.M., and Ghosh, P. (2002). Three-dimensional secretion signals in chaperone-effector complexes of bacterial pathogens. Mol. Cell *9*, 971–980.

Blaylock, B., Riordan, K.E., Missiakas, D.M., and Schneewind, O. (2006). Characterization of the Yersinia enterocolitica Type III Secretion ATPase YscN and Its Regulator, YscL. J. Bacteriol. *188*, 3525–3534.

Buszewski, B., and Noga, S. (2012). Hydrophilic interaction liquid chromatography (HILIC)--a powerful separation technique. Anal. Bioanal. Chem. *402*, 231–247.

Büttner, C.R., Cornelis, G.R., Heinz, D.W., and Niemann, H.H. (2005). Crystal structure of Yersinia enterocolitica type III secretion chaperone SycT. Protein Sci. Publ. Protein Soc. *14*, 1993–2002.

Cheng, L.W., Anderson, D.M., and Schneewind, O. (1997). Two independent type III secretion mechanisms for YopE in Yersinia enterocolitica. Mol. Microbiol. *24*, 757–765.

Cornelis, G.R. (2006). The type III secretion injectisome. Nat. Rev. Microbiol. *4*, 811–825.

Day, J.B., and Plano, G.V. (1998). A complex composed of SycN and YscB functions as a specific chaperone for YopN in Yersinia pestis. Mol. Microbiol. *30*, 777–788.

Edqvist, P.J., Olsson, J., Lavander, M., Sundberg, L., Forsberg, A., Wolf-Watz, H., and Lloyd, S.A. (2003). YscP and YscU regulate substrate specificity of the Yersinia type III secretion system. J. Bacteriol. *185*, 2259–2266.

Van Eerde, A., Hamiaux, C., Pérez, J., Parsot, C., and Dijkstra, B.W. (2004). Structure of Spa15, a type III secretion chaperone from Shigella flexneri with broad specificity. EMBO Rep. *5*, 477–483.

Ferracci, F., Schubot, F.D., Waugh, D.S., and Plano, G.V. (2005). Selection and characterization of Yersinia pestis YopN mutants that constitutively block Yop secretion. Mol. Microbiol. *57*, 970–987.

Galán, J.E., and Wolf-Watz, H. (2006). Protein delivery into eukaryotic cells by type III secretion machines. Nature *444*, 567–573.

Ghosh, P. (2004). Process of protein transport by the type III secretion system. Microbiol. Mol. Biol. Rev. MMBR *68*, 771–795.

Journet, L., Agrain, C., Broz, P., and Cornelis, G.R. (2003). The needle length of bacterial injectisomes is determined by a molecular ruler. Science *302*, 1757–1760.

Kapp, E.A., Schütz, F., Reid, G.E., Eddes, J.S., Moritz, R.L., O'Hair, R.A.J., Speed, T.P., and Simpson, R.J. (2003). Mining a Tandem Mass Spectrometry Database To Determine the Trends and Global Factors Influencing Peptide Fragmentation. Anal. Chem. *75*, 6251–6264.

Lilic, M., Vujanac, M., and Stebbins, C.E. (2006). A common structural motif in the binding of virulence factors to bacterial secretion chaperones. Mol. Cell *21*, 653–664.

Lloyd, S.A., Norman, M., Rosqvist, R., and Wolf-Watz, H. (2001). Yersinia YopE is targeted for type III secretion by N-terminal, not mRNA, signals. Mol. Microbiol. *39*, 520–531.

Locher, M., Lehnert, B., Krauss, K., Heesemann, J., Groll, M., and Wilharm, G. (2005). Crystal structure of the Yersinia enterocolitica type III secretion chaperone SycT. J. Biol. Chem. *280*, 31149–31155.

Luo, Y., Bertero, M.G., Frey, E.A., Pfuetzner, R.A., Wenk, M.R., Creagh, L., Marcus, S.L., Lim, D., Sicheri, F., Kay, C., Haynes, C., Finlay, BB., and Strynadka, NC. (2001). Structural and biochemical characterization of the type III secretion chaperones CesT and SigE. Nat. Struct. Biol. *8*, 1031–1036.

Pallen, M.J., Beatson, S.A., and Bailey, C.M. (2005). Bioinformatics analysis of the locus for enterocyte effacement provides novel insights into type-III secretion. BMC Microbiol. *5*, 9.

Phan, J., Tropea, J.E., and 2004, D.S.W. Structure of the Yersinia pestis type III secretion chaperone SycH in complex with a stable fragment of YscM2. Acta Crystallogr D *60*, 1591–1599.

Riordan, K.E., and Schneewind, O. (2008). YscU cleavage and the assembly of Yersinia type III secretion machine complexes. Mol. Microbiol. *68*, 1485–1501.

Rodgers, L., Gamez, A., Riek, R., and Ghosh, P. (2008). The type III secretion chaperone SycE promotes a localized disorder-to-order transition in the natively unfolded effector YopE. J. Biol. Chem. *283*, 20857–20863.

Rodgers, L., Mukerjea, R., Birtalan, S., Friedberg, D., and Ghosh, P. (2010). A solvent-exposed patch in chaperone-bound YopE is required for translocation by the type III secretion system. J. Bacteriol. *192*, 3114–3122.

Schubot, F.D., Jackson, M.W., Penrose, K.J., Cherry, S., Tropea, J.E., Plano, G.V., and Waugh, D.S. (2005). Three-dimensional structure of a macromolecular assembly that regulates type III secretion in Yersinia pestis. J. Mol. Biol. *346*, 1147–1161.

Singer, A.U., Desveaux, D., Betts, L., Chang, J.H., Nimchuk, Z., Grant, S.R., Dangl, J.L., and Sondek, J. (2004). Crystal structures of the type III effector protein AvrPphF and its chaperone reveal residues required for plant pathogenesis. Struct. Lond. Engl. 1993 *12*, 1669–1681.

Sorg, I., Wagner, S., Amstutz, M., Müller, S.A., Broz, P., Lussi, Y., Engel, A., and Cornelis, G.R. (2007). YscU recognizes translocators as export substrates of the Yersinia injectisome. EMBO J. *26*, 3015–3024.

Stebbins, C.E., and Galán, J.E. (2001). Maintenance of an unfolded polypeptide by a cognate chaperone in bacterial type III secretion. Nature *414*, 77–81.

Wood, S.E., Jin, J., and Lloyd, S.A. (2008). YscP and YscU Switch the Substrate Specificity of the Yersinia Type III Secretion System by Regulating Export of the Inner Rod Protein YscI. J. Bacteriol. *190*, 4252–4262.

Chapter 7:

Concluding Remarks

The type III secretion (T3S) system is a well ordered, finely tuned, and highly evolved mechanism of pathogenesis. The mechanism of effector secretion employed by the T3S occurs in a highly coordinated fashion with multiple components of the T3S injectisome working together to translocate effectors into the host cell.

The T3S apparatus requires multiple components working together to accomplish the task of translocating effector Yops into the host cell. Most if not all these components are critical to the functioning of the T3S system. This was exemplified in our work on characterizing two essential components of the T3S in *Yersinia*, YscD (Chapter 3) and YscO (Chapter 4). In chapter 3, we report the 2.52 Å resolution structure of YscDc and using structural comparison we identified two loop regions necessary for T3S. The findings of chapter 3 indicate the role that YscD plays in the sequential steps required for T3S protein export. Alanine-substitution mutagenesis of these two loop regions indicated the presence of a protein complex including YscD that appeared to be stalled on the route to T3S secretion. This protein complex was hypothesized to form due to a disruption in the dissociation of the SycH-YopH chaperone-effector pair. This disruption caused a protein complex to accumulate which then plugged the apparatus. Using SILAC, other T3S components were identified to be part of the protein complex. Among these T3S components were the putative C-ring YscQ (Bzymek et al., 2012) and the T3S molecular ruler YscP. The result of finding YscQ associated

with the mutated loop regions, L3 and L4, further suggested that the T3S is an ordered system and requires a sequence of events to occur for the transport of effectors. YscQ may be recruited to YscD through SycH, which is the case in both *Salmonella* and *Chlamydia* orthologs of YscQ, SpaO and CdsQ, respectively (Lara-Tejero et al., 2011; Spaeth et al., 2009). Both SpaO and CdsQ have been shown to bind T3S chaperones (Lara-Tejero et al., 2011; Spaeth et al., 2009). The presence of YopH in this stalled apparatus indicates an order of effector translocation. It would be interesting to re-attempt these experiments in a Δ*yopH*, Δ*sycH* or *ΔsycHyopH* background to determine the role of the chaperone in this process, as well as determining which effector would be next in line for translocation. Additionally since *Yersinia* T3S ATPase YscN is most likely responsible for catalyzing the dissociation of SycH from YopH, a possible reason for the formation of this protein complex in these loop substitution mutants is that there is a defect in the recruitment of YscN by these mutant proteins. As the interaction between YscD and YscN may be transient, we may be able to capture it with the addition of an *in vivo* crosslinker such as formaldehyde during the SILAC experiments. It was very interesting that the stalled apparatus also included YscP, as this protein has been shown to be involved in substrate switching (Edqvist et al., 2003) in the T3S system. YscP is itself secreted by the T3S system and perhaps this secretion was inhibited by loop region substitution mutants (Payne and Straley, 1999). YscP has also been shown to interact with YscQ and our study indicates that this interaction may be mediated by YopH, but

further validation using purified components or western analysis is required. In addition to YscU and YscQ, YscP has also been shown to interact with another essential component of the *Yersinia* T3S, YscO.

In Chapter 4 I further explored the protein-protein interactions of the T3S molecular ruler YscP with an essential component of the T3S system, YscO. I found regions of YscO which abrogated secretion, and I found that these regions also affected YscP binding. I found the interaction between YscO and YscP was direct and that the type III secretion substrate specificity switch, or T3S4, domain of YscP was sufficient for this interaction. Previous studies on the control of substrate switching in the *Yersinia* T3S have implicated YscP and the cytoplasmic domain of the inner membrane protein YscU (Allaoui et al., 1994; Edqvist et al., 2003; Riordan and Schneewind, 2008). The findings in Chapter 4 predict a possible role for YscO as the bridge for YscP and YscUc in substrate switching of the T3S in *Yersinia*. This hypothesis would need to be further validated with direct binding assays but we can surmise from my results that the interaction between YscO and the YscP T3S4 domain is essential to type III secretion.

The findings in chapters 3 and 4 indicate the complexity of the T3S system. The mechanisms of effector secretion are coordinated and ordered in such a way that a small change in just one component can have major effects on the secretion and/or translocation of Yops. Prior studies examining individual components of the T3S have not yielded much information on the mechanisms of effector secretion and/or translocation. We have found that many different T3S

components require the presence of the multimeric needle complex to function. This makes characterizing the components as isolated elements outside of this multimeric apparatus problematic. This difficulty is a major factor for why the precise mechanism of secretion or translocation of effectors is still unknown. A new direction in identifying potential interaction partners of the effector YopE and thus answering questions about mechanisms of the T3S is explored in Chapters 5 and 6.

Previous work on the characterization and secretion/translocation of YopE has shown SycE is required for the effective translocation of YopE. The 5'/N-terminal signals, however, have been shown to be sufficient for YopE secretion. There are many *Yerisnia* T3S components hypothesized to interact with and target YopE for secretion or translocation. The major limiting step, however, is the lack of direct evidence for interactions between YopE and specific *Yersinia* T3S components. This was the incentive for trying a different method of determining interacting partners for the secretion and translocation signals of YopE. In Chapter 5, I constructed two vectors to identify potential binding partners of the 5' secretion signal of *yopE* mRNA using reverse-CLIP and RaPID techniques. I found the RaPID technique to be a more promising option than the reverse-CLIP technique. I was able to find a construct that was expressed and capable of being purified through affinity for MS2CP-GFP-SBP. The next steps in using the RaPID technique for determining binding partners for the 5' mRNA signal of YopE is the

quantification of the target construct during purification as well as introducing UV crosslinking.

In chapter 6, I focus on the involvement of SycE in the translocation of the effector YopE. I contributed to work testing a prediction of the translocation signal model (Chapter 2). The hypothesis of SycE-YopE binding to a receptor to target the effector for translocation was tested by disrupting potential receptor binding sites in the effector YopE. The findings in Chapter 2 indicate that the solvent exposed patch of residues in the Cb region of the chaperone bound YopE are crucial for translocation of the effector YopE. Their effect on translocation is consistent with the structure of the chaperone-bound Cb region serving as a signal for translocation. I then set out to determine what this putative receptor for translocation may be.

I found potential binding partners to the first 80 amino acids of the *Yersinia* effector YopE ($YopE_{1-80}$) using a similar technique described in Chapter 5 involving streptavidin affinity purification coupled to tandem mass spectrometry. I used a mutant protein developed from Chapter 2, 3-Ala, to serve as an indicator of potential binding partners required for translocation. I found that under secreting conditions, the inner rod protein YscI selectively bound wild-type Yop_{1-80} and $3\text{-}Ala_{1-80}$. This finding validates a previously indicated role of YscI in conjunction with YscP and YscU as a necessary component for substrate switching in the T3S of *Yersinia* (Wood et al., 2008). This initial finding could be further analyzed with interaction studies between YopE and wild type YscI as

well as known substitution mutants of YscI which abrogate secretion(Wood et al., 2008).

The second potential binding partner found is the ATPase regulator YscL, which selectively bound wild-type $YopE_{1-80}$ and the non-translocating mutant 3-Ala_{1-80}. This is an interesting finding as YscL is the negative regulator of the T3S ATPase YscN. Although studies of other T3S systems have shown interactions between YscN homologs with chaperone-effector pairs, this interaction was not previously observed in *Yersinia.* This may have been due to the interaction being mediated by YscL and this could be further tested by a direct binding study of YscN and SycE-YopE in the presence of YscL. The list of associating proteins to the non-translocating mutant protein 3-Ala was nearly identical to wild-type YopE except in the case of theT3S gate-keeper YopN which was selectively bound by 3-Ala_{1-80}. This was quite interesting to see as there was no host cell present during growth of the bacteria under secreting conditions and indicates the gatekeeper YopN may serve secretion and translocation specific roles. The expression of $YopE_{1-80}$ and 3-Ala_{1-80} in a *ΔsycEΔyopE* background is very important with regards to interaction studies with YopN as this would further indicate a translocation signal is occurring. Additionally, only one or two components of sub-complexes in the T3S associated with our targets. For instance, the protein YscI of the substrate specificity switching complex was found to associate with $YopE_{1-80}$ and 3-Ala_{1-80} whereas YscP and YscU were not bound by either of these constructs. Also in the case of YscL/YscN/YscK, only

YscL was bound to both $YopE_{1-80}$ and $3\text{-}Ala_{1-80}$. Additionally only YopN of the YopN/TyeA/SycN/YscB gate-keeper complex associated with $3\text{-}Ala_{1-80.}$ This indicates the possible necessity of using crosslinking agents to capture any other components of the sub-complexes. The findings in Chapter 3, 5, and 6 indicate a new direction in the determination of binding partners to the secretion and translocation signals of Yops. Using affinity purification coupled to mass spectrometry, I have identified possible binging partners to the secretion signals of YopE and this technique can be applied to different targets in the *Yersinia* T3S to obtain a list of potential interaction partners to a particular target. Applying this method to determine binding partners may reduce disruption of potential complexes of proteins during the purification process. This provides a better approach than previous methods of determining potential binding partners and complexes involved in effector secretion as it maintains the context of the T3S multimeric complex. Since the protein-protein interactions occur in the presence of the multimeric complex, any additional components in the T3S which may be required for these interactions would be available. In addition, we are also including non-secreting conditions to observe any changes in the T3S upon activation of the injectisome. Using affinity purification coupled to tandem mass spectrometry, we can track a specific effector or any other component of the T3S throughout the secretion/translocation process. This technique followed by validation of the potential binding partners, will finally be able to put together the mechanistic pieces of the *Yersinia* T3S puzzle.

REFERENCES

Allaoui, A., Woestyn, S., Sluiters, C., and Cornelis, G.R. (1994). YscU, a Yersinia enterocolitica inner membrane protein involved in Yop secretion. J. Bacteriol. *176*, 4534–4542.

Bzymek, K.P., Hamaoka, B.Y., and Ghosh, P. (2012). Two translation products of Yersinia yscQ assemble to form a complex essential to type III secretion. Biochemistry (Mosc.) *51*, 1669–1677.

Edqvist, P.J., Olsson, J., Lavander, M., Sundberg, L., Forsberg, A., Wolf-Watz, H., and Lloyd, S.A. (2003). YscP and YscU regulate substrate specificity of the Yersinia type III secretion system. J. Bacteriol. *185*, 2259–2266.

Lara-Tejero, M., Kato, J., Wagner, S., Liu, X., and Galán, J.E. (2011). A sorting platform determines the order of protein secretion in bacterial type III systems. Science *331*, 1188–1191.

Payne, P.L., and Straley, S.C. (1999). YscP of Yersinia pestis is a secreted component of the Yop secretion system. J. Bacteriol. *181*, 2852–2862.

Riordan, K.E., and Schneewind, O. (2008). YscU cleavage and the assembly of Yersinia type III secretion machine complexes. Mol. Microbiol. *68*, 1485–1501.

Spaeth, K.E., Chen, Y.-S., and Valdivia, R.H. (2009). The Chlamydia type III secretion system C-ring engages a chaperone-effector protein complex. PLoS Pathog. *5*, e1000579.

Wood, S.E., Jin, J., and Lloyd, S.A. (2008). YscP and YscU switch the substrate specificity of the Yersinia type III secretion system by regulating export of the inner rod protein YscI. J. Bacteriol. *190*, 4252–4262.